Using Holocene sea-level data to improve sea-level predictions for the United Kingdom: a combined empirical and model-based approach

Geoffrey Richards

PhD

University of York

Environment and Geography

September 2018

'We then passed over Newgale sands at which place a very remarkable circumstance occurred. The sandy shores of south Wales laid bare by the extraordinary violence of a storm, the surface of the earth, which had been covered for many ages, reappeared, and discovered the trunk of trees cut off, standing in the very sea itself, the strokes of the hatchet appearing as if made only yesterday. The soil was very black and the wood like ebony. This looked like a grove cut down, perhaps at the time of the deluge, or not long after.'

Giraldus Cambrensis 1188AD

UNIVERSITY OF YORK

Abstract

Department of Environment and Geography

Doctor of Philosophy

Using Holocene sea-level data to improve sea-level predictions for the United Kingdom: a combined empirical and model-based approach

by Geoffrey Richards

The thesis presents new sea-level data for north Wales and western Pembrokeshire. These data are used alongside the existing British sea-level database to assess current GIA models. The suitability of enclosed coastal back-barrier freshwater marshes as archives for Holocene sea level more generally is also evaluated.

This work expands on the work by Gehrels and Anderson (2014) who first demonstrated the suitability of peat deposits in coastal freshwater peat-gravel back-barrier marshes for sea-level reconstructions. The suitability of the method is expanded to include peat-sandy gravel and peat-sand systems.

Groundwater monitoring was used to show that the back-barrier water table is controlled by tide levels. Groundwater modelling experiments were conducted to test the controls of stratigraphy, peat permeability and marsh recharge on the link between groundwater and sea level.

Hand-drilled coring was used to establish the stratigraphy of these sites. Sea-level index points were collected from basal Holocene peat that was dated by radiocarbon methods and is immune to sediment compaction.

Presented here are two new compaction-free sea-level index points for north Wales and six for west Pembrokeshire. The new data show a c.5.2m sea-level rise in north Wales, between c.7400 and 1900 cal years BP. Whilst a mid Holocene highstand can not be ruled out, this data leaves little room for one to have occurred. In western Pembrokeshire sea level rose c.8.2m between c.7000 and 2900 cal years BP.

Current GIA models are shown to over-predict sea level at both sites, possibly due to the under prediction of isostatic rebound. These misfits need to be addressed to improve future predictions of sea-level change for the UK.

Contents

List of Figures

List of Tables

Declaration of Authorship

I, Geoffrey RICHARDS, declare that this thesis titled, 'Using Holocene sea-level data to improve sea-level predictions for the United Kingdom: a combined empirical and model-based approach' and the work presented in it are my own. I confirm that:

- This work was done wholly or mainly while in candidature for a research degree at this University.
- Where any part of this thesis has previously been submitted for a degree or any other qualification at this University or any other institution, this has been clearly stated.
- Where I have consulted the published work of others, this is always clearly attributed.
- Where I have quoted from the work of others, the source is always given. With the exception of such quotations, this thesis is entirely my own work.
- I have acknowledged all main sources of help.
- Where the thesis is based on work done by myself jointly with others, I have made clear exactly what was done by others and what I have contributed myself.

Acknowledgements

I would like to thank everyone who have been a part of my journey towards completing this thesis. Firstly, I would like to thank my supervisor, Prof Roland Gehrels. His support, patience and provision of business meetings has been invaluable in this research. I would also like to thank Prof William Anderson for his unwavering support with groundwater model simulations. Also, to my supervisors Dr Laurence Jones and Dr Christopher Evans for their input throughout.

Thanks also goes to my CASE partner In-Situ Europe for their support with equipment and funding, without which this research would not have been possible. I am grateful to MIKE Powered by DHI, for supplying a licence for their FEFLOW groundwater model and their constant support with hardware failure and surrounding issues. None of this would have been achievable without funding from the Natural Environment Research Council, for which I consider myself fortunate to have received.

The blossoming sea-level group at the University of York have provided much needed enthusiasm and motivation and I am particularly grateful to Graham Rush and Sophie Williams for their emotional support. Thanks to everyone involved in my fieldwork, particularly Tim Jackson, who has worked tirelessly and with unstoppable enthusiasm throughout the most unpleasant of conditions. Thanks also to Rob Mason and Toby Walker for their hard work in the field, they are genuine coring machines.

There are countless friends who have made the experience enjoyable and worthwhile and I thank all of them. Finally, the biggest thank you goes to Louise Richards who, as always, has provided the love and support required to succeed.

Chapter 1

Introduction

1.1 General Introduction

The United Kingdom Climate Impact Programme (UKCIP) has provided predictions of future sea-level change, the most recent report being the UK Climate Projections Science Report: Marine and Coastal Projections (UKCP09) [Lowe et al., 2009]. UKCP09 predictions of future relative sea-level (RSL) change demonstrate that change in mean sea level will not be uniform around the United Kingdom (Figure 1.1) and that significant regional variations are expected due to differential vertical land movements. It is essential that predictions of these variations are reliable and this depends, in part, on an accurate model of Holocene relative sea-level change. As such, understanding the pattern of past relative sea-level change around the United Kingdom is of great importance to society [Gehrels, 2010].

Quaternary sea-level change has been predominantly controlled by the cyclical growth and decay of continental ice. Since the Last Glacial Maximum (LGM), deglaciation has resulted in a transfer of mass from continental ice sheets to oceanic basins [Milne, 2015]. The result of this transfer is that global mean sea level has increased during the Holocene. This increase is often termed *eustatic* sea-level rise [Peltier et al., 2002]. The response of the solid Earth to the loading and unloading of the continental crust and the resulting deformation of the lithosphere is termed *isostasy*. It is the interplay between rising sea level, due to the addition of water to the ocean basins, and the isostatic adjustment of the solid Earth which results in relative sea-level (RSL) change with variations across regions. As these changes are relative, then the terms relative sea-level change and relative land uplift are interchangeable and are used as such in the literature [i.e Shennan et al. [2012]]. Shennan et al. [2012] use geological evidence to produce a map of ongoing relative land uplift for the British Isles (Figure 1.2). Examination of the maps in Figures 1.1 and 1.2 shows similar trends of relative land uplift to those of the predictions of future

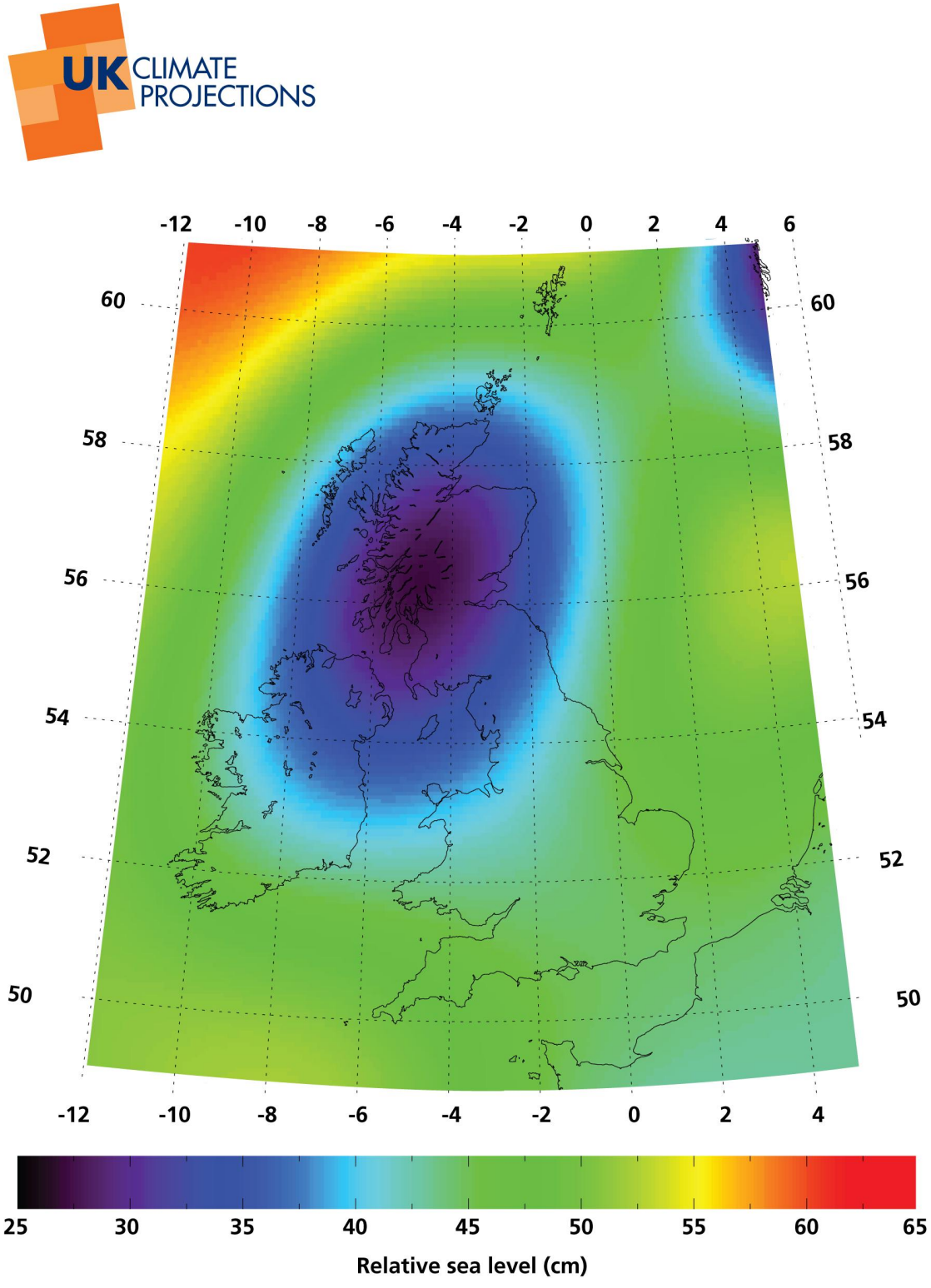

FIGURE 1.1: Predicted regional variation in relative sea-level change around the United Kingdom for 2095. The predicted change is a result of absolute sea-level change averaged for the UK and regional vertical land changes [Lowe et al., 2009].

sea-level change, highlighting that relative land movements play a critical role in the prediction of future sea levels.

Wales is a critical area for models of Holocene sea-level change, because of an isostatic gradient running north to south as a result of Holocene subsidence of the south relative to the north. The models covering these regions are poorly constrained, so further data allows for the improvement of the fit between models and observations. Suitable sites in Wales for Holocene sea-level reconstructions are rare, because Wales contains a limited number of salt marshes and estuaries [Boorman, 2003] due to the rocky geomorphology of the coastline. Barrier systems, on the other hand, are plentiful. Therefore, this work builds on the previous investigation by Gehrels and Anderson [2014], which proposes the necessary conditions for past sea-level data to be archived in a back-barrier freshwater marsh. In this thesis the methods of Gehrels and Anderson are applied to two sites in Wales to test the hypothesis that freshwater peat deposits can have a direct relationship to sea level and as such be suitable archives for past sea level.

1.2 Sea-level Index Points

The geological sea-level data used by Shennan et al. [2012] to construct the map in Figure 1.2 are called sea-level index points (SLIPs). SLIP attributes includes location, age, altitude and a sea-level tendency. The age of the majority of the SLIPs in the British sea-level database is determined by radiocarbon dating, with calibrated ages and some supporting evidence [Shennan et al., 2006]. Constraining the altitude of SLIPs is achieved by assessing the indicative meaning of the sea-level indicator. Indicative meaning include the reference water level and the indicative range of the indicator. The indicative range is the vertical spread over which the indicator could have existed during formation and the reference water level is the midpoint of the indicative range [Milne, 2015]. The indicative meaning is measured relative to contemporary tidal heights (Figure 1.3). The tendency of an index point relates to the increase or decrease of marine influence in stratigraphic context [Shennan et al., 2006].

SLIPs can be categorised into three types. Basal SLIPs are located at the base of the Holocene sequence and as such are not considered to be significantly affected by compaction. These are the preferred SLIPs to use. Intercalated SLIPs are collected from within the Holocene sequence and as such can be displaced downwards by the weight of overlying sediments. Limiting SLIPs give an upper or lower limit of sea level, with samples occurring either in freshwater or fully marine environments. They can only be used to provide the maximum or minimum position of former sea levels [Shennan et al., 2015].

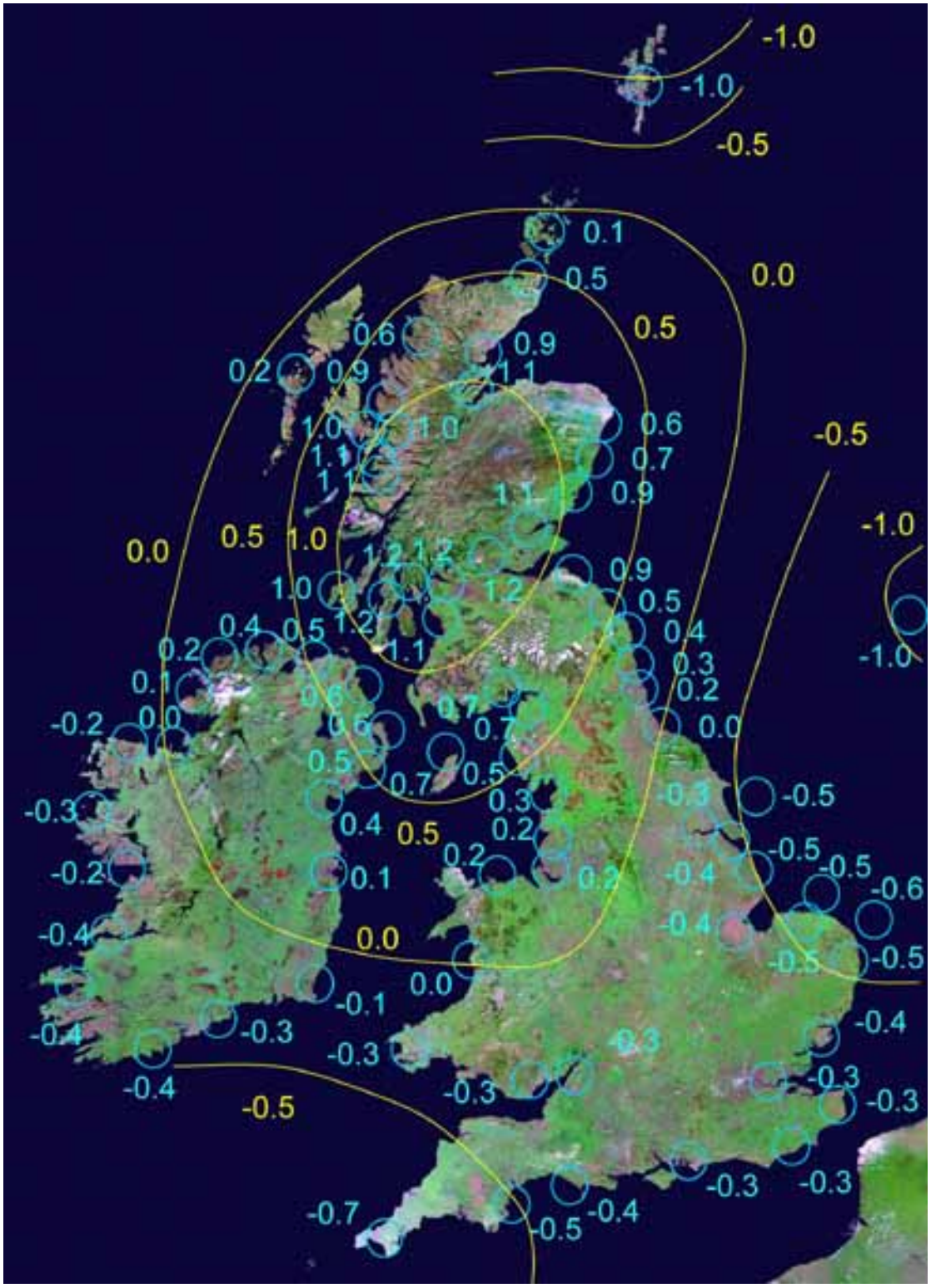

FIGURE 1.2: Rate of relative land change around the British Isles (mm a^{-1}) between 1 ka and the present day. Positive values represent land uplift and negative values subsidence [Shennan et al., 2012].

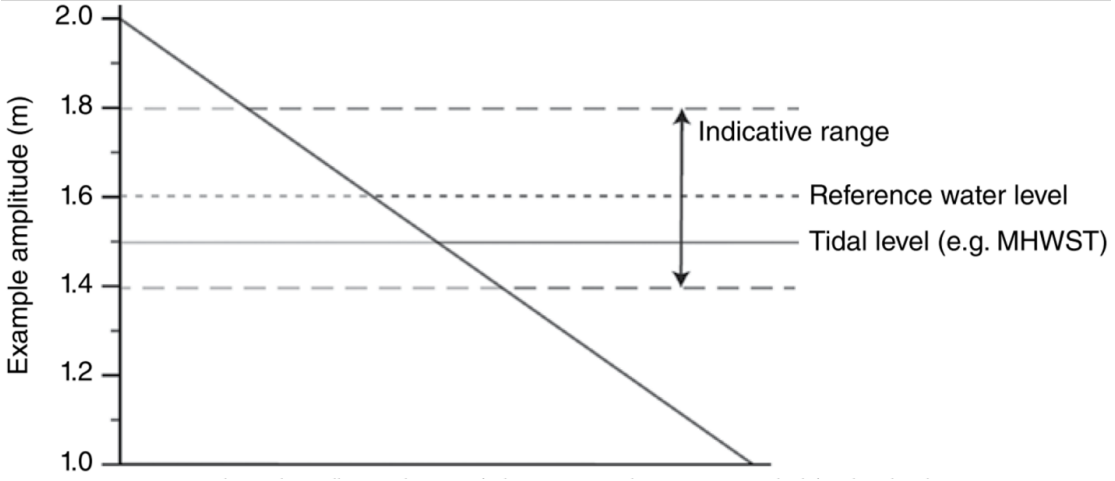

FIGURE 1.3: The indicative range of a SLIP is the potential vertical range of the sample during formation. The reference water level is taken as the mid-point of the indicative range [Milne, 2015].

1.3 Glacial isostatic adjustment modelling

Glacial isostatic adjustment (GIA) numerical models are used to simulate the response of the solid Earth to mass transfer between the oceans and the cryosphere. The change in sea level brought about by this interaction is described by the sea-level equation, such as the simplified version presented by Milne [2015]:

$$S(\theta, \Phi, t) = C(\theta, \Phi)[G(\theta, \Phi, t) - R(\theta, \Phi, t) + H(t)] \tag{1.1}$$

where $S(\theta,\Phi,t)$ represents the change in sea level for a particular location. Changes in the geoid are represented by the term $G(\theta,\Phi,t)$ and changes in the solid Earth by $R(\theta,\Phi,t)$. Conservation of mass is controlled by the term $H(t)$ to ensure that all of the water mass is accounted for when transferred from or to the ocean and $C(\theta,\Phi)$ is the ocean function [Milne, 2015].

There are two main elements to a GIA model, a forcing and a deformation response to the forcing (Figure 1.4). The forcing component is the combination of the rotational changes of the Earth and mass exchange between land and oceans. The deformation response is the change in the solid Earth brought about by the forcing components [Milne, 2015].

GIA models work by solving the generalised sea-level equation [Peltier et al., 2002] and the latest models account for shoreline migration over time, the advance/retreat of ice sheets, ablating marine based ice and the changes in Earth's rotation vector caused by the influence of GIA [Bradley et al., 2011, Milne et al., 2006, Shennan et al., 2006]. GIA models can produce

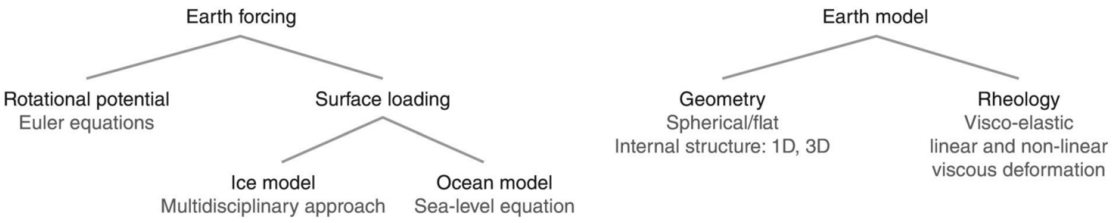

FIGURE 1.4: The key elements that comprise the Earth forcing and Earth model components of GIA models. Earth forcing and earth properties (determined by the earth model) control how the earth deforms due to variations in ice and ocean loading [Milne, 2015].

predictions of vertical land uplift and subsidence (Figure 1.5), such as those reflected in the sea-level predictions produced by UKCIP (Figure 1.1).

The prediction of vertical land movements by GIA models is reliant upon an Earth model which simulates the response of the mantle to loading and unloading. The small size of the British Ice Sheet means that the upper mantle is primarily responsible for the degree of rebound observed around the British Isles, with the impact of the lower mantle being negligible [Lambeck, 1993a]. The more recent models use a three layer model as in Milne et al. [2006], Shennan et al. [2006] and Bradley et al. [2011]. The first two layers represent the lithosphere and upper mantle, extending to a depth of 670m [Bradley et al., 2011, Milne et al., 2006] and the deepest layer represents the lower mantle. The thickness of the lithosphere varies between models, typically a 96km or 71km thick lithosphere is used [Bradley et al., 2011, Shennan et al., 2006]. The viscosity of the lithosphere is typically 10^{43} Pa s [Bradley et al., 2011, Milne et al., 2006, Shennan et al., 2006]. Viscosity ranges for the upper and lower mantle are typically 10^{20}-10^{21} and 10^{21}-10^{22} respectively.

Typically, GIA models for the British Isles use a nested ice model based on low resolution global ice models such as those presented by Bassett et al. [2005], and high resolution British-Irish ice sheet models such as Peltier et al. [2002]. Shennan et al. [2000] highlighted that by not accounting for topography under the ice sheet, in areas such as Scotland, the ice thickness would be overestimated. As such, more recent ice models make adaptations to correct for this issue, such as Bradley et al. [2011].

GIA models predict past sea levels from SLIPs and the predictions are typically presented as curves (Figure 1.6). Each SLIP includes a range of possible ages and heights, which are usually represented as crosses. The horizontal axis of a cross shows the range in age of the SLIP. The vertical axis shows the indicative range and the combined estimations of height error, which includes errors introduced by a variety of factors which include surveying, autocompaction, angle of borehole, datum errors and uncertainties in paleotides [Gehrels et al., 1996]. The GIA modelled curves presented by Shennan et al. [2012] clearly show the non-uniform nature of Holocene sea-level change around the United Kingdom (Figure 1.6).

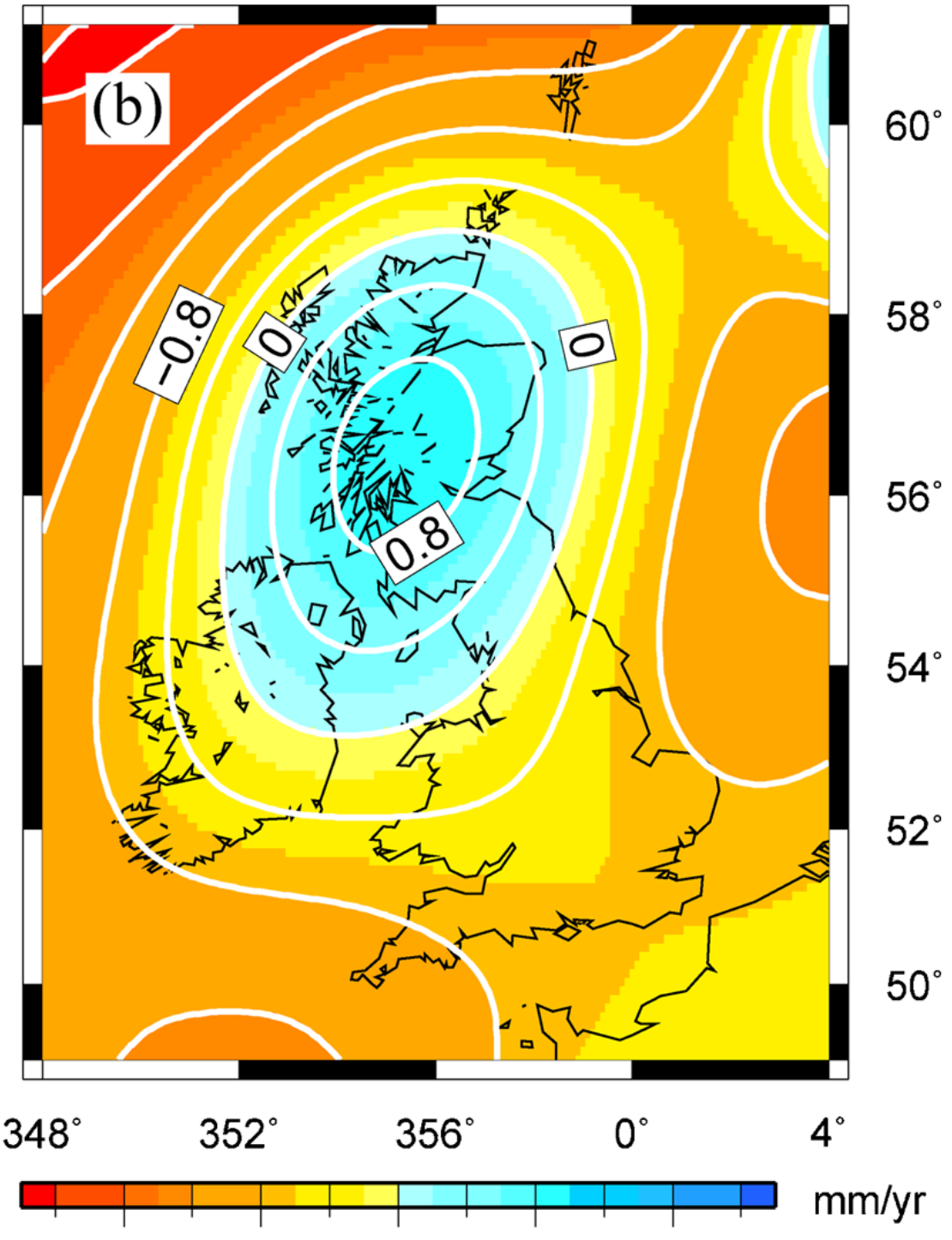

FIGURE 1.5: Glacial Isostatic Adjustment model prediction of present day vertical land uplift in the British Isles in mm/yr. Predictions include relevant ocean loading and rotational components [Bradley et al., 2011].

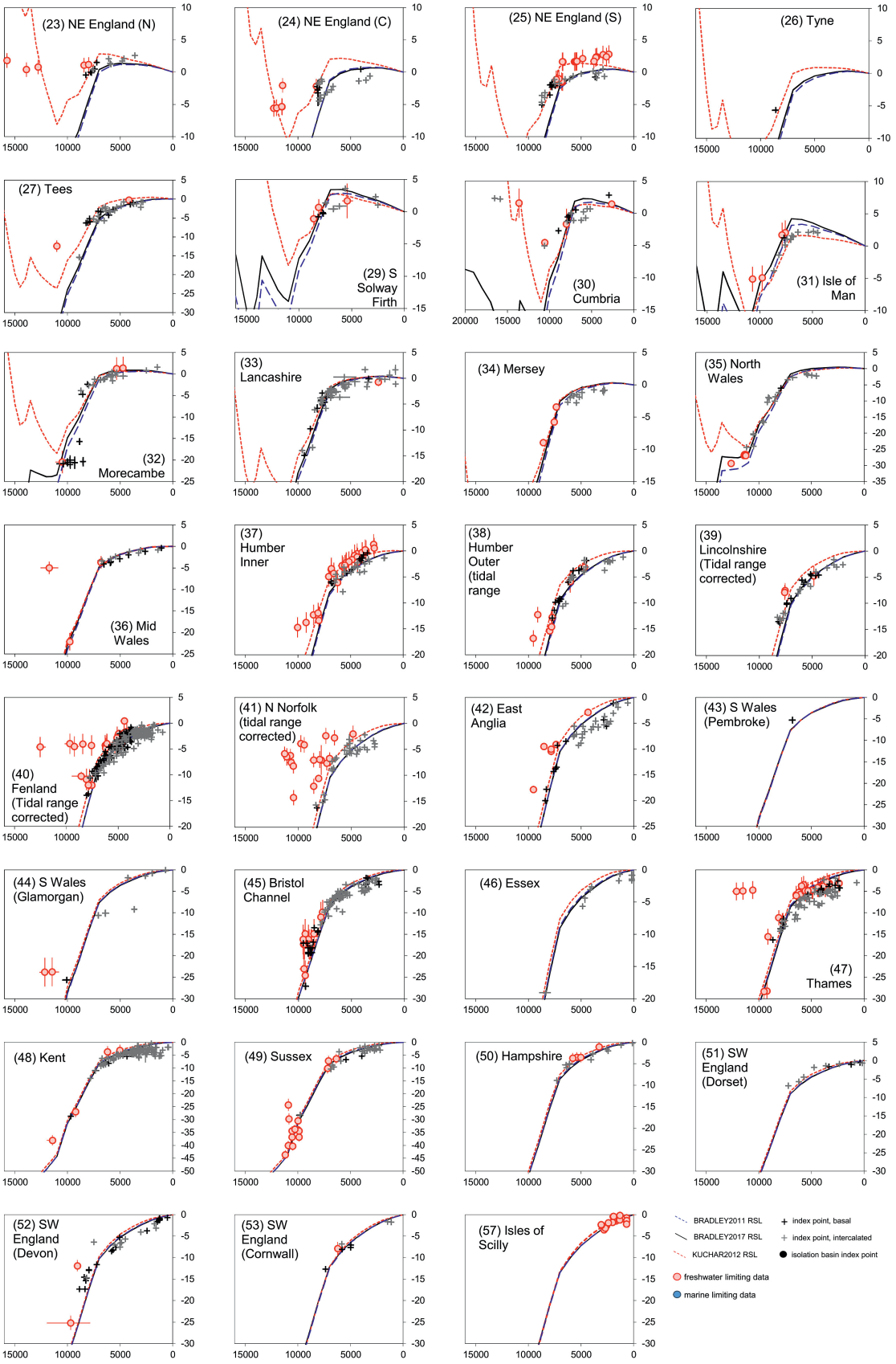

FIGURE 1.6: Example plots from the Sea-level Index Point Database for the United Kingdom and relative sea-level curves from three Glacial Isostatic Adjustment models. Horizontal bars represent the age error at 95% probability in years BP. The vertical error bar represents the combined elevation errors [Shennan et al., 2018].

There are key misfits apparent between the modelled predictions and the geological data. GIA models predict too large a magnitude oscillation events associated with melt water pulse 1A in Scotland [Bradley et al., 2011]. The models underestimate the magnitude of sea-level fall, during the late Devensian in Scotland [Bradley et al., 2011] and underestimate the magnitude of land uplift in central Scotland [Gehrels, 2010]. These local misfits could be of key importance for the validity of GIA modelling.

Wales in particular has key misfits between the modelled Holocene sea-level change and the available SLIPs. For example the GIA model presented by Peltier et al. [2002] predicts a middle Holocene sea-level highstand in north Wales which is not supported by the current SLIP database. This highstand is a time of maximum sea-level height, subsequent to which sea level has gradually decreased to modern day levels. The model presented by Bradley et al. [2011] does not predict any highstand in north Wales (Figure 1.7). However, this is based on only a small number of SLIPs resulting in uncertainty in the pattern of Holocene sea-level change in Wales and a requirement for the collection of more SLIPs to better constrain the models.

1.4 Holocene Sea-level Change in Wales

Patterns of predicted Holocene RSL change show clear differences between north Wales and south Wales. The general pattern of south Wales RSL change is one of steady rise, although there are few SLIPs to constrain the data (Figure 1.7). Models for north Wales disagree on the pattern of sea-level change with, as mentioned, some predicting a middle Holocene highstand.

The misfits in Wales, between geological data and models, have wider implications. If GIA models fail to predict accurately the sea-level history in this region, the GIA models are potentially inaccurate and an attempt should be made to improve them before they are used to predict future sea-level changes for all of the UK. Whilst mid Wales has a good coverage of sea-level data, there is a lack of sea-level data for north and south Wales. North Wales has no data younger than 4000 years BP [Roberts et al., 2011] and south Wales has only one index point in Pembrokeshire [Heyworth and Kidson, 1982, Shennan et al., 2018] and nine collected in Glamorgan, along with three limiting points [Edwards, 2006, Heyworth and Kidson, 1982, Shennan et al., 2018].

1.5 Study Areas

Former coastal environments in Wales, from which sea-level index points have been collected, include estuaries, salt marshes, tidal flats and drowned forests. In Wales and elsewhere, open back-barrier systems have been used to reconstruct Holocene sea-level change, despite problems

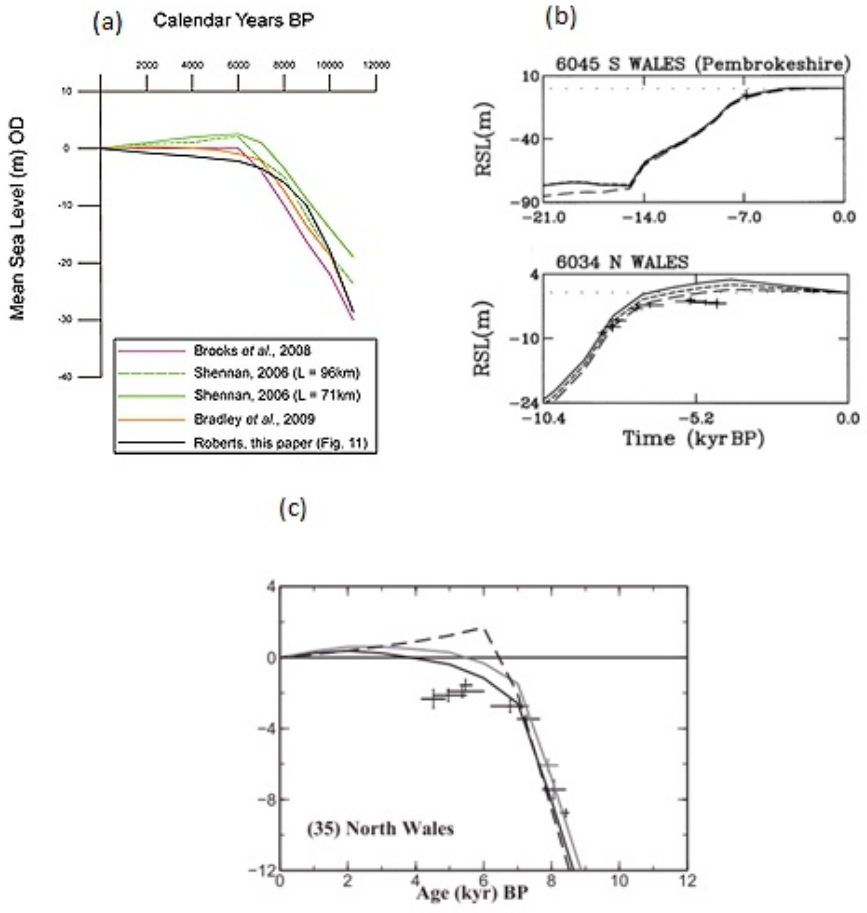

FIGURE 1.7: Modelled sea-level curves for Wales presented by (a) Roberts et al. [2011] for north Wales; (b) Peltier et al. [2002] for north Wales and Pembrokeshire; and (c) Bradley et al. [2011] for north Wales. SLIPs are shown as crosses, which indicate the elevation error with vertical bars and age error with horizontal.

of sediment being reworked by coastal processes [Gehrels and Anderson, 2014]. Many back-barrier systems in Wales, however, are closed, and contain deposits of freshwater peat. In a recent paper Gehrels and Anderson [2014] show that these systems can be suitable environments for sea-level reconstructions, provided that the groundwater table was coupled to sea level during the period that is covered by the sea-level reconstruction. In this thesis, the findings of Gehrels and Anderson [2014] are tested with the aim to identify back barrier systems that can provide new sea-level index points in south-west and north Wales.

The sites chosen for this work are barrier-impounded freshwater coastal marshes in Anglesey and western Pembrokeshire (Figure 1.8). Peat is formed and preserved in freshwater marshlands and preliminary investigations suggested that at both sites the peat is continuous, showing no sign of reworking. This was indicative that the system had remained closed, with no tidal inlet, and no erosion by migrating tidal creeks. Before the sites were selected monitoring wells were installed in the marsh, recording groundwater data at 15 minute intervals, that appeared to show a tidal signal, possibly demonstrating the coupling of sea level with the groundwater level. Longer records were collected as part of this study, to demonstrate the coupling with statistical certainty. The two sites have been chosen to examine differences between northern and southern Wales Holocene sea-level change due to GIA. The chosen sites also represent two different coastal barrier types, with Abermawr in the south of Wales being a gravel barrier system and Rhoscolyn in the north being a sand barrier system. One of the aims of this thesis, therefore, is to explore whether the methodology suggested by Gehrels and Anderson [2014] for a gravel barrier system can be extended to include sand barriers.

1.5.1 Rhoscolyn

Rhoscolyn (SH 275753) is located in north Wales on Holy Island, which is connected to the Isle of Anglesey in north Wales (Figure 1.9). The site lies in the bay of Borthwen and has been developed around the far edges, where houses and a car park have been built. Rhoscolyn marsh and Holy Island in general, have not been subjected to any previous sea-level reconstruction studies.

The back-barrier system is a freshwater marsh, fully enclosed by a sand barrier running parallel to the shoreline. It is roughly square in shape, extending approximately 0.55km inland and covering an area of around 0.3km^2. The vegetation is dominated by *Phragmites* and drainage is via a single culvert, which exits below the sand barrier through a tidal sluice. A small pond is present in the south east of the marsh. The beach is predominantly sandy, leading to a rocky shoreline to the south

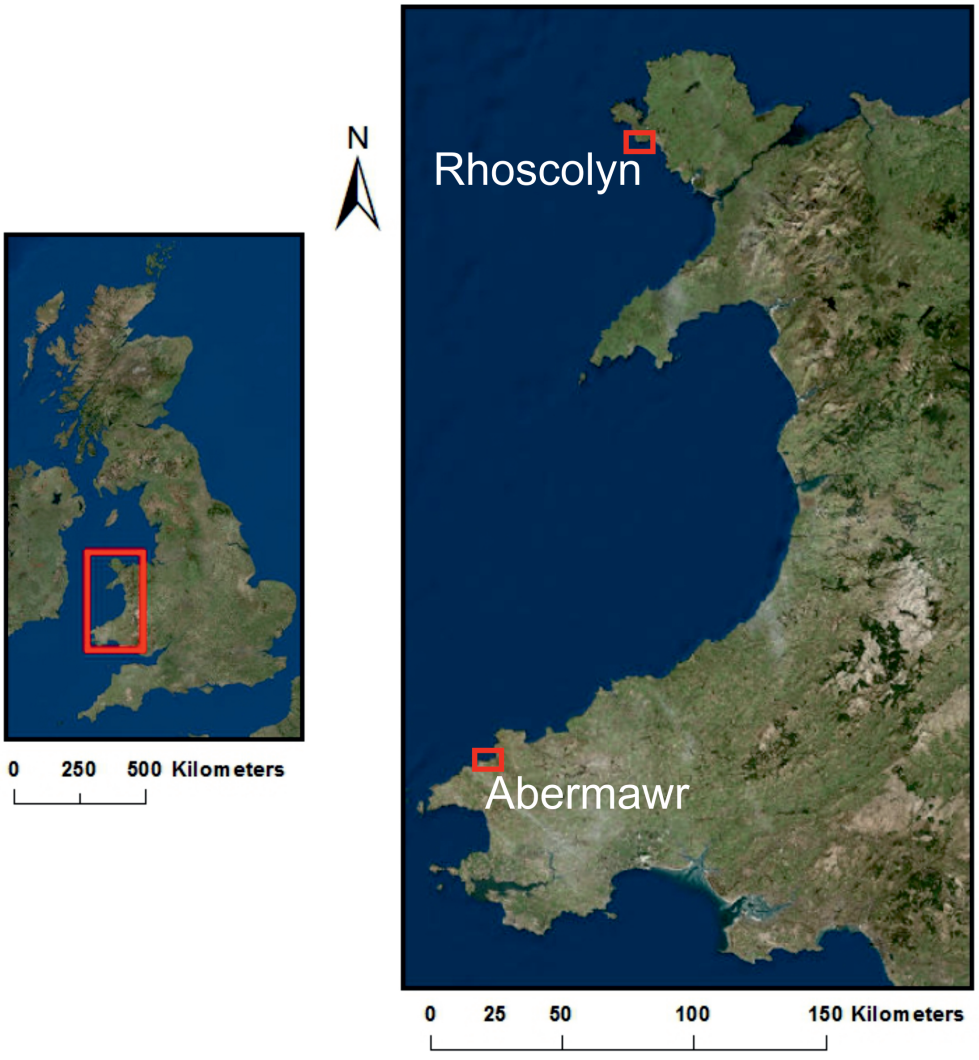

FIGURE 1.8: Location of Wales within the UK. Rhoscolyn in Anglesey and Abermawr in west Pembrokeshire.

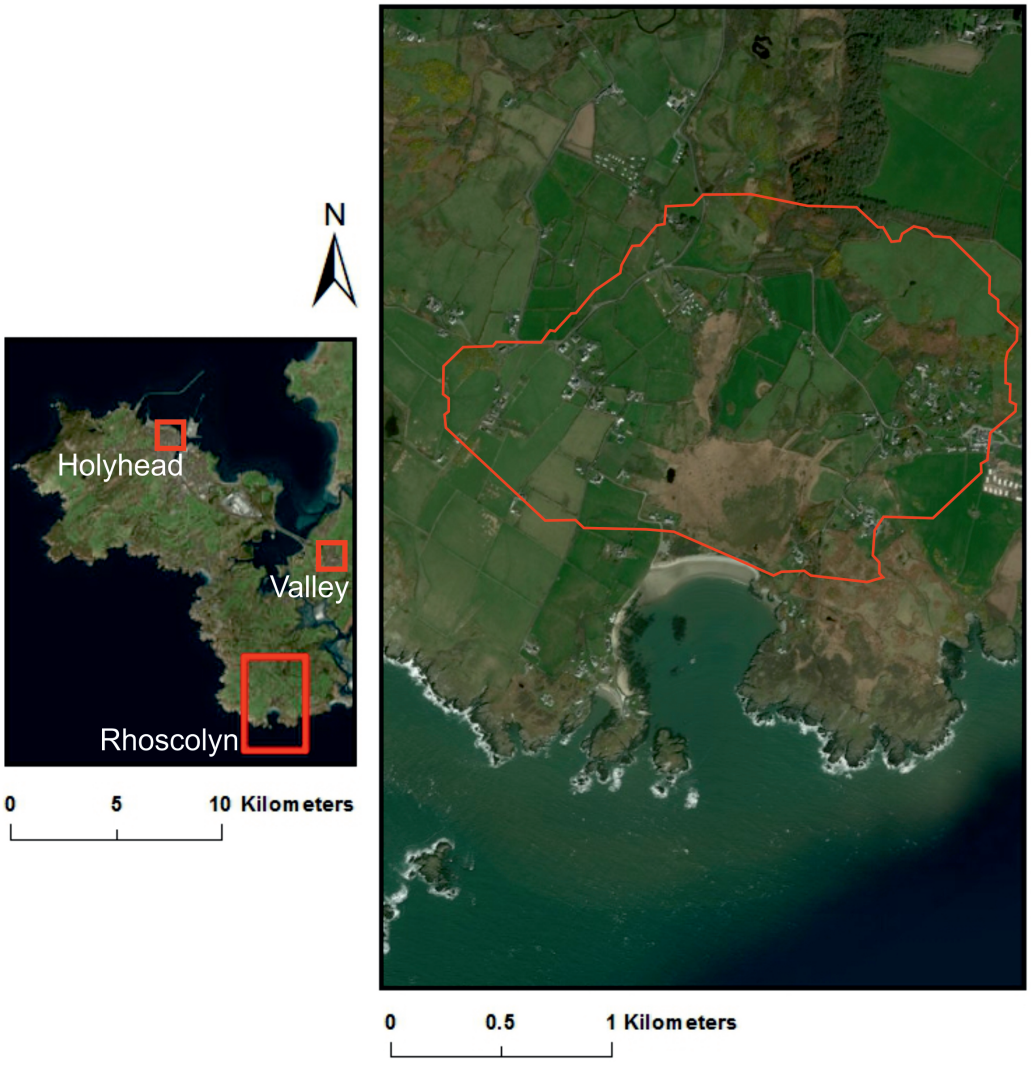

FIGURE 1.9: The location of Rhoscolyn marsh in relation to the Anglesey and the United Kingdom. Also shown is the location of the tide gauge (Holyhead) and weather station (Valley) used in this study. Outlined on the marsh is the catchment area for the site.

The catchment area for Rhoscolyn marsh is small (Figure 1.9). There are no rivers feeding into the marsh, only a small stream. As such, the total net annual average flow accumulation (based on climate data for 2000-2010) is small. On average the net annual flow is 364,688 m^3/yr.

The Rhoscolyn back-barrier system overlies late Precambrian rocks comprising the South Stack and New Harbour Groups. These consist of the interbedded psammites and pelites of the South Stack Group and the pelites of the New Harbour Group. The geology of Rhoscolyn has been the subject of many investigations [Collins and Buchan, 2004, Hassani et al., 2004, Lisle, 1988, Roper, 1992, Treagus et al., 2003], focusing on the nature and age of an anticline contained within the South Stack Group. Underlying the freshwater peat, the surface deposits are dominated by glacial till. The British Geological Survey also indicates tidal flat deposits of clay and silt, at the rear of the marsh.

The Holyhead tide gauge (SH 2553 8287) is the most proximal to Rhoscolyn (Figure 1.10), with records covering the period between 1938-2016. The record shows a gradual increase of 2.26mm per year through this period (Figure 1.10). MHWS is 2.61m OD and MHWN is 1.46m OD. MLWS is -2.34m OD and MLWN is -1.03m OD. The mean springs range is 4.95m compared the the mean neap range of 2.49m.

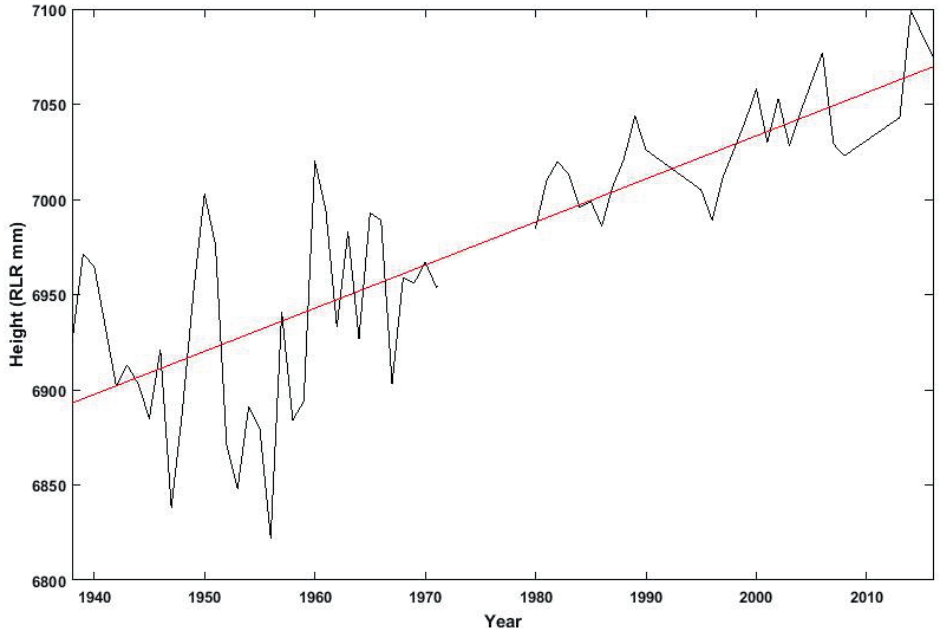

FIGURE 1.10: The tide gauge record for Holyhead 1938-2016, showing an average of 2.26mm per year RSL rise. Sea-level heights are revised to a local reference (RLR) to correct for datum changes through time. The linear trend of sea-level rise is shown by the red dotted line [Holgate et al., 2013, PSMSL, 2017].

Weather records are taken from the station at Valley. The local rainfall shows clear seasonality (Figure 1.11), with a large spike between November 2015 and January 2016. The rainfall during

December 2015 coincides with the occurrence of storms Desmond and Eva, which resulted in heavy rainfall at the beginning and end of the month respectively.

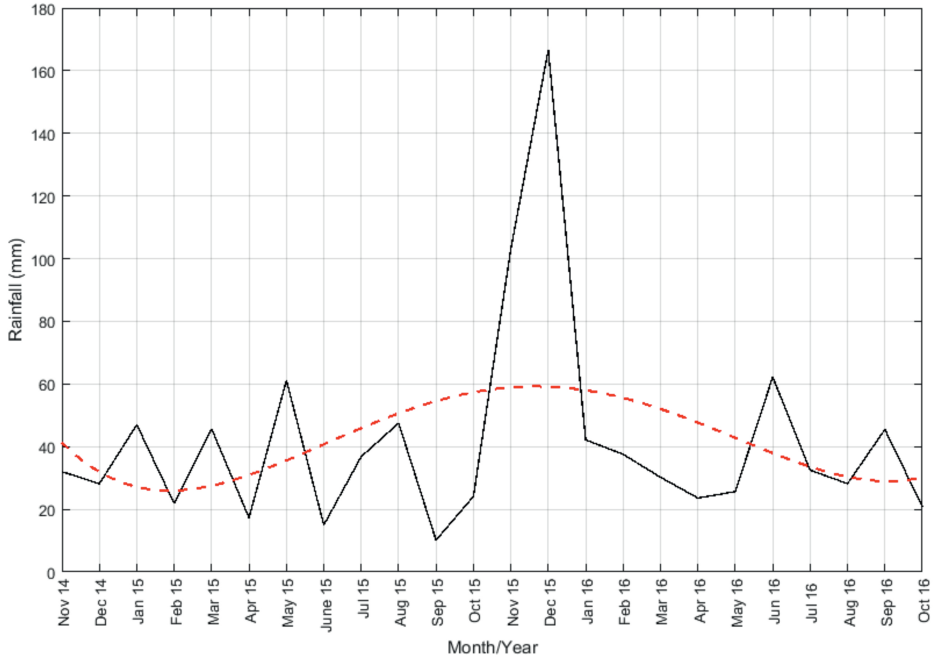

FIGURE 1.11: Monthly mean rainfall data taken from the Valley weather station during the period of water-level observations at Rhoscolyn. Dashed red line shows the overall trend, suggesting seasonality. However, the record is too short to be certain of a seasonal trend.

1.5.2 Abermawr

Abermawr (SM 883346) is located in south Wales on the west coast of Pembrokeshire (Figure 1.12). The site is a remote beach, comprised of a sandy foreshore and an upper sandy gravel barrier. During low tide, freshwater channels form along the lower part of the barrier, parallel to the shoreline. These channels are caused by the discharge of a subterranean estuary, flowing from the freshwater marsh, under the barrier and into the sea. Storm waves expose a drowned forest on the foreshore, when a sufficient quantity of sand is displaced offshore. This usually occurs during the winter months and is once again fully concealed with sand by late spring.

The back-barrier system is a freshwater peat marsh, fully enclosed by the gravel barrier running parallel to the shoreline. The marsh extends approximately 0.45km inland and covers an area of around 0.1km^2. The vegetation is dominated by *Phragmites* extending roughly 0.25km inland before giving way to an alder forest in the back marsh. There is a drowned forest on the foreshore which is only occasionally exposed as the result of significant storm events. The preserved trees appear to be alder, as in the modern back marsh. The drowned forest provides evidence of the transgressive nature of the barrier.

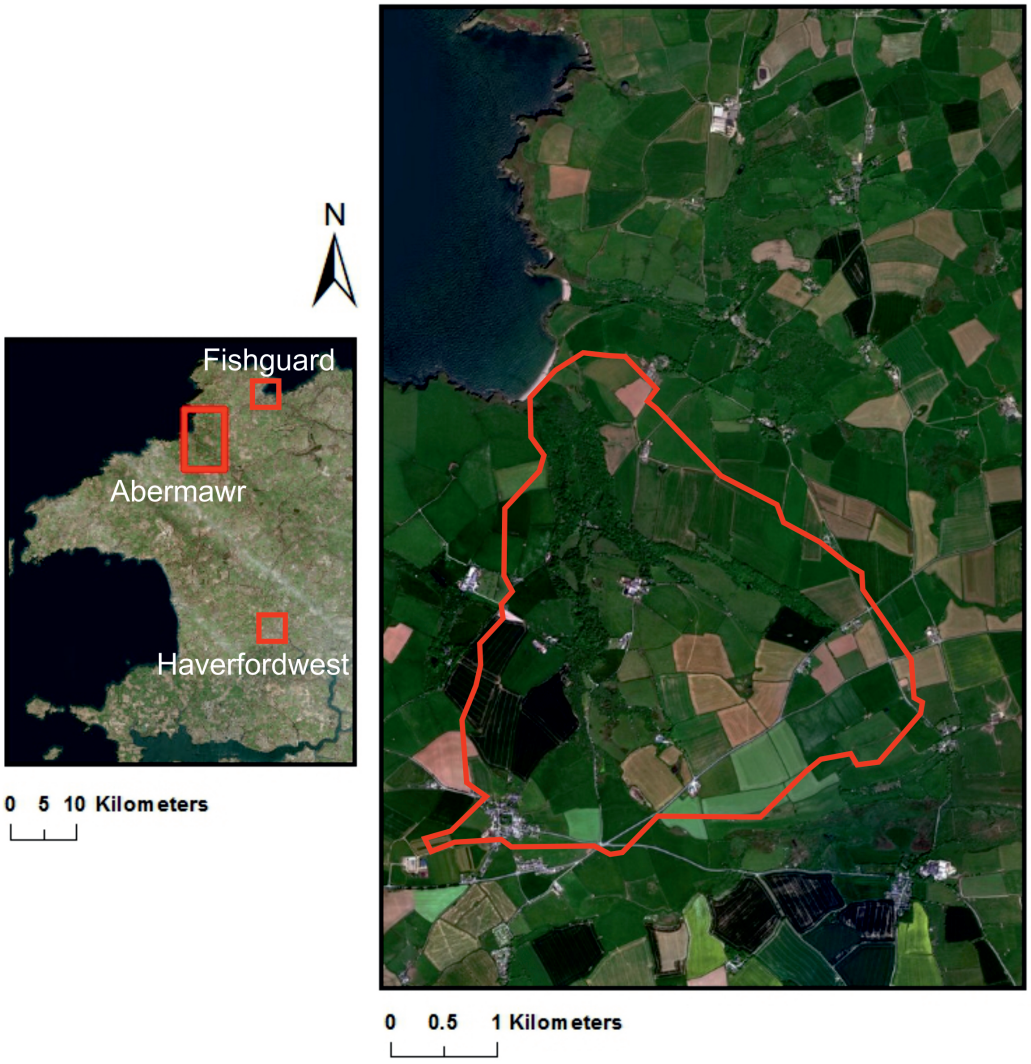

FIGURE 1.12: Location of the Abermawr site. Also shown are the locations of tide gauge (Fishguard) and weather station (Haverfordwest). The catchment area for the site is also outlined.

As with Rhoscolyn marsh, the catchment area for Abermawr is small (Figure 1.12). There is a small river feeding into the marsh and so the total net annual average flow accumulation is an order of magnitude larger. On average the net annual flow is 3,175,796 m^3/yr.

Abermawr, along with the broader Pembrokeshire region, was investigated for archaeological remains as part of the archaeological monitoring of the intertidal and coastal zone report for Pembrokeshire, undertaken in 2003 [Crane, 2004]. Flints and flint fragments were recovered from the pasture land to the north-east and further finds were made in the exposed drowned forest. Two radiocarbon dates are presented in the report, from peat dated from the submerged forest. The location of the dates is unclear as they were obtained from one of three archaeological pits located SM8820834532, SM8822534554 or SM8825034584. The two dates are classified as an older lower peat and a younger upper peat. They are not suitable for sea-level reconstructions, due to the imprecise nature of their location and elevation. The upper peat was dated is 4500 ^{14}C year ± 60 BP and the lower peat dated 7640 ^{14}C year ± 150 BP.

The Abermawr back-barrier system overlies upper Cambrian and Ordovician rocks comprising the Lingula Flangs and Ogof Hen formations. These consist of the sandstone and mudstone of the Lingula Flags formation and the Mudstone of the Ogof Hen formation [BGS, 2016a]. The surface geology is dominated by fluvial and glaciofluvial deposits, comprising of sand, gravel and glacial till [BGS, 2016b]. The glacial till deposits were located under the freshwater peat during this work. The area is subjected to high erosion, with the cliff eroding at a rate of c. 0.5 m/y [Duigan et al., 2014].

Tidal data are taken from the nearby tide-gauge of Fishguard [Holgate et al., 2013]. The highest astronomical tide is 3.06 m OD and the lowest astronomical tide -2.24 m OD. Tidal range during neaps is 1.56 m, with mean high water being 1.12 m OD and mean low water -0.44 m OD. The range is much greater during spring tides, with a range of 4.01 m. During the mean high springs water level is 2.4 m OD and mean low water is -1.61 m OD. Fishguard tide-gauge records cover a period between 1974 and 2015 (Figure 1.13) and shows a gradual increase of 4.64mm per year through this period.

Rainfall data was collected from Haverford West (Figure 1.12) and shows a small seasonal signal (Figure 1.14), with a large spike between November 2015 and January 2016. The rainfall during December 2015 coincides with the occurrence of storms Desmond and Eva, which resulted in heavy rainfall at the beginning and end of the month respectively. The large peak between November 2016 and January 2017 roughly coincides with the occurrence of storm Barbara around this time.

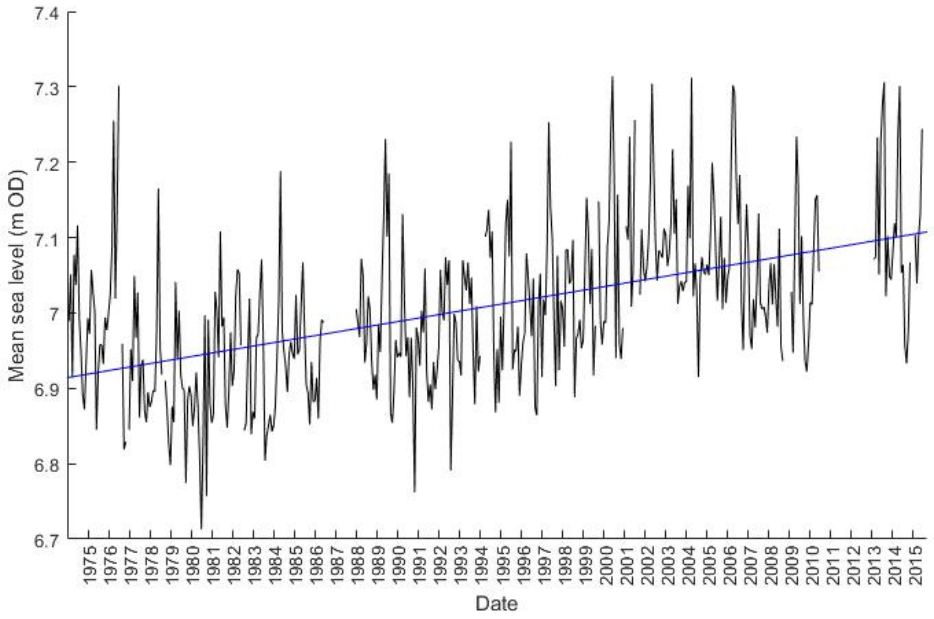

FIGURE 1.13: The tide gauge record for Fishguard 1938-2015. Sea-level heights are revised to a local reference (RLR) to correct for datum changes through time. The linear trend of sea-level rise is shown by the blue line [Holgate et al., 2013, PSMSL, 2017].

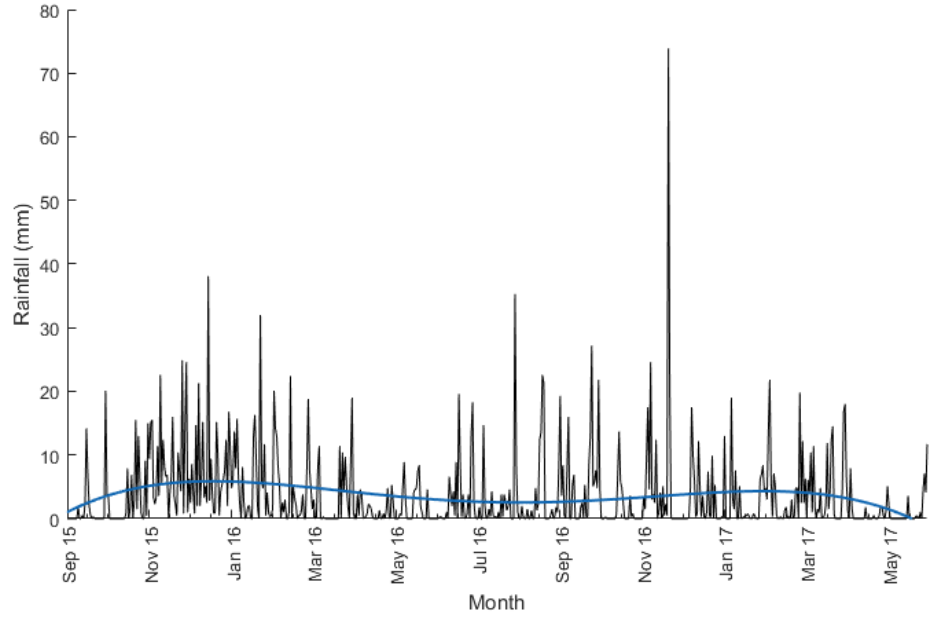

FIGURE 1.14: Rainfall data taken from the Haverford West weather station, covering the period of this study. The blue trend line show seasonality, with rainfall highs during the winter months.

1.6 Aims and Objectives

The aim of this work is to establish Holocene RSL histories for Anglesey and western Pembrokeshire. In conjunction with previously published SLIPs, the new data will be used to assess current GIA models. This is achieved using novel modelling methods alongside traditional sampling and monitoring techniques.

A secondary aim of this work is to evaluate whether SLIPs can be obtained from both sand and sandy gravel barrier systems. The connectivity between the groundwater and sea level is controlled by permeability and as such it may vary between the two systems. The monitoring and modelling of the groundwater and sea-level variations will enable a better understanding of the differences between these systems.

In order to achieve the aims of this project, the following objectives are undertaken:

1) document the lithostratigraphy of the Abermawr and Rhoscolyn marshlands from cores using hand coring methods;

2) assess the effects of seasonality and tidal oscillations on the groundwater regime of the Abermawr and Rhoscolyn marshlands, via groundwater monitoring wells;

3) understand the conditions that make back-barrier peat suitable for sea-level reconstruction, utilising groundwater modelling.

1.7 Synopsis

There is disagreement regarding the history of Holocene RSL change in north Wales, with some GIA models predicting a mid Holocene highstand whilst others do not. There is also a lack of sea-level data for north Wales, with no data younger than 4000 ka BP available and a paucity of Holocene sea-level data for south Wales. Pembrokeshire only has a single data point available to constrain GIA models. Gehrels and Anderson [2014] demonstrated that coastal back-barrier freshwater marshes are suitable environments for reconstructing Holocene RSL histories. This research builds upon their work to exploit previously ignored environments to produce new sea-level data. These data will be collected from Rhoscolyn in Anglesey and Abermawr in Pembrokeshire and fill a vital gap in the SLIP database. They will contribute to the resolution of current debates surrounding the mid Holocene highstand. As Rhoscolyn is a sand barrier system and Abermawr is a gravel barrier system, this work will also compare the two systems in terms of the suitability for sea-level reconstructions

Chapter 2

Previous Investigations

2.1 Introduction

This chapter reviews four areas of coastal and sea-level science that underpin this thesis. First, glacial isostatic adjustment (GIA) models are reviewed as they form the basis for sea-level predictions in the UK. Sea-level data provide the constraints for the GIA models, and therefore, second, the current state of the sea-level database for Wales is reviewed. Third, this work reviews coastal back-barrier freshwater evolution to assess the suitability of these marshes as sea-level archives. Finally, a review of coastal groundwater is presented as the methodology used to reconstruct past sea level, in this work, relies on an understanding of the link between a tidally oscillating ocean and groundwater levels in the back-barrier system.

2.2 Coastal Back-barrier Freshwater Marshes

Coastal barrier systems are dynamic depositional environments of great importance to sea-level reconstructions, as Holocene sea-level rise has resulted in the formation of a sedimentary archive from which sea-level histories can be reconstructed [Kraft and Chrzastowski, 1985]. This study depends on an understanding of how the shoreline retreats horizontally under conditions of rising sea level.

Schwartz [1967] demonstrated the validity of Bruun Theory with regards to the response of shore erosion to RSL rise. Since then, there has been a wealth of literature on the subject i.e [Bruun, 1988, FitzGerald et al., 2008, Forbes et al., 1995, Jennings et al., 1998, Orford et al., 2002] and advances made in the understanding of barrier response to RSL rise. The precise nature of this response varies between individual barriers, but the geological record shows that barrier systems have evolved dramatically in response to Holocene sea-level rise [FitzGerald et al., 2008].

Kraft and Chrzastowski [1985] present a number of processes which can cause coastal barrier systems to vary, both temporally and geographically, across the vertical and lateral planes. Eustatic sea-level change is only one of several controls on the transgressive/regressive nature of a barrier, but it should be considered as majorly significant. In fact, Kraft and Chrzastowski [1985] consider it to be of such significance to Holocene coastal barrier evolution as to require particular attention.

Of interest to this study is the evolution of bay-blocking barriers [Otvos, 2012], discussed as baymouth barriers by Kraft and Chrzastowski [1985]. These barriers run parallel to the shoreline and are anchored to the mainland at both ends. They are typically the result of wave action and form a distinct barrier between the mainland and open marine conditions. Towards the mainland, the barrier system may be comprised of lagoon, marsh and swamp zonation. The barrier itself is often elevated to such an extent as to allow for the growth of vegetation.

Kraft and Chrzastowski [1985] discuss the difficulties in fully understanding the origin and formation of a transgressive bay-blocking barrier. It is probable that they formed offshore on the continental shelf and have since transgressed as a result of Holocene sea-level rise. In areas with a neutral or negative tectonic influence, transgression is the normal coastal movement. However, small changes in the rate of sea-level rise can result in periods of regression. As such, for areas which are dominated by transgressive barrier systems, it is not unusual to find evidence of regressive periods.

The position of the leading edge of the Holocene transgression is of great importance to sea-level studies. Kraft and Chrzastowski [1985] present a schematic of a lagoon-barrier system along the Delaware coast (Figure 2.1). This sheltered lagoon remains marginal marine as inlets and ebayments allow for the ocean to influence the back-barrier system. It is significant that the basal unit associated with the Holocene transgression is not formed along the coastline, but rather at the landwards edge of the back-barrier system.

Perhaps the most influential conceptual model of shoreline response to rising sea level is presented by Bruun [1962]. One of the key features of this model is that so long as there is plentiful sediment supply, the landwards movement of the shoreline is a function of the slope of the profile and sea level rise. This can be calculated from:

$$R = \frac{1}{tan\theta} S \tag{2.1}$$

where R is the horizontal recession of the shoreline, S is the increase in sea level and $tan\theta$ is the average slope of the near shore. Although later work, such as Davidson-Arnott [2005] (Figure 2.2), has refined elements of this work with regards to the direction of sediment transport, the calculation for horizontal shoreline recession has remained unaltered.

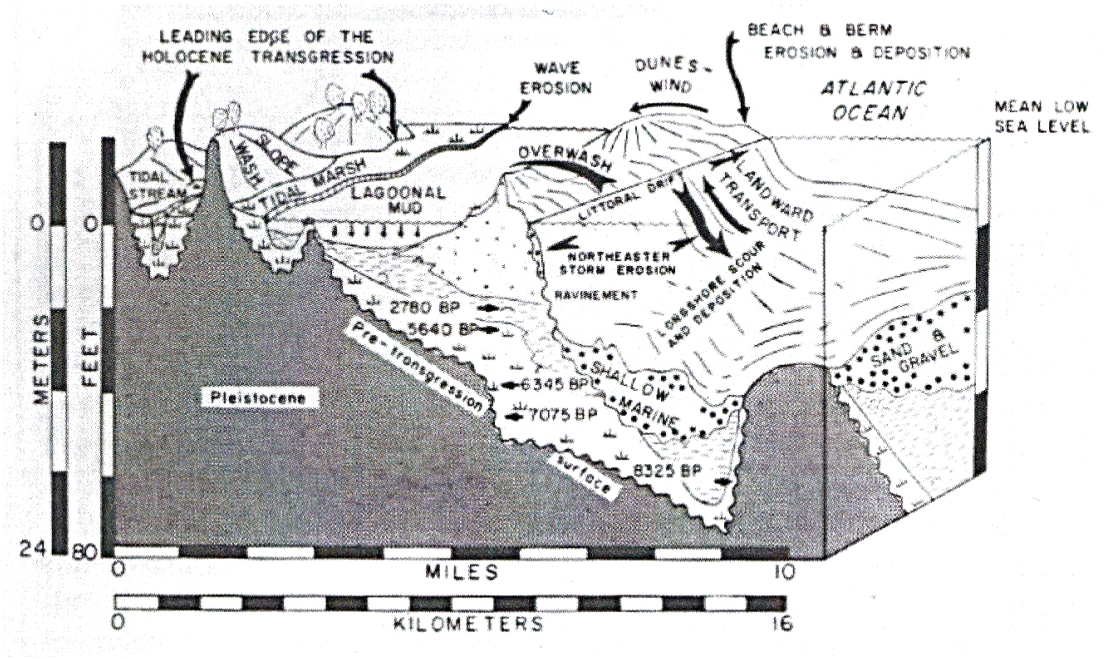

FIGURE 2.1: A transgressive lagoon-barrier system from the coast of Delaware, showing the various factors influencing the system and the location of the leading edge of the Holocene transgression [Kraft and Chrzastowski, 1985].

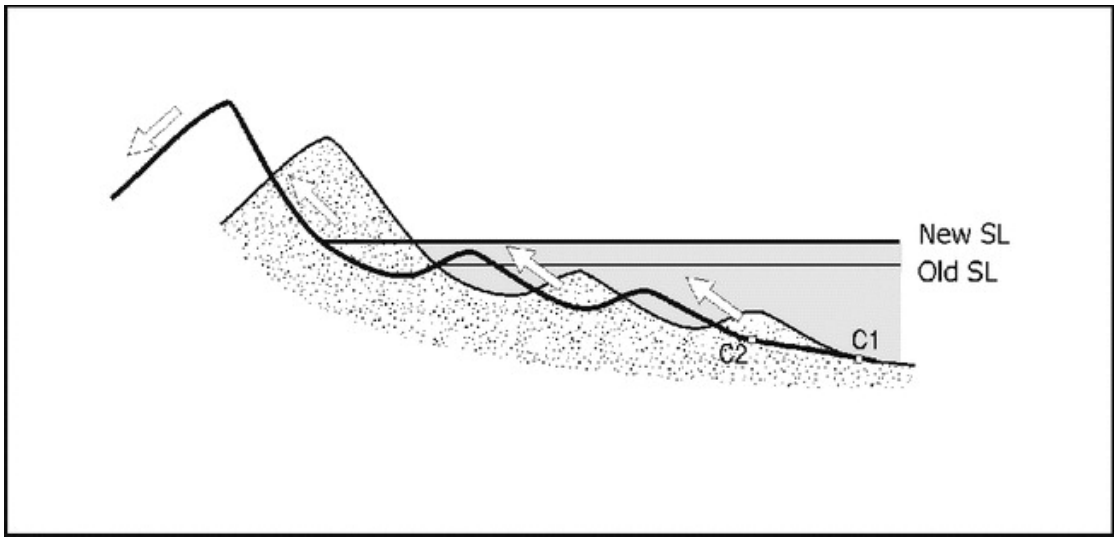

FIGURE 2.2: The landwards migration of a sand barrier under rising relative sea level. C1 shows the original position of the barrier and C2 the new position following sea-level rise [Davidson-Arnott, 2005].

The work by Bruun [1962] and studies which followed, for example Davidson-Arnott [2005], Schwartz [1967] were mainly concerned with the transgression of sand barriers. When considering barrier responses to rising sea level, it is important to note that the lithofacies and morphodynamic processes of gravel coastlines will not be the same as sandy coastlines [Orford et al., 2002]. Despite these differences, both have been shown to respond to rising RSL by migrating onshore [Davidson-Arnott, 2005, Orford et al., 2002]. Gravel coastlines exist where there a supply of gravel from locally eroding shorelines, although such coastlines may still contain large volumes of sand [Orford et al., 2002]. Here gravel barriers form from coarse-clastic sediment and are important features in the study of Quaternary sea level [Orford et al., 1991]. Orford et al. [1991] details the three phases of gravel barrier development, the initiation phase, the established phase and the breakdown phase.

During the initiation phase, gravel barriers originally form as drift-aligned barriers, when there is a surplus of sediment supply, but will become swash-aligned when sediment supply is reduced (Figure 2.3) [Orford et al., 1991, 2002]. The availability of sediment is mainly controlled by RSL change, with a rise in RSL leading to a greater supply of sediment due to erosion. It is possible that under rapid RSL rise barriers can become prograding, but with a constant supply of sediment they are more likely to be transgressive [Orford et al., 2002]. When the sediment supply is large enough, tidal inlets do not form and there is the possibility of the formation of a carr in the back barrier [Jennings et al., 1998]. During the established phase drift-aligned barriers extend and thicken, whereas swash-aligned barriers move landwards [Orford et al., 1991]. Landward migration is driven by rollover at a rate controlled by the rate of RSL rise, the degree of storminess, the geometry of the barrier and the position of the headlands [Orford et al., 1991]. If sediment supply becomes insufficient for barrier growth, then the barrier will enter the breakdown phase. Drift-aligned barriers will eventually become segmented and swash-aligned barriers continue to migrate landwards, which may lead to the barrier becoming stretched and eventually breaching [Orford et al., 1991].

2.3 Coastal Groundwater

This study aims to show that groundwater levels at the chosen sites are ultimately controlled by tidal amplitude at the coast and as such are suitable archives of sea-level data. Therefore, it is important to fully understand the relationship between coastal groundwater and the associated tidal influence upon the aquifer. Understanding the relationship between tidal oscillations and groundwater levels is complicated by the influence of both landwards and seawards factors. Vallejos et al. [2015] consider the key drivers to be tidal oscillations, wave action, variations in atmospheric pressure and rainfall recharge events.

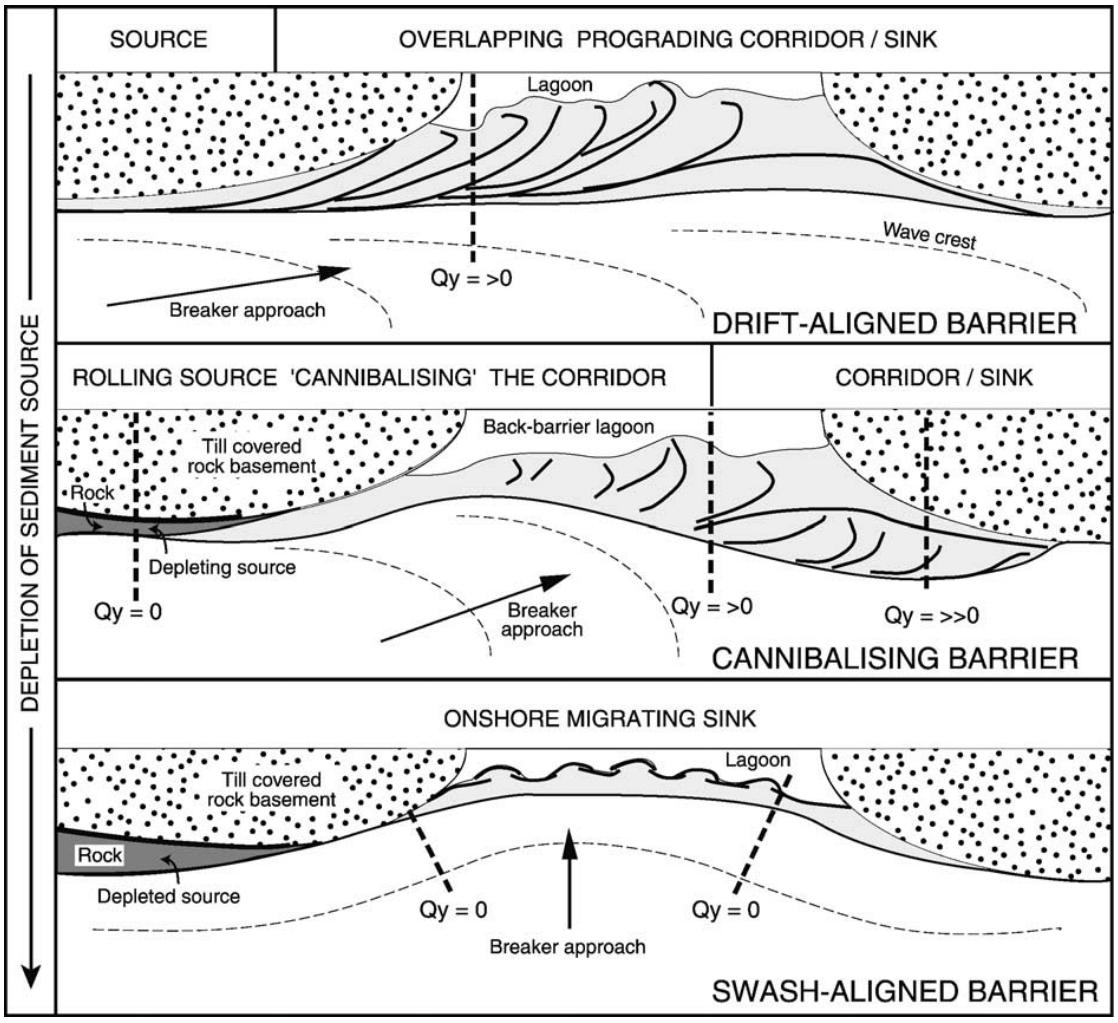

FIGURE 2.3: The stages of gravel barrier development, from drift-aligned under conditions of sediment surplus (Qy = >0), to swash aligned as sediment supply is reduced (Qy = 0). When sediment is depleted, the drift-aligned barrier is cannibalised before transforming to a swash-aligned barrier [Orford et al., 2002].

Where fresh and saline water meet, mixing occurs. The zone of mixing between coastal groundwater and oceans was described as a subterranean estuary (Figure 2.4) by Moore [1999], who likened them to surface estuaries in the way they interact with the ocean, including the effects of tidal forcing and sea-level change. This hydrological connection allows for tidal oscillations to change groundwater levels, this is a component of tidal forcing [Xun et al., 2015]. Tidal oscillations are a significant part of tidal forcing and propagate landwards in the groundwater. This landwards propagation is out of phase with the tidal oscillations and the amplitude is attenuated [Robinson et al., 2007]. Robinson et al. [2007] demonstrate that increased tidal forcing results in an increase in the distance that the oscillations are propagated through the groundwater.

Tidal oscillations have an important influence on the development of a subterranean estuary, especially in macro-tidal barrier systems with a moderate wave climate where groundwater

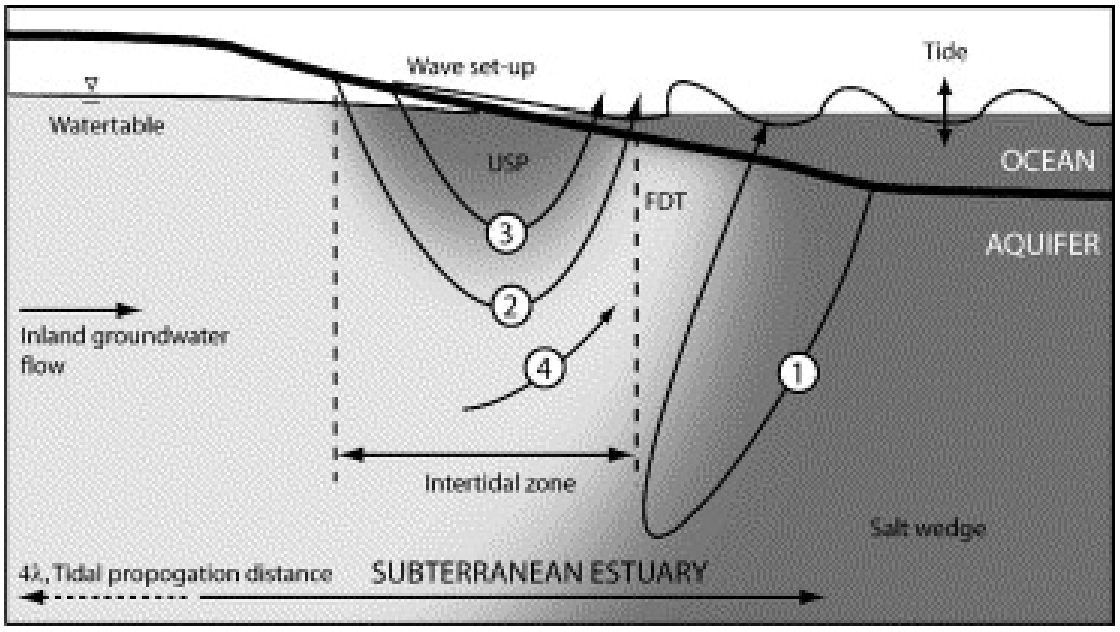

FIGURE 2.4: Subterranean estuary showing tidally induced features. Clear is the upper saline plume (USP) and a freshwater discharge tube (FDT). Tidal propagation distance, and as such the landward extent of the subterranean estuary, is controlled by the extent of tidal influence on the coastal groundwater [Robinson et al., 2007].

fluctuates with tidal changes. In such systems an upper saline plume and freshwater discharge tube will develop [Anderson Jr., 2015]. Gehrels and Anderson [2014] used the US Geological Survey's coupled groundwater flow - solute/heat transport finite-element code SUTRA (Saturated-Unsaturated TRAnsport) to model the relationship between groundwater within a freshwater coastal back-barrier marsh and tidal oscillations. The SUTRA model was set up as a shore-perpendicular cross section which extended 75m offshore and 100m behind a gravel barrier, into the freshwater marsh. A simplified hydro-stratigraphy was used to establish a two layer aquifer system of peat and gravel.

The amplitude of the oscillations in the groundwater is smaller than the tidal oscillations that cause them and they decrease exponentially as they travel landwards. This decrease in amplitude is termed tidal efficiency and combined with the fact that the time at which they occur lags tidal movement in a linear relationship, can be utilised to infer the characteristics of a coastal aquifer [Xun et al., 2015].

Identifying tidal oscillations within groundwater levels can be problematic as there can be several signals compounded within groundwater fluctuations. Geng and Boufadel [2017] utilised spectral analyses to examine groundwater fluctuations in the time-frequency domain. This technique was able to identify a range of tidal influences (diurnal, semidiurnal, terdiurnal and quarterdiurnal) on the groundwater level. Gehrels and Anderson [2014] also demonstrated the influence of tidal forcing on groundwater levels, with spectral analysis.

2.4 Freshwater peat formation as a result of sea-level rise

When peat-lands form and expand as a result of the rising elevation of groundwater, it is referred to as paludification, a process which is often accompanied by forest retreat [CRAWFORD et al., 2003]. This process is so ubiquitous in northern Europe, that it is mostly considered an accepted natural process. The formation of peat via paludification, as opposed to terrestrialisation (the infilling of a water body by organic material) was first proposed by Canjander [1913] and is now accepted as one of two major pathways of peat formation.

Paludification can be initiated by reducing the permeability of the ground. As discussed, rising sea levels during the Holocene have been responsible for landward migration of offshore barriers. These barriers can reduce permeability of the land and result in increased wetness of the soil. This provides the first stage of peat formation via paludification.

Canjander [1913] proposed that contiguous paludification could occur if the groundwater within a landscape became influenced by an adjoining area. Rising sea levels result in the adjoining landscape becoming wetter and via the groundwater processes described above, this results in higher water levels in the back-barrier area. This is not an unusual process for the United Kingdom, areas such as The Wash, the Somerset Levels, Thorne and Hatfield Moors and the Norfolk Broads have had their formation linked to rising Holocene sea levels.

Once peatland growth is initiated, the elevated groundwater levels have an effect on the adjacent land. Peatlands can expand horizontally and vertically via the process of paludification [Wheeler and Shaw, 1995], a process that is often accompanied by the replacement of forests with plants suitable to wetter environments [CRAWFORD et al., 2003].

This is clear at both of the sites in the study. The stratigraphy shows a clear transition between forested carr to a *phragmites* reed bed. The current vegetation zonation also supports this at both sites, as the forested carr is still present at the most landward section of the marsh and also outcrops along the beach. As such, it is reasonable to expect both formation and expansion of peat to have been driven by rising Holocene sea level.

2.5 Post-glacial Sea-level Data for North Wales

2.5.1 The current database

All of the published sea-level data within the north Wales database [Shennan et al., 2018] were collected from the north coast and the Isle of Anglesey and include 24 SLIPs, of which 5 are limiting points (Table A.1). This study incorporates the entire database for this region, along with corrections to error and indicative meanings that have been refined over the many iterations

of the database. The data cover the majority of the north Wales coastline, from Rhyl in the east to Malltraeth in the west. The period covered by the data spans a period between c.11,000 cal yr BP and c.4500 yr cal BP. The lack of data in the last 4500 years is addressed in this study.

The Holocene sea-level data for north Wales show a history of a rapid rise during the early Holocene followed by a slower rise during the mid Holocene, before stabilising during the late Holocene. (Figure 2.5). The existing data shows a rise of c. 21m at a rate of 5.8 mm/y, between c. 11000 and 7300 cal years BP. The rate reduces to 1.0 mm/y and shows a total rise of c. 2m between c. 7300 and 5500 cal years BP. Sea-level change then stabilises around this time, with the data showing a negligible fall of c. 1m between c. 5500 to 4500 cal years BP, at a rate of 0.75 mm/y.

Compared to the data, the model of Bradley et al. [2011] over predicts sea-level rise during the early Holocene, showing a c. 25m rise at a rate of 6.5 mm/y for the same period. The mid Holocene data is in agreement with the model, which predicts a c. 2m rise at rate of 1.1 mm/y. The lack of data for the late Holocene makes comparison with the model difficult, with the model showing a negligible rise at a rate of 0.3 mm/y for the same period.

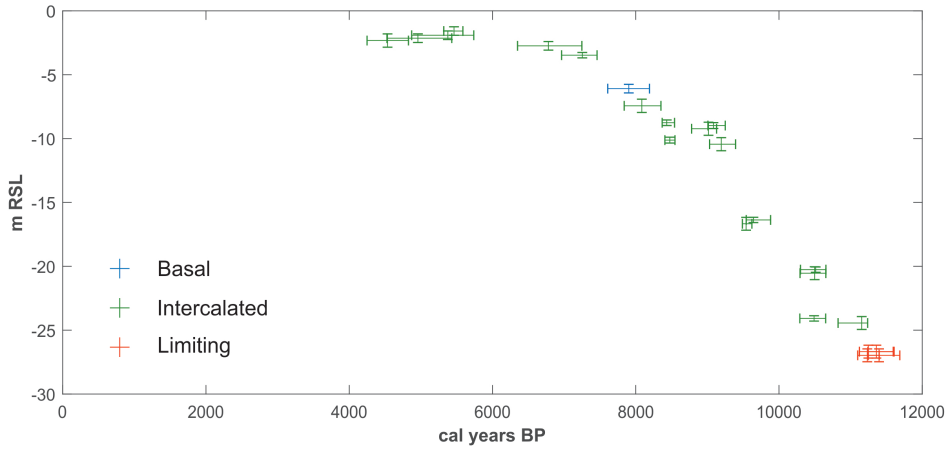

FIGURE 2.5: The current available data for north Wales, calibrated using CALIB 5.0. Note the lack of data for the late Holocene. Vertical and horizontal error bars represent errors in elevation and age respectively.

2.5.2 Previous investigations

Exposed peat beds in Rhyl were investigated by Bibby [1940]. The exposed beds, which were situated on the shoreline landwards against the sea wall, had traditionally been classified as "upper forest" and "lower forest" beds. Landward coring on the adjacent golf course revealed a ca. 1.8m silt layer separating two distinct peat beds. Bedlington [1994] states that work by

Tooley (unpublished) produced a date (Hv4348) of 4725 ± 65 ^{14}C yr BP from the peat beds at Rhyl (SJ0310.8261).

Harkness and Wilson [1974] produced a further date (SRR-61), from Llandudno station (SH7754.8191), of 7635 ± 52 ^{14}C yr BP. The peat bed was present at a depth between -5.21 m OD to -4.16 m OD. The peat was deposited on top of 3.24m of estuarine clay, which was underlain by Irish Sea boulder clay. Covering the peat bed were estuarine clay, beach deposits and blown sand.

These data are also reported in Heyworth and Kidson [1982] and used to produce a sea-level curve for north Wales. This early work shows a rapid sea-level rise in north Wales from c.8000 ^{14}C yr BP, slowing down in the late Holocene. In total the curve shows a rise of c.9 m over a period of c.4000 years between c. 8000 and 4000 ^{14}C yr BP. The date from Rhyl beach was also accepted in reviews by Bedlington [1994] and Roberts [2006]. Roberts et al. [2011] highlight inadequacies in the defined altitude, a lack of palaeoenvironmental context and a need for a large compression correction with regards to the Llandudno Station data and classified this point as a limiting index point. However, these concerns have been addressed over time and is included in the current database as an intercalated index point.

Bedlington [1994] presented seven new SLIPs for north Wales, utilising a combined lithostratigraphic and biostratigraphic approach, alongside radiocarbon dating. These are integrated into existing data to produce a time-altitude sea-level curve. The curve suggests that north Wales experienced rapid sea-level rise between early and middle Holocene. The rate between 8000-7000 cal yr BP was greater than 7mm/yr, reducing to ca. 3.5mm/yr between 7000-6000 cal yr BP.

Two cores taken at Hendre Fawr (SH9660.7712) produced 4 acceptable SLIPs. A date of 4345 ±145 ^{14}C yr BP (HV17810) was obtained from +1.87 m OD. This regressive overlap was interpreted, from the pollen assemblage, as being formed in a salt-marsh environment. At +1.7 m OD a transgressive overlap was dated at 4685 ±175 ^{14}C yr BP (HV17811) and interpreted as an upper marsh environment form the biostratigraphy. A further regressive overlap was dated at 5935 ±190 ^{14}C yr BP (HV17812) at +1.25 m OD and interpreted as deposited at MHWS. Bedlington [1994] rejects a date of 5530 ±385 ^{14}C yr BP (HV17813) at -0.93 m OD, due to the large age error, despite having good indicative meaning. A final date of 7080 ±155 ^{14}C yr BP (HV17814) is obtained from -2.49 m OD. This is taken from basal peat and is interpreted as the start of a transition from a terrestrial environment through to a lower marsh environment.

Two cores from Malltraeth Marsh (SH4735.7445) produced 2 acceptable SLIPs. A date of 4035 ±100 BP (HV17820) was obtained from +1.00 m OD. The date is obtained from the base of woody peat with light grey clay underlying and is interpreted as a regressive overlap. Although there are no pollen or diatoms preserved within this core, Bedlington [1994] states that a proximal core obtained by Tooley (unpublished) allowed for pollen and diatom analyses and the point is interpreted as being formed at MHWS. A date of 7255 ±130 BP (HV17819) was obtained from

-4.11 m OD from organic material close to the base of the core along with a date of 7435 ±185 BP at -3.96 m OD. These dates are age inverted and cannot both be accepted. Bedlington [1994] accepts the youngest date, based on the pollen assemblage data.

A core at Morfa Penrhyn (SH8218.8079) produced an acceptable SLIP. A date of 6335 ±115 BP (HV 17815) was obtained from +0.28 m OD. The diatom and pollen analyses suggest a regressive overlap.

Roberts [2006] combined a micropalaeontological, sedimentological and geophysical approach, in conjunction with radiocarbon dating, to collect sea-level data from the Menai Strait. Three cores were collected and ten new SLIPs were added to the database. These new data are used, in combination with existing data, to produce a sea-level curve for north Wales. The majority of sea-level rise is predicted to occur earlier in the Holocene than the curves presented by Heyworth and Kidson [1982] and Bedlington [1994]. Three distinct periods are identifiable. Between 11 kyr and 9 kyr ago sea level rose ca. 18m at a rate of 6mm per year. This is followed by a slower rate between 9 kyr and 6 kyr ago, when sea level rose ca. 8m at a rate of 3mm per year. From 6 kyr onwards, the curve shows a steady increase until modern day.

Core CJSC 1 [Roberts, 2006] was taken from the sea floor of the Menai Strait (SH5830.7365) at a sea-bed depth of -4.12m OD, to a depth of -35.42m OD. Between -20.84m OD and -20.66m OD a fibrous peat was deposited on a sandy silt and overlain by a laminated silty clay. A dated sample from the organics at -20.84m OD produced a date of 9714 ±49 ^{14}C yr BP (SUERC-2492) and a further sample from -20.66m OD produced a date of 9296 ±53 BP (SUERC-2491). Although the pollen evidence underestimates the SUERC-2492 date by around 800 calibrated years, both dates are accepted into the database as there is no evidence of contamination by allochthonous carbon.

Core CJSC 2 was taken from the sea floor of the Menai Strait (SH5975.7465) at a sea-bed depth of -7.51 m OD, to a depth of -32.01 m OD. Between -16.94m OD and -16.85m OD a fibrous organic material was deposited on a laminated silt and overlain by a laminated fine grained silty clay. A dated sample from the organics at -16.94m OD produced a date of 9301 ±54 ^{14}C yr BP (SUERC-2503) and a further sample from -16.87m OD produced a date of 9308 ±45 ^{14}C yr BP (SUERC-2502). Although the pollen data are limited, they do support the ^{14}C date and both are accepted into the database.

Between -13.08m OD and -12.97m OD an organic sediment was deposited on a silty clay with large quantities of organic detritus and overlain by clay. A dated sample from the organics at -13.07m OD produced a date of 8581 ±40 ^{14}C yr BP (SUERC-2498) and a further sample from -12.97m OD produced a date of 8698 ±43 ^{14}C yr BP (SUERC2497). Although Roberts [2006] acknowledges some difficulty in inferring the indicative meaning from the samples, the dates are accepted into the database.

Core CJSC 3 was taken from inter-tidal mudflats on the Menai Strait (SH5845.7335) at a sea-bed depth of -3.05m OD, to a depth of -9.05m OD. Between -7.89m OD and -7.77m OD fibrous material with a large organic content was deposited on a silty clay and overlain by a laminated silty clay containing organic material. A dated sample from the organics at -7.89m OD produced a date of 8227 ±40 ^{14}C yr BP (SUERC-2512) and a further sample from -7.77m OD produced a date of 7689 ±38 ^{14}C yr BP (SUERC-2511). The date of 8227 ±40 BP corresponds well with the pollen record and is included in the database. Roberts [2006] acknowledges that the date of 7689 ±38 BP is ca. 400 calibrated years younger than the age suggested by the pollen record and by dates obtained from the surrounding material. Roberts [2006] also acknowledges a limited degree of accuracy with regards to interpreting the indicative meaning for this sample. Although both dates were accepted by Roberts (2006), only the date of 8227 ±40 is accepted into this database due to inaccuracies in dating and indicative meaning associated with the younger sample. A correction to the inferred MSL from SUERC-2498 is also made, due to what appears to be a transcription error. Roberts et al. [2011] calculates MSL from an original altitude of -6.84m OD rather than -7.89m OD, this is corrected within this database.

Between -6.69m OD and -6.64m OD a fibrous material with a large organic content was deposited on laminated silty clay and overlain by grey silty clay. A dated sample at -6.69m OD produced a date of 8084 ±41 ^{14}C yr BP (SUERC-2510) and a further sample from -6.64m OD produced a date of 8152 ±38 ^{14}C yr BP (SUERC-2509). SUERC-2510 is ca.800 calibrated years older than the age suggested by the pollen record and is age inverted when compared with SUERC-2509. SUERC-2509 is >1000 calibrated years older than suggested by the pollen record. Roberts [2006] acknowledges the discrepancies in the dates of these sample and they are accepted into the current database.

2.6 Post-glacial Sea-level Data for mid Wales

2.6.1 The current database

All of the sea-level data for mid Wales have been collected between Aberystwyth and Ynyslay and include 14 SLIPs (Table A.2). This study incorporates the entire database for the region as presented by Shennan et al. [2018], despite difficulties in tracing all of the SLIPs to the original studies. The period covered by the data spans a period between c.6700 cal yr BP and c.1100 cal yr BP.

The Holocene sea-level data for mid Wales show a history of a continual gradual rise from the mid to late Holocene (Figure 2.6), although there is a distinct slow down starting c. 4100 cal years BP. Between c. 6700 to 4100 cal years BP, sea-level rose c. 2m at a rate of around 9 mm/y.

This slowed to around 3 mm/y between c. 4100 to 1100 cal years BP, when sea-level rose c. 1m. There is a lack of data covering the early Holocene period.

For the period between c. 6700 to 4100 cal years BP, the GIA model presented by Bradley et al. [2011] over predicts the rate of sea-level rise by 4 mm/y, compared to the existing data. This is a difference of around c. 1m of total sea-level rise for this period. The model is a better fit for the data during the late Holocene. Between c. 4100 to 1100 cal years BP, the model over predicts the rate by 1 mm/y.

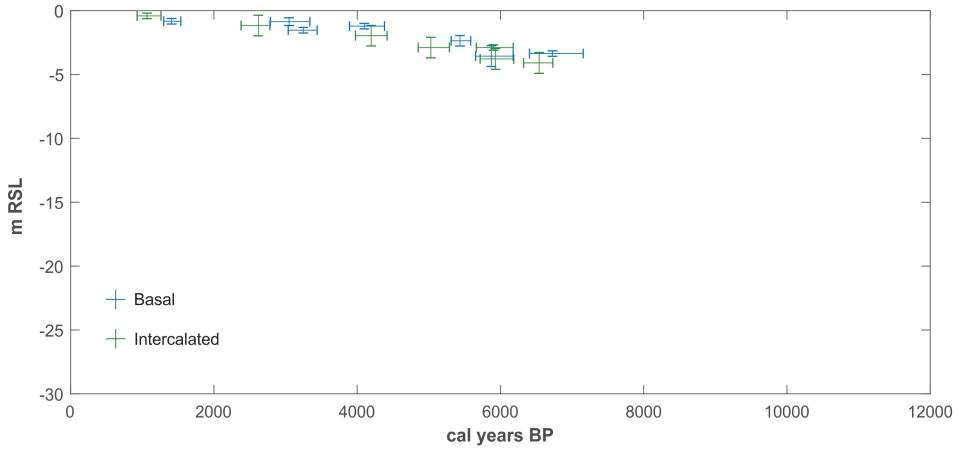

FIGURE 2.6: Mid Wales SLIP data, calibrated using CALIB 5.0. Note the lack of data for the mid to early Holocene. Age error is represented by horizontal bars and elevation error by vertical bars.

2.6.2 Previous investigations

SLIPs were obtained from Borth Bog which extends ca.5km between Aberystwyth and Ynyslas. The deposits consisted on fen, alder carr and forest beds, which are deposited on a salt marsh clay. Further SLIPs were obtained from a submerged forest present at Clarach Bay. These deposits are described in detail by Wilks [1977] and published by Heyworth and Kidson [1982].

Wilks [1977] presents data from a single core taken from Clarach Valley SN 5880 8300, borehole 1, showing a gradually rising water table and transition from forest to marsh. A date of 5740 ±80 ^{14}C yr BP (HAR301) was obtained from a depth of -1.51m OD and was interpreted as having formed during the freshwater to high marsh transition, supported by diatom analyses. This date was interpreted as relating to RSL of -4.09 ±0.82m. A further date of 5170 ±90 ^{14}C yr BP (HAR300) was obtained from a depth of -1.27m OD. Diatom analyses supported an interpretation of freshwater to high marsh transition. This was related to a RSL of -3.78 ±0.81m. A third date of 5130 ±100 ^{14}C yr BP (HAR299) was collected from the same core at a depth of -1.08m OD and interpreted as forming during the freshwater to high marsh transition. The

RSL associated with this date is taken as -3.56 ±0.82m. A fourth date of 4410 ±60 ^{14}C yr BP (HAR1576) was collected from a depth of -0.35m OD and once again interpreted as being formed during the freshwater to high marsh transition. The associated RSL is reported as -2.89 ± 0.80m. A fifth date of 2560 ±80 ^{14}C yr BP (HAR1575) was collected from a depth of 1.38m OD. Despite contradictory evidence with the pollen and diatom assemblages, it is interpreted as forming during the freshwater to high marsh transition and related to RSL of 1.16 ± 0.80m. A sixth date of 1140 ±80 ^{14}C yr BP (HAR1572) was collected from a depth of 1.93m OD. Wilks [1977] present many uncertainties around this sea level point and highlight landward barrier migration as a factor. Nevertheless, it is interpreted as forming in the high marsh at a RSL of -0.41 ± 0.22m.

Three SLIPs are presented by Wilks [1977] from a single core taken at Ynyslas (SN 6100 9300) and interpreted from stratigraphy, pollen and diatoms. A date of 5150 ±90 ^{14}C yr BP (HAR1020) was collected from -0.25m OD and interpreted as a high marsh environment. This is related to a RSL of -2.89 ± 0.22m. A second date of 4700 ±70 ^{14}C yr BP (HAR1019) was collected from 0.27m OD and interpreted as forming in a high marsh environment. The date was related to a RSL of 2.36 ± 0.41m. A third date of 3740 ± 10 ^{14}C yr BP (HAR1018) was collected from 1.12m OD and interpreted as being formed in newly developed, intermittent, high marsh environment. RSL was inferred to be 1.21 ± 0.22m.

Two further slips are presented by Wilks [1977] from a separate core at Ynyslas. A date of 3050 ±10 ^{14}C yr BP (HAR1017) was collected from 1.00m OD and interpreted as the start of a freshwater to high marsh transition. RSL was inferred to be -1.53 ± 0.22m. A second date of 1510 ± 70 ^{14}C yr BP (HAR1016) was collected from 1.80m OD and interpreted as forming in a high marsh environment. RSL is inferred as 0.83 ± 0.22m.

2.7 Post-glacial Sea-level Data for Pembrokeshire and Glamorgan

2.7.1 The current database

The published data for Pembrokeshire is combined with that of Glamorgan, to enable comparisons across a region with very similar predicted sea-level histories, which was predicted by the GIA model of Bradley et al. [2011]. This is based on the correlation matrix presented by Shennan et al. [2018], which shows a 0.999 correlation coefficient between the two regions. The database contains 1 SLIP for Pembrokeshire and 12 for Glamorgan, of which 3 are limiting points (Table A.3). The period covered by the database is between c. 10000 to 700 cal years BP. The lack of comparative data from Pembrokeshire is addressed in this study.

The data contained within the combined Pembrokeshire and Glamorgan database shows continual rise until c. 4000 cal years BP, when sea-level becomes stable (Figure 2.7). There are three distinct periods of RSL change. The most rapid rise occurs between c. 10000 to 6500 cal years BP, when sea-level rose c. 18m at a rate of 5.1 mm/y. The rate of change slowed between c. 6500 to 4000 cal years BP to a rise of 2.2 mm/y, with a total rise of c. 5.5m. From c. 4000 cal years BP to present day sea-level rise is low, showing a c. 2m rise at a rate of 0.5 mm/y. There is a distinct gap in the data connecting the mid and early Holocene, which is addressed in this study.

For the period 10000 to 6500 cal years BP, the GIA model for Pembrokeshire by Bradley et al. [2011], over predicts the rate of sea-level rise compared to the data. The model predicts a rise of c. 22m at a rate 6.1 mm/y, The mid Holocene prediction is a better fit, at 1.8 mm/y and a total rise of c. 4m. The model accurately predicts the almost flat sea-level rate for the late Holocene period between c. 4000 cal years BP to present day, at a rate of 0.6 mm/y and a total rise of c. 2.5m.

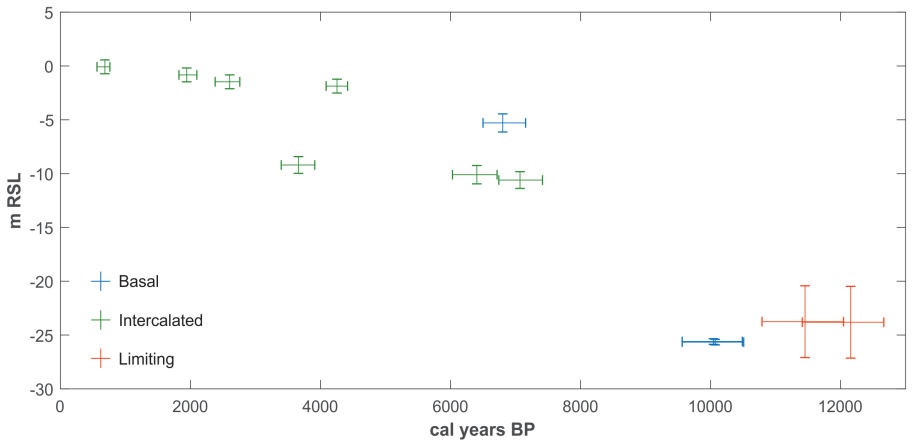

FIGURE 2.7: South Wales SLIP data, calibrated using CALIB 5.0. Gaps in the data exist between the early to mid Holocene and mid to late Holocene. Vertical and horizontal bars represent errors in elevation and age respectively.

2.7.2 Previous investigations

There is limited information available for the data presented by Heyworth and Kidson [1982]. This study relies on the details in the sea-level database presented by Shennan et al. [2018].There is a single sample collected from Pembroke Dock from a height of -2.00m OD and dated at 5960 ± 120 ^{14}C yr BP (Q530). It is interpreted as being formed at RSL -5.29 ± 0.84m.

3 dates were obtained from Margam for the Glamorgan database. A date of 3402 ± 108 ^{14}C yr BP (Q265) was collected from a height of -2.4m OD and interpreted as forming in the high marsh environment. This was related to a RSL of -9.20 ± 0.78m, which is not in keeping with the overall database, as the date appears to be too young for this interpretation. A further dare of 5605 ± 126 ^{14}C yr BP (Q274) was collected at a height of -3.1m OD and interpreted as forming at the freshwater to high marsh transition, when RSL was -10.10 ± 0.85m. The final date from Margam is 6184 ± 143 ^{14}C yr BP (Q275) from a sample obtained at a height of -3.2m OD. This was interpreted as forming when RSL was -10.60 ± 0.78m, in a high marsh environment.

A further 2 dates are incorporated into the Glamorgan database from Port Talbot. A date of 8970 ± 160 ^{14}C yr BP (Q663) was obtained from a height of -18.80 m OD and interpreted as forming in the high marsh environment, when RSL was -25.60 ± 0.26m. This is supported by a similar date of 8990 ± 170 ^{14}C yr BP (Q662), obtained from a height of -18.86m OD, also interpreted as forming in the high marsh environment when RSL was -25.66 ± 0.26m.

Edwards [2006] presents 4 dates from Stavel Hagar in the Glamorgan database. These are all based on a local foraminifera transfer function. A date of 1990 ± 50 ^{14}C yr BP (CAMS41310) was collected from a height of 3.30m OD and was formed when RSL was -0.83 ± 0.64m. A second date of 2540 ± 60 ^{14}C yr BP (CAMS41309) was collected from a height of 2.65m OD and interpreted as forming when RSL was -1.47 ± 0.64m. A third date of 3840 ± 60 ^{14}C yr BP (CAMS41308) was collected from 2.2m OD and related to RSL -1.87± 0.64m. The fourth date presented is 740 ± 50 ^{14}C yr BP (CAMS41307), collected from a height of 4.10m OD and forming when RSL was -0.08 ± 0.64m.

2.8 Glacial Isostatic Adjustment Models

The model presented by Lambeck [1993a] made significant advances for GIA modelling in general, and was the first one applied in detail to the British Isles. Modelling results showed variability in predicted post-glacial sea-level histories for Wales (Figure 2.8). The model was based around an Earth model with radial symmetry and the rheology of a Maxwell body, with viscosity changing with depth. A three layer Earth model was used, to model a lithosphere and a lower and upper mantle, with a lithospheric thickness of 100km. The GIA model included high resolution models for the British ice sheet and the Fennoscandian ice sheet as well as far-field ice models for the Laurentide, Barents-Kara and Antarctic ice sheets. Early results demonstrated large variations in sea-level change around the United Kingdom and the isostatic response being most sensitive to changes in upper mantle viscosity. The model used a time scale in radiocarbon years and ice retreat occurred between 13,000 ^{14}C yr BP and 9000 ^{14}C yr BP, by which time complete deglaciation had occurred. The Loch Lomond advance is not accounted for. During

the last glacial maximum (LGM) the British ice sheet joined with the Fennoscandian ice sheet over a limited area of the western North Sea and split around 16,000 ^{14}C yr BP.

Sea-level predictions from this model do not match the geological observations for sites within the boundaries of the former ice sheet and the centre of rebound is in the wrong location. Lambeck [1993a] gives several reasons for the discrepancies. There are uncertainties in the timing of maximum glaciation, which could have occurred earlier than 18,000 yr BP and when using 23,000 yr BP some of the discrepancy is removed. The maximum extent of glaciation may have been overestimated and the ice volumes could be too large.

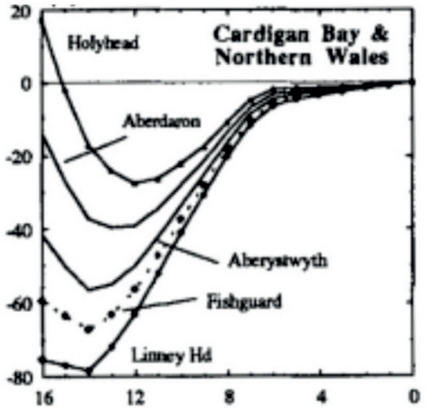

FIGURE 2.8: The non-uniformity of sea-level curves for Wales, demonstrating the need for more localised reconstructions. The Holyhead curve is located proximal to the Rhoscolyn site in this study and the Fishguard site is proximal to the Abermawr site [Lambeck, 1993a]. Note that the dates for these sea-level curves are presented as ^{14}C yr BP

Lambeck [1993b] refined the ice model to incorporate the Loch Lomand advance and to remove the North Sea ice coverage. The thickness of the British ice sheet was also reduced, giving a thickest point of ca. 1300m. Five curves are generated for Wales and the Aberystwyth curve is compared to synthetic SLIPs based around the exposed tree stump data from Borth Bog, Mid Wales (Figure 2.8). As such, this curve is not actually compared to geological data. Although the curve follows the general pattern of sea-level rise as shown by the synthetic SLIPs, it under predicts the height of sea level at all times.

Lambeck et al. [1996] further refined the model to test the impact of varying lithosphere thicknesses. The best fits with geological data were obtained with a maximum ice thickness of ca. 1500m, and a five layer earth model with a lithosphere thickness ca. 65km. Although the sea-level curve better fit the observed data, sea level was still under predicted at all times.

Peltier et al. [2002] were able to make use of an expanded sea-level index point database for the United Kingdom [Shennan and Horton, 2002], to assess the suitability of a thin lithosphere Earth model and a reduced thickness ice model. There are some key differences between the model presented by Peltier et al. [2002] and that of Lambeck [1993b], including a lithosphere thickness of 90km and the calibration of ^{14}C dates to calendar years.

Four outputs were produced for Wales (Figure 2.9) to represent the alternative modelling inputs. The areas further away from the centre of the ice sheet are less sensitive to variations in ice and lithosphere thickness. The north Wales curve is substantially more sensitive to changes in model parameters and the fit is much better for the thin ice and thin lithosphere model.

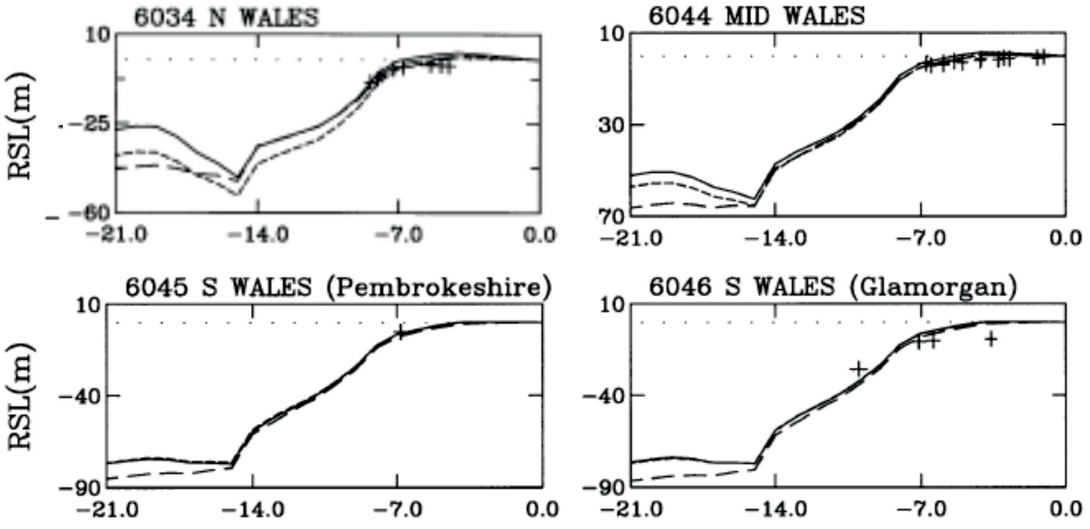

FIGURE 2.9: GIA modelled regional sea-level curves for Wales from Peltier et al. [2002]. Three model parameters are displayed. The solid line represents a thin ice model and a thin lithosphere; the long dash represents a thick ice model and a thick lithosphere; the short dash represents a thin ice model and a thick lithosphere. Age is shown as cal years BP.

For both north and mid Wales the model predicts a highstand occurring ca. 4000 cal yr BP. Peltier et al. [2002] state that such a highstand should result in raised beaches being preserved in the region. So far there is no observable evidence in either north or mid Wales to support the predictions. Sensitivity modelling showed that changes in the local ice load do not remove the highstand.

Peltier et al. [2002] introduced a continuation of Holocene eustatic sea-level rise beyond 4000 yr BP, in an attempt to drown the highstand. Although the highstand is reduced, it did not disappear entirely. Furthermore, the resulting sea-level curves from Scotland and north-east England did not match SLIPs, leading Peltier et al. [2002] to consider such adjustments to the eustatic function to be unacceptable.

Shennan et al. [2006] included shoreline migration, areas of ablating marine based ice and changes in the Earth's rotation vector. The Earth model used was a three layer model and simulations were run to assess 71km and 96km thick lithospheres. Perhaps the most important feature when compared to Peltier et al. [2002], Lambeck [1993a,b] and Lambeck et al. [1996] is the inclusion of topography when considering ice thickness.

When allowing for topography in the model and with the assumption that no isostatic equilibrium was reached during the LGM, only a 71km thick lithosphere produced acceptable results. The combination of these two factors results in a reduction in the magnitude of the misfits. The curve is a reasonable fit to the Welsh data (Figure 2.10), accurately predicting sea level during the early Holocene. The larger misfit during the mid/late Holocene is with intercalated index points which may have been displaced. The mid Wales model over-predicts sea level at all times, although the highstand present in the model by Peltier et al. [2002] has been removed. The Pembrokeshire curve only relates to a single data point, so meaningful comparisons are not possible (Figure 2.10).

The model presented by Bradley et al. [2011] shares many features with the Shennan et al. [2006] model. A key feature of the Bradley et al. [2011] model is 5 m of eustatic sea-level rise between 7 cal yr BP and 2 cal yr BP. The model also uses sea-level data from both Great Britain and Ireland to compare model predictions with. These changes result in substantial reduction in the misfits for mid Wales, with the over prediction of sea level height much reduced (Figure 2.11). The model under-predicts sea level during the mid-Holocene and the fit is slightly worse than that provided by Shennan et al. [2006]. However, the fit is much improved towards the late Holocene. The model no longer predicts a mid-Holocene highstand.

Shennan et al. [2018] present an updated post-glacial sea-level database for the British Isles. This is used to test the regional relationships between patterns of Holocene RSL change. The misfits between observed data and modelled sea-level change are reduced for north and Mid Wales but there is little difference in the fit for Pembrokeshire and Glamorgan (Figure 2.12). North and mid

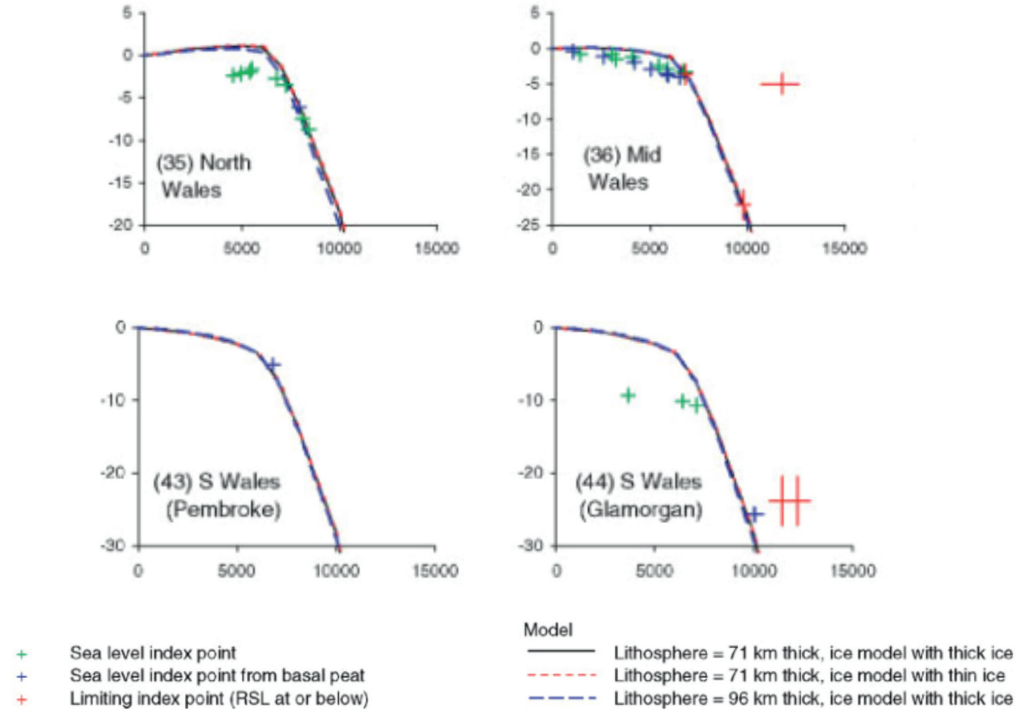

FIGURE 2.10: The sea-level curves for Wales when taking into account North Sea ice coverage, both thick ice and thin ice. Note that the north Wales curve shows the mid-Holocene highstand [Shennan et al., 2006].

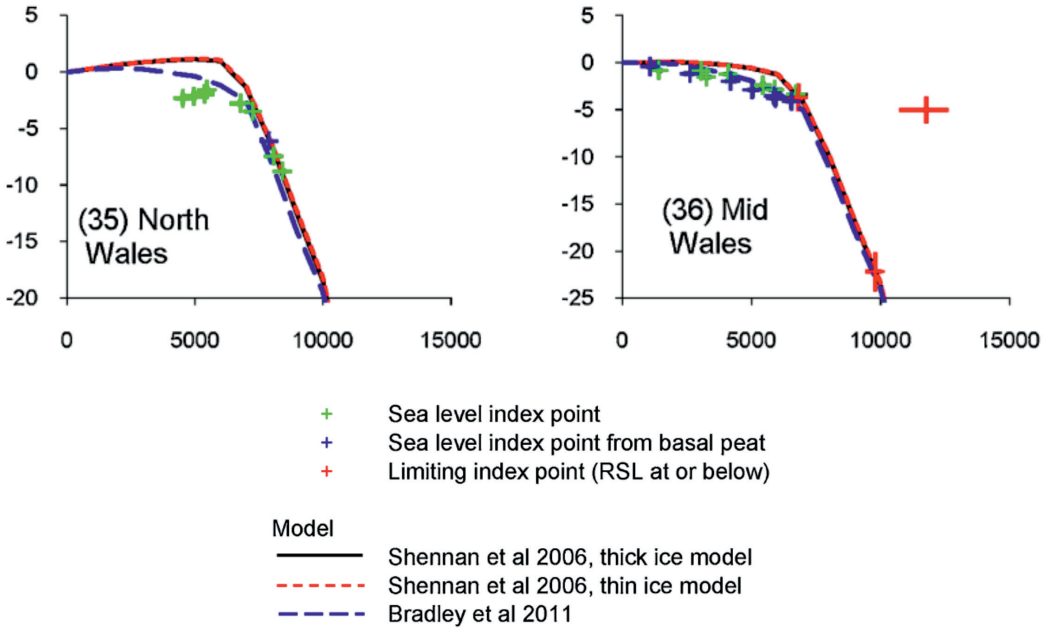

FIGURE 2.11: Sea-level curves for Wales as presented by Bradley et al. [2011]. The sea-level curves are displayed alongside those presented by Shennan et al. [2006] for comparison. The mid-Holocene highstand has been removed from the north Wales model.

Wales are included as regionally similar, as are Pembrokeshire and Glamorgan, with correlation coefficients of 0.99 and 0.999 respectively.

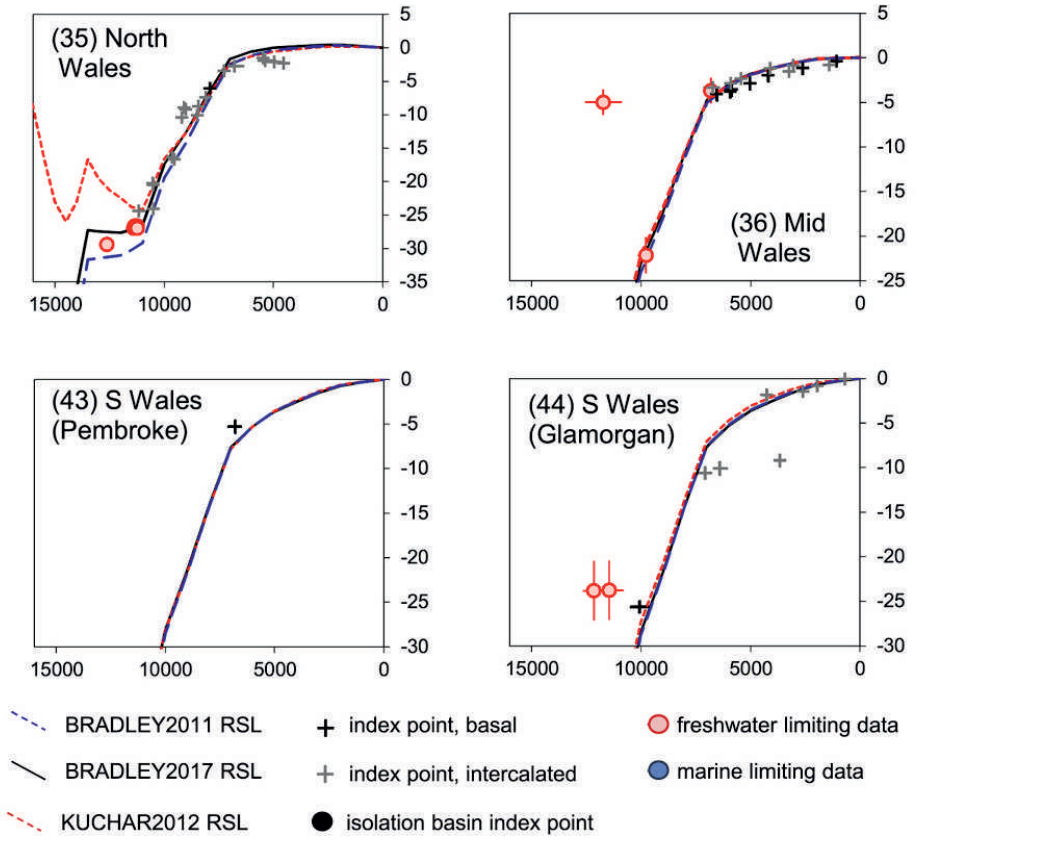

FIGURE 2.12: Sea-level curves for Wales as presented by Shennan et al. [2018]. All three models show similar sea-level histories, with the exception of the early Holocene for north Wales.

2.9 Synopsis

The existing database for SLIP Britain has gaps in key areas. For North Wales, there is a lack of data younger than c.4500 cal years BP. For Pembrokeshire, there is only a single data point. Even when combined with the Glamorgan database, there is a lack of data between the early and mid Holocene period.

Subterranean estuaries have been shown to directly connect groundwater to the sea, with oscillations propagating a distance onshore. This link between the two water levels can, under certain conditions, make freshwater back-barrier wetlands suitable archives for past sea-level.

Chapter 3

Methods

3.1 General Introduction

This work combines empirical observations with modelling to reconstruct Holocene sea-level changes. Groundwater oscillations resulting from tidal forcing were observed in wells over a three year period. Stratigraphy was established by hand coring. Samples for radiocarbon dating were collected from the cores to generate SLIPs. All heights were surveyed with DGPS. A groundwater model elucidated the conditions under which the horizontal migration and vertical growth of a freshwater back-barrier marsh is controlled by sea-level rise.

3.2 Groundwater Monitoring

Groundwater monitoring wells were installed on a transect perpendicular to the barrier, positioned centrally on the marsh. The wells were located at 20m, 60m and 90m (Figure 3.1) (Rhoscolyn) and 40m, 60m and 80m (Abermawr) (Figure 3.2) behind the barrier crest to identify the tidal signal and the degree of attenuation occurring over distance.

In Abermawr, the groundwater was monitored using Level TROLL 700 data loggers, which measure fluctuations in temperature and pressure every 15s. At Rhoscolyn, groundwater monitoring was carried out with Aqua TROLL 200 data loggers, which measure salinity as an additional parameter. Five of the loggers were vented, with a single non-vented logger at Rhoscolyn. This non-vented logger was corrected for changes in atmospheric pressure, which was monitored using a BaroTROLL 500 data logger. The pressure data from the loggers were used to calculate changes in the height of the water table. The height calculation, along with temperature and pressure data, provide information on seasonality, high rainfall and possible over wash events within the marsh.

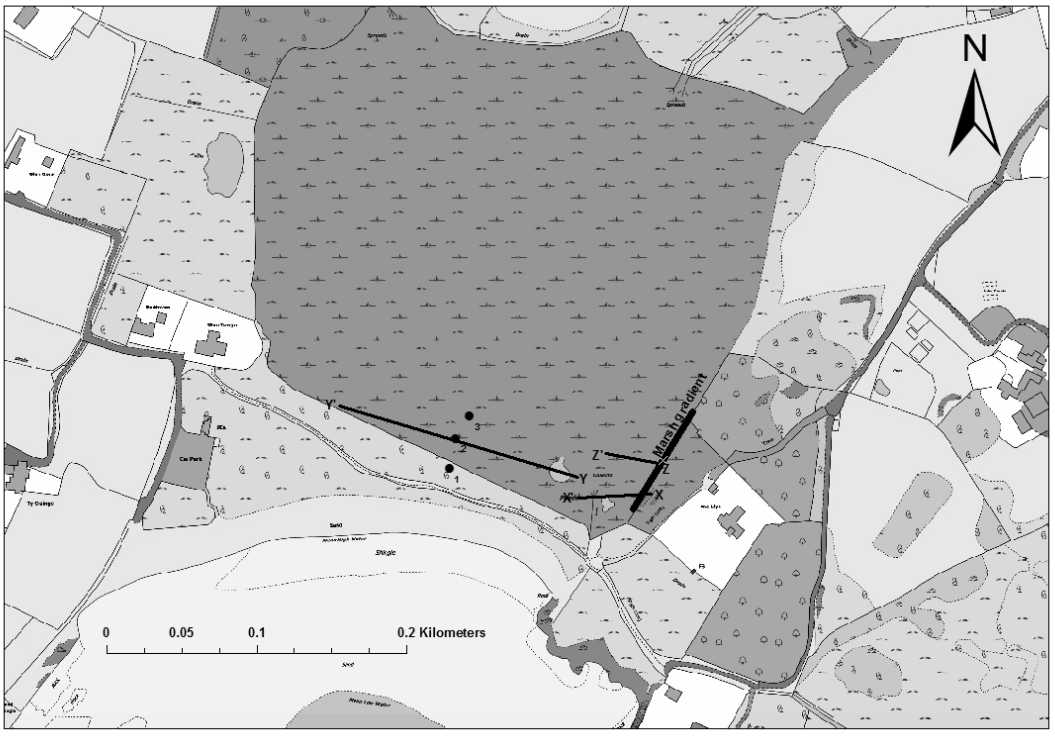

FIGURE 3.1: Rhoscolyn marsh back-barrier system, showing the location of monitoring wells 1-3 and coring transects X'-X, Y'-Y and Z'-Z. Also shown is the GPS transect used to calculate the groundwater gradient.

27 consecutive months of data were collected across all three wells at Abermawr and 17 consecutive months from wells 2 and 3 at Rhoscolyn. Rhoscolyn Well 1 gathered data for 32 consecutive months. The data is plotted as a time series in Matlab to identify tidal oscillations. Tidal data for Abermawr were taken from the Fishguard tide gauge and from Holyhead for the Rhoscolyn site [Holgate et al., 2013], covering the same period as the data loggers.

Cross wavelet and wavelet coherence analysis was applied to the tide gauge and groundwater data sets, using a Matlab script made available by Grinsted et al. [2004]. This enabled the simultaneous analyses of two time series data sets to examine relationships between the signal in time frequency space. A three step approach was taken to analyse the data. First a continuous wavelet transform (CWT) was applied to both datasets, before applying a cross wavelet transform (XWT) to test for significant power correlations in the signal. Finally, the coherence of the wavelets in time frequency space was tested for significance. All significance tests were against red noise, using Monte Carlo methods.

A Morlet wavelet was used as a consecutive bandpass filter across both time series. This process of CWT shifts the time series data into time frequency space and enables comparisons of wavelet power. The process produces edge effects, which are highlighted via a cone of influence, where

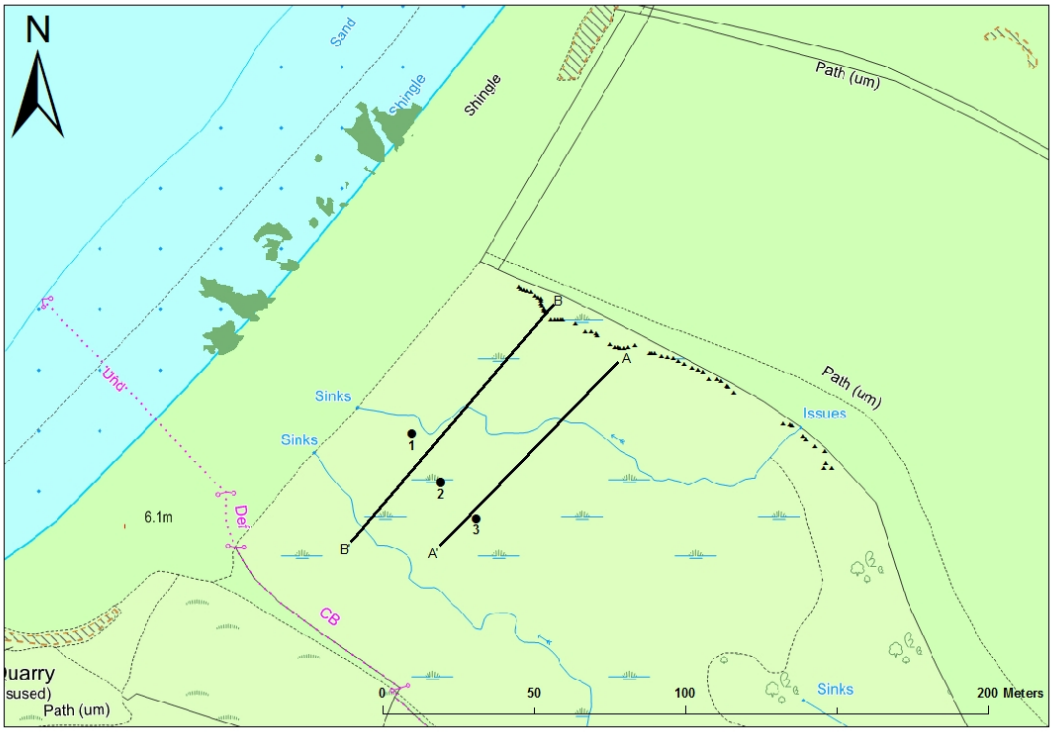

FIGURE 3.2: Abermawr marsh back-barrier system, showing the location of monitoring wells 1-3 and coring transects A'-A, and B'-B. Also marked in green are the ancient peat beds on the foreshore. The individual data points collected for groundwater gradient calculations are also shown.

results are not reliable and should be ignored [Grinsted et al., 2004]. Once transformed via CWT, XWT analysis is performed to test the significance between areas of common high power (Figure 3.3). Areas significant at the 5% level against red noise are shown with a thick contour. If one signal is dependent upon the other, it is probable that they will be phase locked. The phase relationship at any individual point in time frequency space is shown with an arrow [Grinsted et al., 2004].

XWT highlights areas of common power between two sets of time series data. It is also possible to check the significance of the coherence in time frequency space, between the two sets of data. Grinsted et al. [2004] define wavelet coherence as a*"localised correlation coefficient in time frequency space"*. When compared to XWT (Figure 3.3), it is clear that wavelet coherence identifies the same relationships (Figure 3.4) but is capable of being a more powerful tool to identify correlations in variation.

The oscillations within groundwater, as a result of tidal oscillations, reduces with distance away from the coast. Groundwater wells measured the propagation of tidal oscillations through the marsh. The use of three wells enabled the calculation of attenuation of the tidal signal with distance into the marsh, as a measure tidal efficiency. The tidal efficiency of a system is the ratio

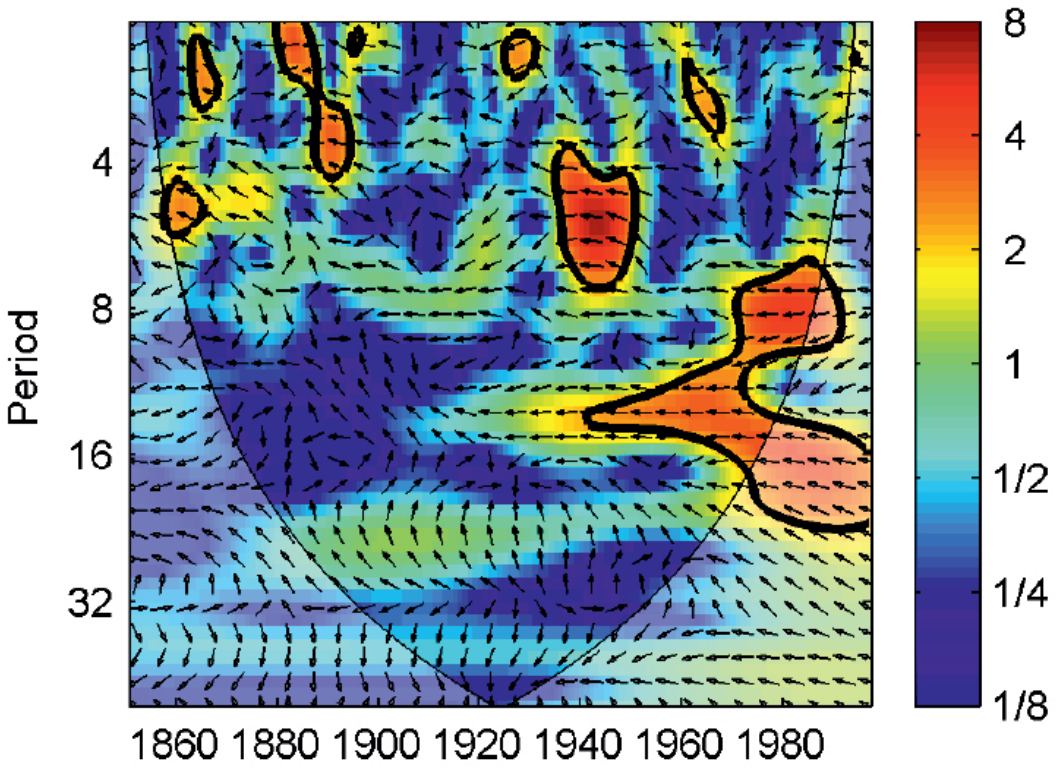

FIGURE 3.3: An example of time series data after cross wavelet transformation. The cone of influence, showing edge effects, is highlighted by the light contour. Significance at 5% against red noise is highlighted with a thick contour. The phase shift between the two series is shown with arrows [Grinsted et al., 2004].

of the amplitude of tidal oscillations and the change in amplitude of and aquifer in response to those oscillations. It can be simply represented as:

$$TE = \frac{H_x}{H_o} \tag{3.1}$$

where TE is tidal efficiency, H_x is is the tidal amplitude and H_o is the tidal response at a given distance. TE has been shown to reduce linearly with distance [Erskine, 1991] and this relationship is used to calculate a starting point for barrier and marsh hydraulic conductivity (K) values.

3.3 Hand Coring

An Eijkelkamp gouge corer was used to undertake a stratigraphy survey along a shore parallel transect behind the barrier. Thress transects at Rhoscolyn (Figure 3.1) and two transects at Abermawr (Figure 3.2) extending the width of the marsh were sampled and described, providing

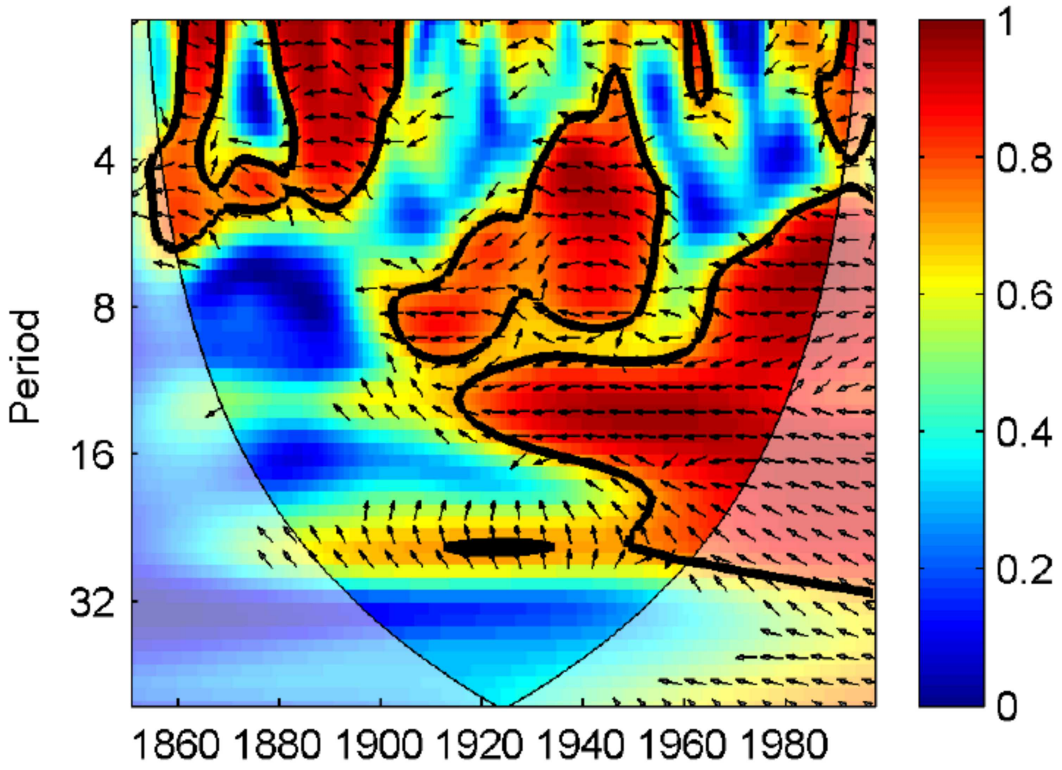

FIGURE 3.4: An example of wavelet coherence analysis, based on the same data as figure 3.3. Note that the significant relationship between the time series data is expanded beyond that of XWT [Grinsted et al., 2004].

a picture of the morphology of the valley floor and the stratigraphy of the Holocene infill. The stratigraphy was described using an adapted Troels-Smith [1955] method.

A "Russian" chamber corer was used to collect samples for analysis in the laboratory and to obtain samples for radiocarbon dating. The 0.5m chamber has a diameter of 50mm and secures the sediment sample using a blade and fin which closes around the sample prior to extraction. The interface between the Holocene base and freshwater peat was sampled. Longer cores were collected to provide the option of micro-fossil analysis, encompassing the vertical extent of the marsh. This was achieved using the method as described in Vleeschouwer et al. [2010], whereby two boreholes are created side by side, allowing for cores to be collected with a 0.1m overlap. This removes the effects of the 0.1m cone on the bottom of the chamber, which doesn't sample the subsurface but does disturb the underlying sediment. Samples collected in this way are ideal for micro-fossil analyses and radiocarbon dating as the degree of sediment disturbance is greatly reduced [Shennan et al., 2015]. The main problems associated with the use of a chamber corer are related to the difficulty in collecting stiff sediment. The chamber can become easily clogged with organic detritus and large pebbles, as well as difficulty in retrieving samples containing stiff clay [Shennan et al., 2015].

3.4 Differential GPS

Differential GPS combines a roving segment with a base station to achieve centimetre accuracy measurements in real time. A Trimble Differential GPS was used to survey the marsh, corrected to UK Ordnance Datum. Height and location were measured simultaneously with the stratigraphical survey / basal sampling at each sampled borehole. A further survey was undertaken in the marsh to measure the topographic gradient at the edge of the marsh to estimate the gradient in the groundwater in the area where basal peat is formed as per Gehrels and Anderson [2014]. A shore perpendicular survey over the crest of the barrier and along the beach to the position of low tide was also performed to provide accurate height information for the groundwater model. A further survey of the drowned forest was made to map the extent and height of the exposed foreshore peat beds.

3.5 Groundwater Modelling

Groundwater modelling is used to test the suitability of the Rhoscolyn and Abermawr sites for Holocene sea-level reconstructions. It is possible that the barrier systems became decoupled from sea level in the past. Increased recharge or decreased discharge could result in an elevated water table and ponding in the marsh. The increased height of the groundwater level could result in decoupling from the sea and the vertical shift of new peat growth not being the result of sea-level rise. Likewise, it is possible that decreased recharge or increased discharge could result in the lowering of the groundwater level. Modelling was used to check for the effects of ponding and desiccation on the system and monitor recovery times.

Two dimensional numerical simulations were performed with FEFLOW, a finite element model which has been applied to several coastal groundwater / ocean interactions (eg. Loáiciga et al. [2011], Michael et al. [2005], Smith [2004]). The model domain (Figure 3.5) extends landwards and seaward from the barrier crest. The Rhoscolyn model extends 135m seawards and 50m landwards, whilst the Abermawr model extends 150m seawards and 50m landwards. The model domain for Rhoscolyn comprises 9659 nodes and 8904 elements and Abermawr comprises 16182 nodes and 16736 elements.

No flow boundaries are applied to the base and the edges of the model and a tidally oscillating head applied to the seawards edge, with data taken from the Fishguard and Holyhead tide stations for the two sites. Constant recharge rates of 0.00123 m/d are applied to the peat at zero concentration salinity, whilst a salinity concentration of 35 kg / m^3 were applied along the barrier edge.

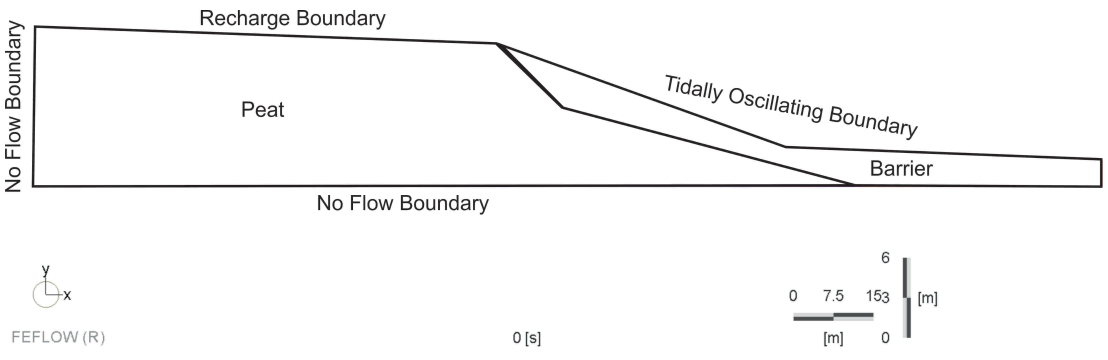

FIGURE 3.5: Generic model domain for the simulations used for Abermawr and Rhoscolyn. The system is simplified to a two layer model, with a no flow boundary on the landwards side and the base of the model. Recharge is applied to the marsh surface and a oscillating tidal time series is applied to the barrier boundary.

The hydrostratigraphy was simplified to a peat-sand barrier (Rhoscolyn) and a peat-sandy gravel barrier (Abermawr) (Table 3.1). Hydraulic conductivity (K) was calculated in 1m strips, to mitigate the fact that the layers aren't parallel. There are several steps to this process and requires the calculation of tidal efficiency from the field data.

Parameter	Rhoscolyn	Abermawr
Peat Properties		
Hydraulic Conductivity (m/d)	0.144	0.001
Recharge (m/d)	0.00123	0.00123
Barrier Properties		
Hydraulic Conductivity (m/d)	55.1	27
Both Layers		
Porosity	0.3	0.3

TABLE 3.1: Hydrological model base case parameters.

Firstly, the thickness of the layers are estimated from the surface of the land, the base of the barrier and the top of the pre-Holocene substrate. In this study, linear equations are used to interpolate between measurements. Ideally, ground penetrating radar would have provided more precise data, but at both sites the signal was too weak to be useful. Estimated K values, along with the estimated thickness of each layer enables the calculation of the aquifer thickness from,

$$\frac{(bbarrier * Kbarrier) + (bpeat * Kpeat)}{(bbarrier + bpeat)} \tag{3.2}$$

where bbarrier is the thickness of the barrier layer, bpeat is the thickness of the peat layer, kbarrier is the hydraulic conductivity of the barrier and kpeat the hydraulic conductivity of the peat.

Next, time series data was compared between the local tide gauge and well 1 at each site. For a particular period, peaks recorded by the tide gauge were matched to those occurring within the groundwater. At both sites the groundwater record is extremely noisy and matching peaks is not always possible. Neither site showed a semi-diurnal groundwater response to tidal forcing, rather there was a single peak as a result of the full diurnal cycle (Figure 3.7).

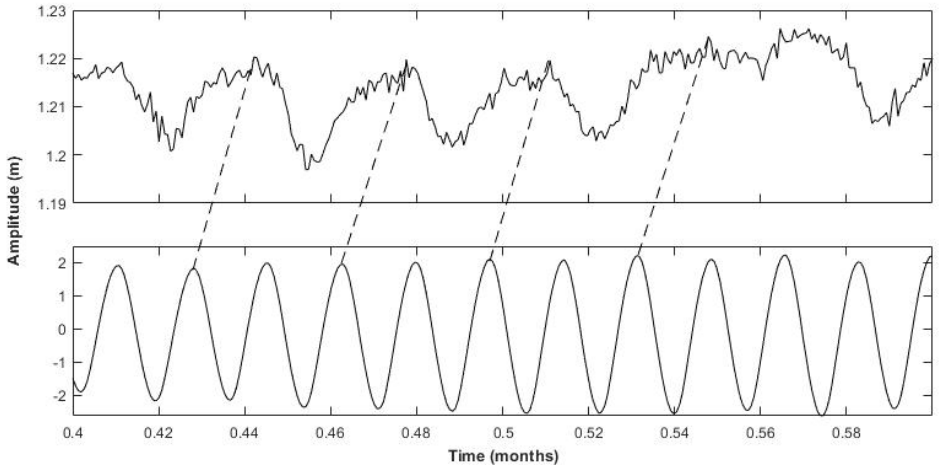

FIGURE 3.6: An example of how tidal and groundwater peaks were matched from a 7 day period recording in well 1 at Rhoscolyn. The dashed line represents paired tidal and groundwater peaks. The second high tide of each day was paired with the following peak in groundwater. This was taken as the time lag between high tide and the groundwater response.

The change in amplitude of the groundwater response with distance from the tidal peak, allows the calculation of tidal efficiency. This can then be compared to an analytical solution based on estimated K values for each layer. The analytical solution is calculated from,

$$TE = exp\frac{-x\sqrt{\pi S}}{(t_0 T_e)} \tag{3.3}$$

where t_0 is the length of the tidal cycle in days, T_e is transmissivity calculated from aquifer thickness and S is the storativity of the aquifer, estimated to be 0.10. The K values for the barrier and peat were changed iteratively, until a best fit solution was found for the analytical solution to the field data (Figure 3.7.)

Sensitivity experiments were carried out to examine the changes in groundwater elevation as a result of variations in peat and barrier permeability. In both cases, barrier permeability was increased and decreased from the base case values, by an order of magnitude. These changes had very little impact on groundwater elevation, with less than 20cm fluctuations in groundwater at both sites.

Changes in peat permeability were much more significant. As with the barrier permeability, values were raised and lowered by an order of magnitude. Lower permeability of the peat resulted

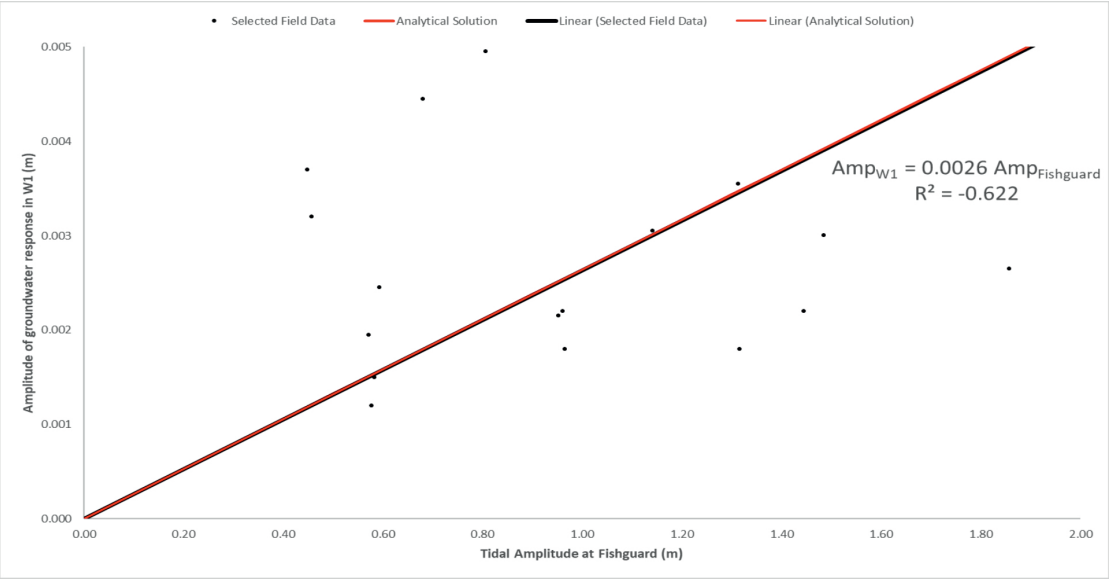

FIGURE 3.7: Analytical Solution calculations of permeability. Black line represents the linear fit for the field data, forced to intersect zero. Red line represents the analytical solution, the result of varying peat and barrier permeability until it fit the field data.

in ponding across the marsh, with water levels over 1m above the surface at both sites. Higher permeability resulted in the water table dropping significantly at both sites, by over 2m from the base case scenario. One of the preconditions of this methodology is that the main control on groundwater elevation is the peat permeability, as opposed to that of the barrier. These sensitivity experiments demonstrate that to be the case. The high sensitivity to changes in peat permeability also provide justification to the values chosen in the base case scenario.

Once the base case model was calibrated to the field data, sensitivity experiments were used to investigate how the back-barrier marsh responds to flooding and dessication events. The boundary condition in the peat was set to simulate these events for 6 month periods, before resetting to base conditions to monitor response and recovery characteristics.

3.6 AMS ^{14}C Radiocarbon Dating

For a SLIP to be acceptable, it requires a robust age. For Holocene peats, radiocarbon dating is typical across several studies. This work uses radiocarbon dates obtained from Accelerator Mass Spectrometry, which allows for precise dating of small samples [Lowe, 2015], to date basal peat samples. This was necessary for this study, as only small samples had been preserved in the peat.

Samples were selected to be in the closest proximity to the basal peat as possible, in accordance with Gehrels [1999]. Basal samples were selected to produce compaction free SLIPs to establish the Holocene sea-level trend. The core was sampled in 1cm sections, with the edges removed to

avoid contamination. Plant macrofossils, embedded within the horizontal plane, were selected and picked with tweezers. Samples were washed with distilled water and dried at 50^0C overnight, before being refrigerated in an airtight container.

AMS ^{14}C analyses was performed by the Natural Environment Research Council (NERC) Radiocarbon Laboratory. Calibration was carried out using CALIB 7.1 [Stuiver and Reimer, 2018] and dates were calibrated to cal years BP. Calibration is required as the amount of ^{14}C has changed over time [Lowe, 2015]. Marine reservoir effects can also be an issue and result in older ages than expected. However, as the sites are freshwater environments this is not an issue. Local groundwater could be a source of error due to the introduction of younger carbon into the system.

3.7 Palaeosea-level Determinations

The reconstruction of past mean sea level (SL), from basal peat, follows the relationship $SL = H - I$, where H is the OD height of the sample and I is the indicative meaning [Gehrels, 1999]. The procedure for calculating past sea level from freshwater back-barrier peat is described by Gehrels and Anderson [2014] and we follow the same method here.

The original indicative meaning of a sample is taken as the average height of peat formation directly behind the barrier, marked A in Figure 3.8. The height of the sample is directly measured by DGPS and is marked B. At this point it would be possible to calculate past sea level, using previously stated relationship. However, this is complicated by the existence of a gradient in the groundwater. As our sample formed a distance behind the barrier, we must correct for the influence of the gradient, marked C. As such, we calculate an original past mean sea level from $SL = H - I - GW$, where GW is the correction for the groundwater gradient.

This gives rise to a further complication. When sea level was lower, the position of the barrier would have been further offshore as shown by Bruun [1962], where the position of the palaeo barrier can be calculated from:

$$R = \frac{1}{tan\theta} S \tag{3.4}$$

This means that the sample was formed further away from the barrier than in our original calculations, marked D in Figure 3.8. As such, the sample is further along the groundwater gradient than previously measured and so the correction must be amended and sea level recalculated. This recalculation results in a new sea level prediction and the barrier must be further shifted down the beach slope, marked E. This process is repeated iteratively, until there is no significant movement of the barrier over three iterations.

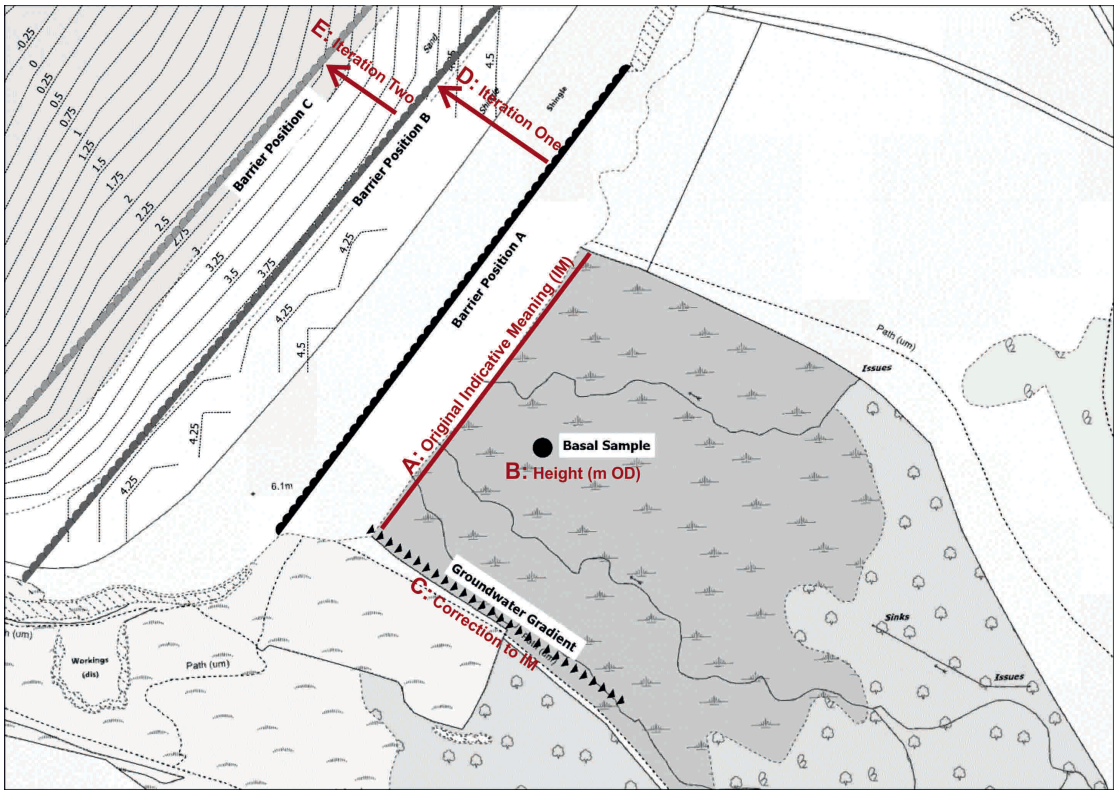

FIGURE 3.8: (The iterative steps, labelled A-E, in calculating the relationship between the basal sample and past sea level. A = average height of the marsh behind the barrier. B = the height of the basal sample. C = the measured slope in the groundwater. D = the previous position of the barrier, under conditions of lower sea level. E = the final position of the barrier after no change in indicitive meaning over three iterations.)

This method is most sensitive to errors in groundwater predictions, which are large enough to overprint any other errors which may occur. This study takes ± two standard errors in the groundwater gradient and recalculates each individual SLIP based on the new groundwater gradient. The difference in the predicted sea level is taken as the vertical error.

3.8 Synopsis

This section describes the methodology employed to reconstruct sea-level change from freshwater back-barrier marshes in Wales. It shows how groundwater modelling is utilised to examine the conditions necessary for this methodology to be utilised more broadly. Hand coring is used to understand the stratigraphy of the marsh and to collect samples for radiocarbon dating. Groundwater monitoring enables the identification of a tidal connection and provides data for model calibration. DGPS allows for the measurement of accurate heights, used both in sea-level reconstruction and groundwater modelling.

Chapter 4

Results: Rhoscolyn

4.1 General Introduction

In this chapter two basal SLIPs are presented, collected from a freshwater peat-sand enclosed back-barrier system at Rhoscolyn in north Wales. SLIPs were collected to fill the younger than 4000 cal years BP gap in the sea-level database, in order to test for the existence of a mid Holocene highstand in north Wales. Furthermore, the suitability of these types of systems as archives for past sea level was assessed.

4.2 Lithostratigraphy

A total of five radiocarbon dates were collected for sub-sampling from three transects, X, Y and z, running oblique and parallel to the shoreline (Figure 3.1). A simplified extended stratigraphy is shown in Figures 4.1, 4.2 and 4.3.

A total of 10 cores were taken along transect X (Figure 4.1), which extends 55m, with 2 cores sub-sampled for dating (index points 12 and 13). The general trend is of *Phragmites* peat overlying woody peat, which in turn overlies a pre-Holocene substrate of glacial till. A layer of sandy *Phragmites* peat is found across the transect, around 3.4m OD at its deepest point in the middle of the marsh. This is could be either slopewash or overwash from a storm event. A units of clayey peat is present along the entire transect, shallowest at the edges (between 3-3.5m OD) and deeper in the middle of the marsh (around 1.5m OD). This is interpreted as slope wash.

Sixteen cores were taken from transect Y (Figure 4.2), which extends 161m, with one core sub-sampled for dating (index point 16). The general trend is of *Phragmites* peat overlying woody peat, which in turn overlies a pre-Holocene substrate of glacial till. The western edge (Y′) is

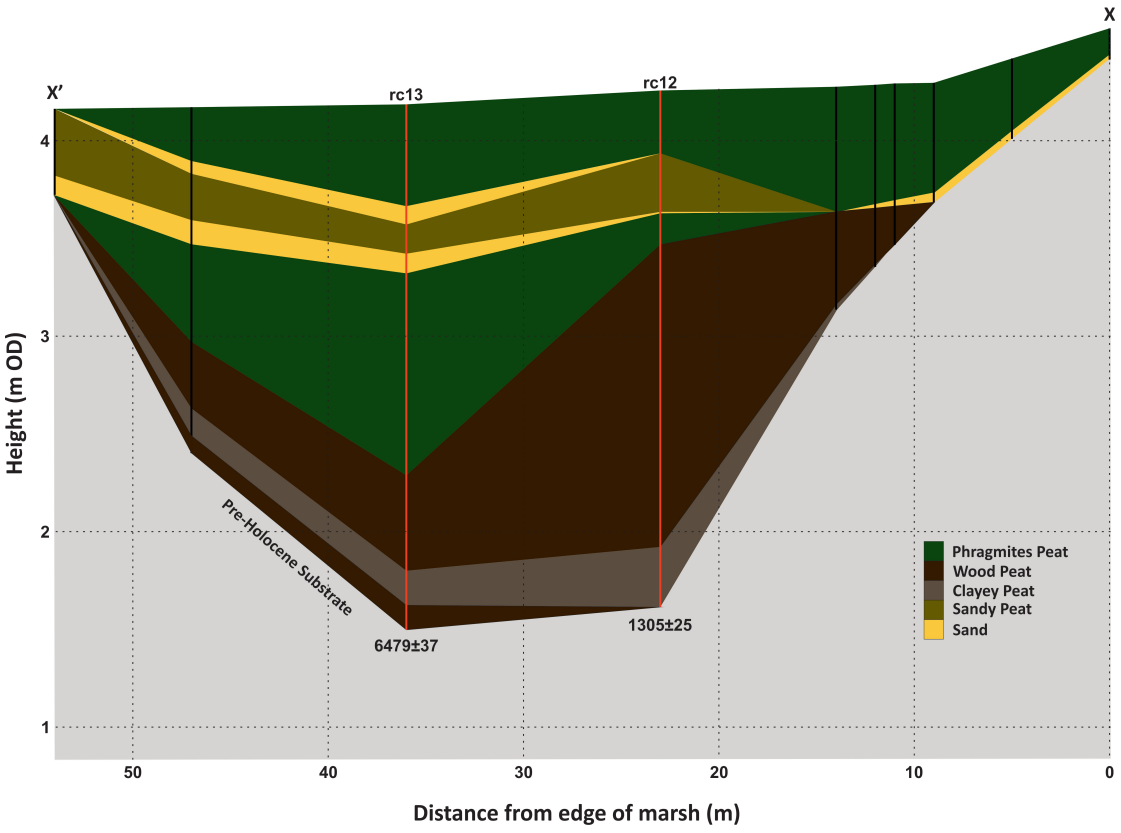

FIGURE 4.1: Shore normal stratigraphy for transect X, running west (X′) to east (X), with a simplified stratigraphy from 10 cores. See figure 3.1 for location.

dominated by sandy *Phragmites* peat. There is a large sand body, between 3.5 to 5.5m OD, spanning the woody peat and *Phragmites* peat layers. This is interpreted as overwash, possibly from a large storm event. The eastern edge (Y) has a small sand layer at the interface of the *Phragmites* and woody peat, which progresses into a unit of sandy peat. There is a small clay layer just above 2m OD, at the eastern end. Between 75 to 100m, there are two sandy *Phragmites* peat units at around 5m OD.

A total of 11 cores were taken from transect Z (Figure 4.3), which extends 38m, with two cores sub-sampled for dating (index points 9 and 14). The general trend is *Phragmites* peat overlaying woody peat, which in turn overlies a pre-Holocene substrate of glacial till. Two bands of sand run from the western side of the transect (Z'), to around 15m from the edge, at a depth between 4-4.5m OD. As with the sandy layers in the other transect, this could be the result of storm driven over wash. There is a layer of clayey peat towards the western edge of the marsh, between the Holocene base and the woody peat.

The stratigraphy shows the potential evidence of an open channel. There is a large body of sand, which could be open water, but it does not cut to the base of the marsh. There is no evidence

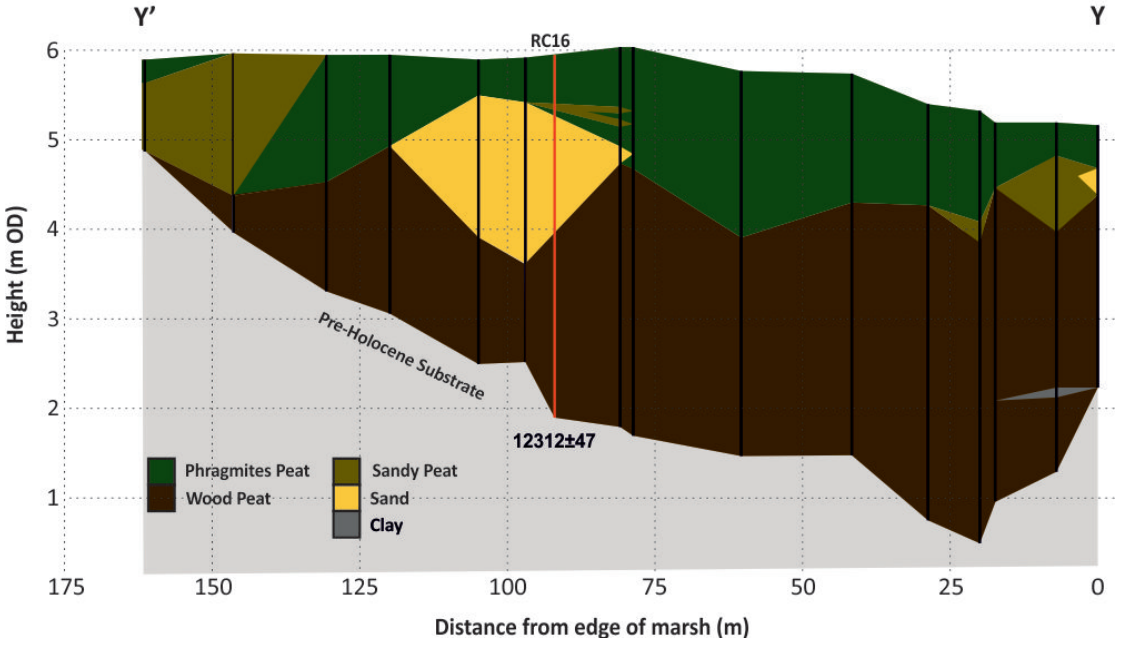

FIGURE 4.2: Shore normal stratigraphy for transect Y, running west (Y′) to east (Y), with a simplified stratigraphy from 16 cores. See figure 3.1 for location.

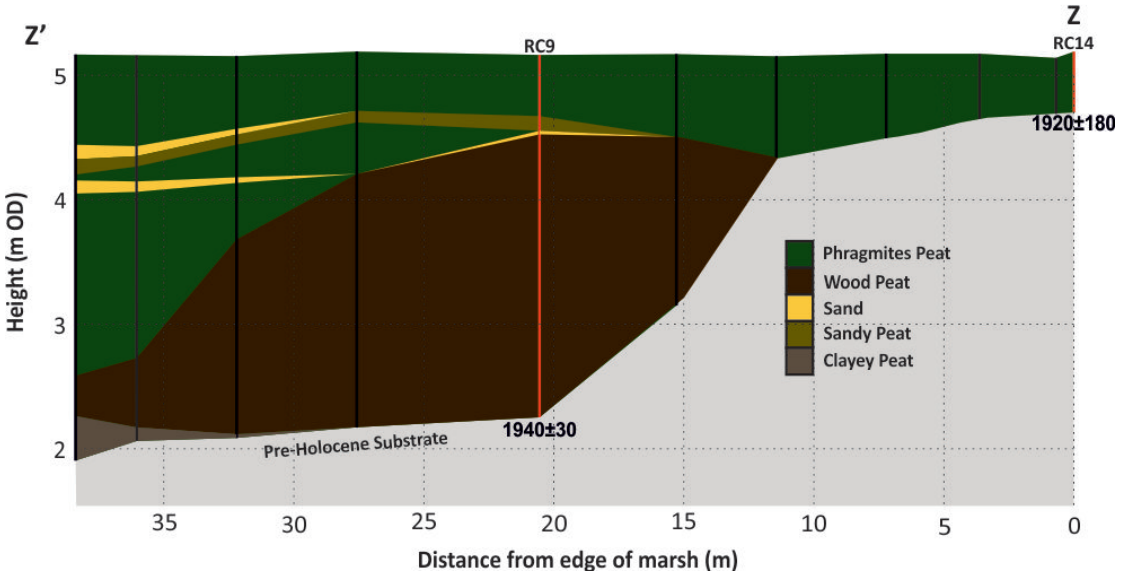

FIGURE 4.3: Shore normal stratigraphy for transect Z, running west (Z′) to east (Z), with a simplified stratigraphy from 11 cores. See figire 3.1 for location.

of oxidation within the peat or gyttja type deposits. This supports the idea that this was not a chanel and the marsh has been resistant to ponding or dessication events over time.

4.3 Chronology

Five age measurements by AMS ^{14}C dating of basal sediment cores rc0716002, rc0716005, rh4, rh5 and RHmarsh100 (Table 4.1). For all cores, a single date was obtained from plant macrofossils. Two further dates were returned as modern samples and as such were discarded.

Core rc0716002 was dated at 4.05m depth (1.72m OD) and produced a ^{14}C age of 12312 ± 47, calibrated to a median age of 14258 cal years BP. Core rc0716005 was dated at 2.91m depth (2.25m OD) and produced a ^{14}C of 1940 ± 30, calibrated to a median age of 1890 cal years BP. Core rh4 was dated at a 2.57m depth (1.69m OD) and produced a ^{14}C of 1305 ± 25, calibrated to a median age of 1251 cal years BP. Core rh5 was dated at 2.65m depth (1.54m OD) and produced a ^{14}C of 6479 ± 37, calibrated to a median age of 7381 cal years BP. Core RHmarsh100 was dated at a 0.49m depth and produced a ^{14}C age of 1920 ± 180, calibrated to a median age of 1870 cal years BP.

The ages for cores rh5 and RHmarsh100 are consistent with what would be expected from the height they were collected. The age for rc0716002 is much older than anticipated and whilst it is likely to be correct, it dates an older fen or swamp that existed before 12,000 years ago. The peat that formed in response to sea-level rise has transgressed this older swamp. The ages from cores rc0716005 and rh4 are younger than anticipated, potentially as a result of sampling more modern remains of rhizomes or roots. The peat was expected to have formed during a time of stable sea level. As a result, there was a lack of accommodation space created to allow for the vertical growth of the marsh. This allows for the ongoing growth of *Phragmites* at roughly the same level, meaning the roots have time to penetrate the underlying peat. Whilst these three dates are included in indicative meaning calculations, they are expected to be rejected as acceptable SLIPs.

4.4 Groundwater Monitoring

4.4.1 Well data

Monitoring wells were positioned 20m (SH 27405 75164), 60m (SH 27409 75185) and 87m (SH 27419 75199) behind the crest of the barrier. Well 1 and 3 cover an uninterrupted period of 21 months, whilst well 2 covers 18 months. All three wells monitor changes in height, temperature and salinity (Figure 4.4, 4.5 and 4.6.

Index number	9	12	13	14	16
Radiocarbon lab. number	UCIAMS-192865	UCIAMS-192866	SUERC-72897	UCIAMS-192868	SUERC-76468
Core	rc0716005	rh4	rh5	RHmarsh100	rc0716002
Material	Plant macrofossil	Plant macrofossil	Plant macrofossil	Plant macrofossil	Plant macrofossil
14C Enrichment (% Modern ± 1σ)	78.56 ± 0.26	85.03 ± 0.26	44.64 ± 0.20	78.76 ± 1.67	21.59 ± 0.13
14C age (years BP ± 1σ)	1940 ± 30	1305 ± 25	6479 ± 37	1920 ± 180	12312 ± 47
Calibrated BP ± 1σ age ranges	(1865-1927)	(1187-1204)	(7330-7359)	(1625-1670)	(14115-14364)
		(1242-1248)	(7368-7394)	(1690-2063)	
		(1256-1284)	(7412-7432)	(2085-2103)	
Calibrated BP ± 2σ age ranges	(1821-1949)	(1183-1211)	(7315-7459)	(1420-1459)	(14072-14614)
	(1963-1967)	(1226-1290)		(1519-2321)	
Median calibrated age (cal yrs BP)	1890	1251	7381	1870	14258
Carbon content (% by weight)	41.1	66.2	59.6	12.7	57.7
$\delta^{13}C_{VPDB}$ ‰(±0.1)	-19	-18	-28.3	-17.3	-27.6

TABLE 4.1: Rhoscolyn radiocarbon dates and associated errors. All dates were obtained from plant microfossils.

Monitoring Well 1 shows no clear tidal signal in the water depth, salinity or temperature fluctuations (Figure 4.4). Water depth responded to rainfall, with a large peak at the end of December 2015 slightly lagging the high peak in local rainfall (Figure 1.11). Salinity increased during the winter storm season in 2014/15 and 2015/16, probably as a result of wind driven storm waves over-topping the barrier. Temperature was seasonally driven, showing clear cooling during the winter and warming during the summer.

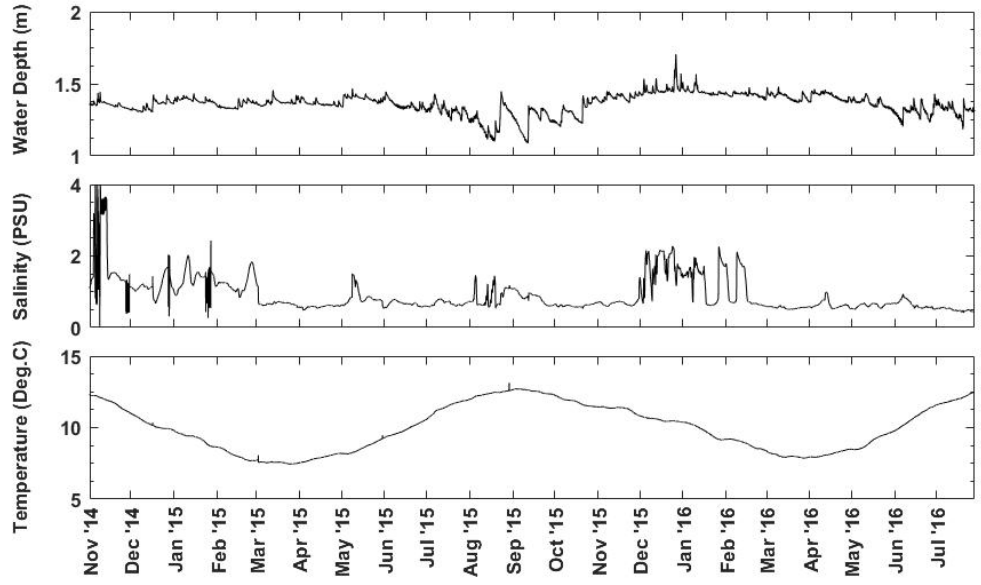

FIGURE 4.4: Well 1 groundwater data. Water depth (top) shows some seasonality, along with temperature (bottom). Salinity (middle) spikes occur during the storm season.

Monitoring Well 2 has a water depth record which is very noisy until September 2015; this is probably caused by a trapped sediment particle, which subsequently became dislodged. The logger shows no clear tidal signal in the water depth, salinity or temperature fluctuations (Figure 4.5). Water depth responded to rainfall, with a large peak at the end of December 2015 slightly

lagging the high peak in local rainfall (Figure 1.11). Salinity was stable, showing only two large dips around June and September 2015. These dips coincide with removal of the wells to download data and salinity quickly returned to roughly normal parameters, although there is a slight decline over time as it continues to stabilise. Temperature was seasonally driven, showing clear cooling during the winter and warming during the summer.

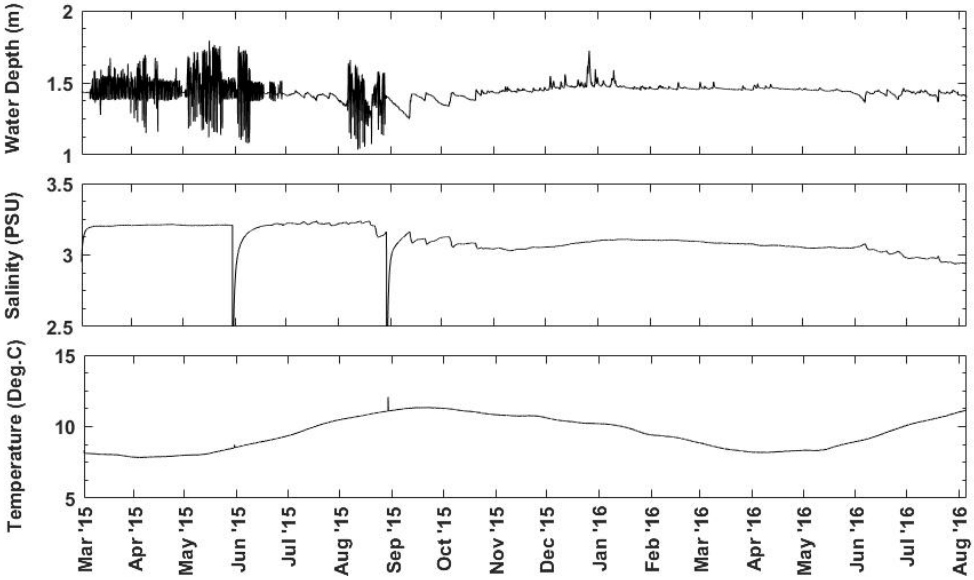

FIGURE 4.5: Well 2 groundwater data. The signal is noisy at the start of the record, with no clear seasonality in water depth (top.) Salinity (middle) is stable throughout the record, despite a general reduction over time. Temperature (bottom) is seasonally driven.

Monitoring Well 3 shows no clear tidal signal in the water depth, salinity or temperature fluctuations (Figure 4.6). Water depth responded to rainfall, with a large peak at the end of December 2015 slightly lagging the high peak in local rainfall (Figure 1.11). Salinity was stable, showing only two large dips around June and September 2015. These dips coincide with removal of the wells to download data and quickly recovered in June but never returned to pre-extraction levels following September. This was probably result of a combination of mixing induced by removing the well and because the well was replaced at a slightly different depth. Temperature was seasonally driven, showing clear cooling during the winter and warming during the summer.

4.4.2 Spectral analyses

Spectral analysis has been successfully used to identify tidal oscillations in coastal groundwater [Gehrels and Anderson, 2014, Geng and Boufadel, 2017]. Here, the presence of the spring-neaps tidal cycle (0.7μHz), the diurnal (10μHz) and semidiurnal (20μHz) periods (Figure 4.7) are tested (Table 4.2). The monitoring wells were compared to the Holyhead tide gauge, which

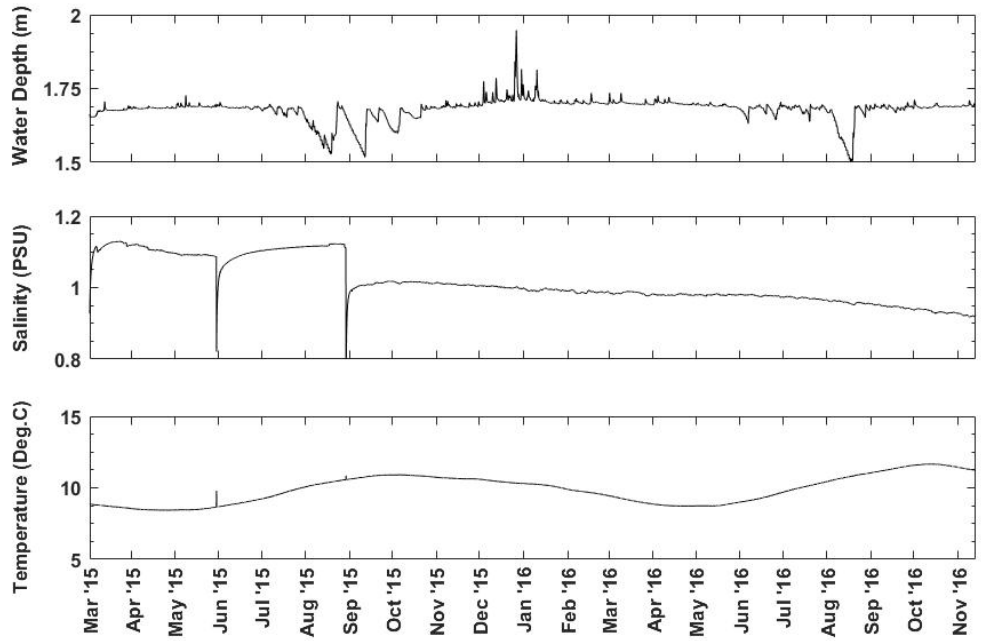

FIGURE 4.6: Well 3 groundwater data. Water depth (top) shows some seasonality, along with temperature (bottom). Salinity (middle) is generally stable, but reduces over time.

SITE	SEMI-DIURNAL (μ HZ)	FISHER G	P VALUE	DIURNAL (μ HZ)	FISHER G	P VALUE	SPRING-NEAP (μ HZ)	FISHER G	P VALUE
Holyhead	20.1	0.117	0	10.36	0.001	0.486	0.74	0.013	0
WELL 1	20.12	0	3.47×10^{11}	10.39	0	4.25	0.79	0.001	0
WELL 2	20.80	0.007	0	10.39	0.049	0	0.78	0.005	0
WELL 3	20.82	0	1.6×10^{12}	10.37	0	2.91×10^{6}	0.77	0.004	0

TABLE 4.2: Rhoscolyn peak frequency significance in water elevation, as tested by Fisher G statistic. Reported frequencies represent the highest peak around the expected tidal constituent.

is the nearest available to the site. The peaks at and proximal to the expected periodicities were tested for significance utilising the Fisher G statistic.

The semidiurnal tide occurs at a frequency of around 20μHz and is significant (p=o) in both the tide gauge and well 2 data. The diurnal tide occurs at a frequency of around 10μHz and is significant (p=0) in both the tide gauge and well 2 data. Spring-neap cycles occur at a frequency of around 0.7μHz and is significant (p=0) in all three wells and the tide gauge data.

The lack of a significant semi-diurnal and diurnal tidal signal in well 1 is problematic. It would be expected that the well closest to shoreline would have the greatest tidal signal, decreasing in amplitude the further landwards the well is placed. This unexpected result, along with the fact that the semi-diurnal tide were only significant in a single well, meant that further analyses was necessary.

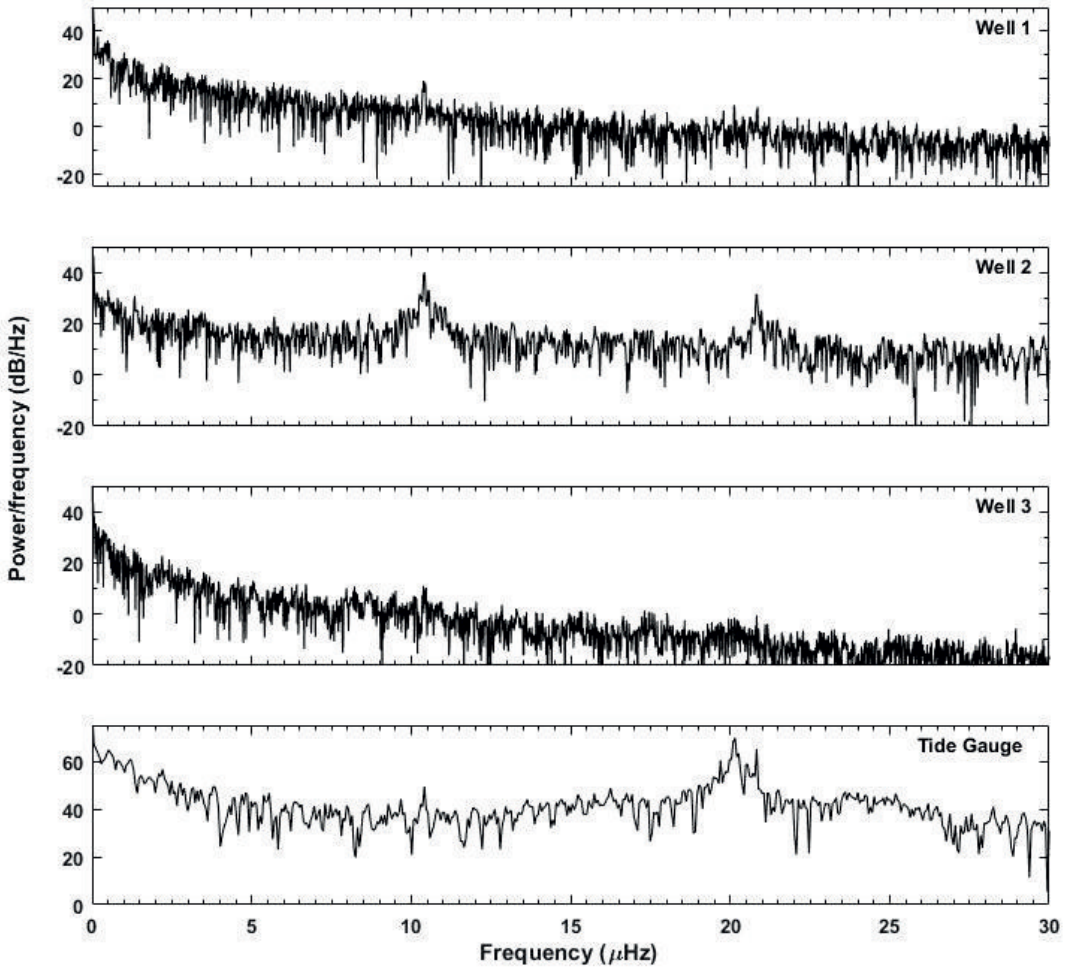

FIGURE 4.7: Spectral analyses showing the frequency of peaks in water elevation. Ground water monitoring wells are shown alongside the Holyhead tide gauge for comparison. Semi-diurnal tides occur around 20 μHZ, diurnal tides around 10.4 μHZ and spring-neap tides around 0.75 μHZ.

4.4.3 Wavelet analyses

Several studies have used wavelet analysis to identify relationships between two sets of geophysical time series data, in particular via the use of wavelet coherence [Grinsted et al., 2004, Gu et al., 2014]. Here the relationship between tide gauge data from the Holyhead tide gauge and groundwater elevation data from the Rhoscolyn monitoring wells was tested. In all three wells, the semi-diurnal and diurnal tide were shown to be significantly correlated to the 95th significance level against red noise, determined using Monte Carlo methods (Figure 4.8).

Correlation is not significant throughout the year, which may be related to spring/neap cycles and/or weather conditions at the time. The most noticeable absence of coherence is during the winter months of 2015, which coincides with a high rainfall peak in the weather data and elevated groundwater levels in the well data. It would seem reasonable that, for this short period,

the relationship between groundwater and the tide was masked by these events. There is also a reduction in coherence the further landwards the well is located. This is as a result of tidal efficiencies and the tidal signal attenuating as it travels through the subsurface.

The spring/neap cycle is only significantly detected in well 1 and 2 and only intermittently. This could be for a result of the signal being too small against the background noise of the system or a consequence of the sand barrier permeability. However, when taken alongside the spectral analysis there is good evidence for the spring-neap cycle being recorded in the back-barrier groundwater oscillations.

4.5 Groundwater Model

The Rhoscolyn model base conditions were not stable with a recharge boundary, so a fixed boundary head of 5m was applied on the landwards side to establish suitable conditions. This was reduced to simulate drought conditions and a fixed boundary was added to the top to simulate flood conditions. The hydraulic conductivity of the peat was 0.14m/d, similar to the base conditions. However, the base conditions for barrier hydraulic conductivity for the sand barrier (55.1m/d) did not produce results that represented reality. A barrier hydraulic conductivity of 15m/d was applied and improved the model performance.

The groundwater model at Rhoscolyn then produced a consistent groundwater height and a realistic mixing zone (Figure 4.9). This represents the current conditions within the marsh, where groundwater elevation is controlled by sea-level height. The base model reproduces a slight gradient in the groundwater table, as observed in the field.

Monitoring wells placed within the model, record a spring-neap cycle within the back-barrier peat. This is consistent with the significant detection of the spring-neap cycle using spectral analysis (Table 4.2) and the intermittent signal in wavelet analysis (Figure 4.8). This demonstrates that the model is capable of reproducing conditions observed in the field.

Drought conditions were simulated in the marsh by changing the fixed hydraulic head to 4m, which lowered the groundwater (Figure 4.10). These were run for six and twelve month drought periods, followed by a recovery period of twelve months. Groundwater height is decreased during the drought periods, with the gradient reversed compared to base conditions. There is no observable difference between a six and twelve month drought, in the reduction in groundwater height. Following the drought, the system fully returns to base conditions within a twelve month period. This holds true for both the six and twelve month droughts.

Flood conditions were simulated by applying a 6.4m hydraulic head to the landward side and the top of the marsh, which elevated groundwater to a height where flooding would occur within

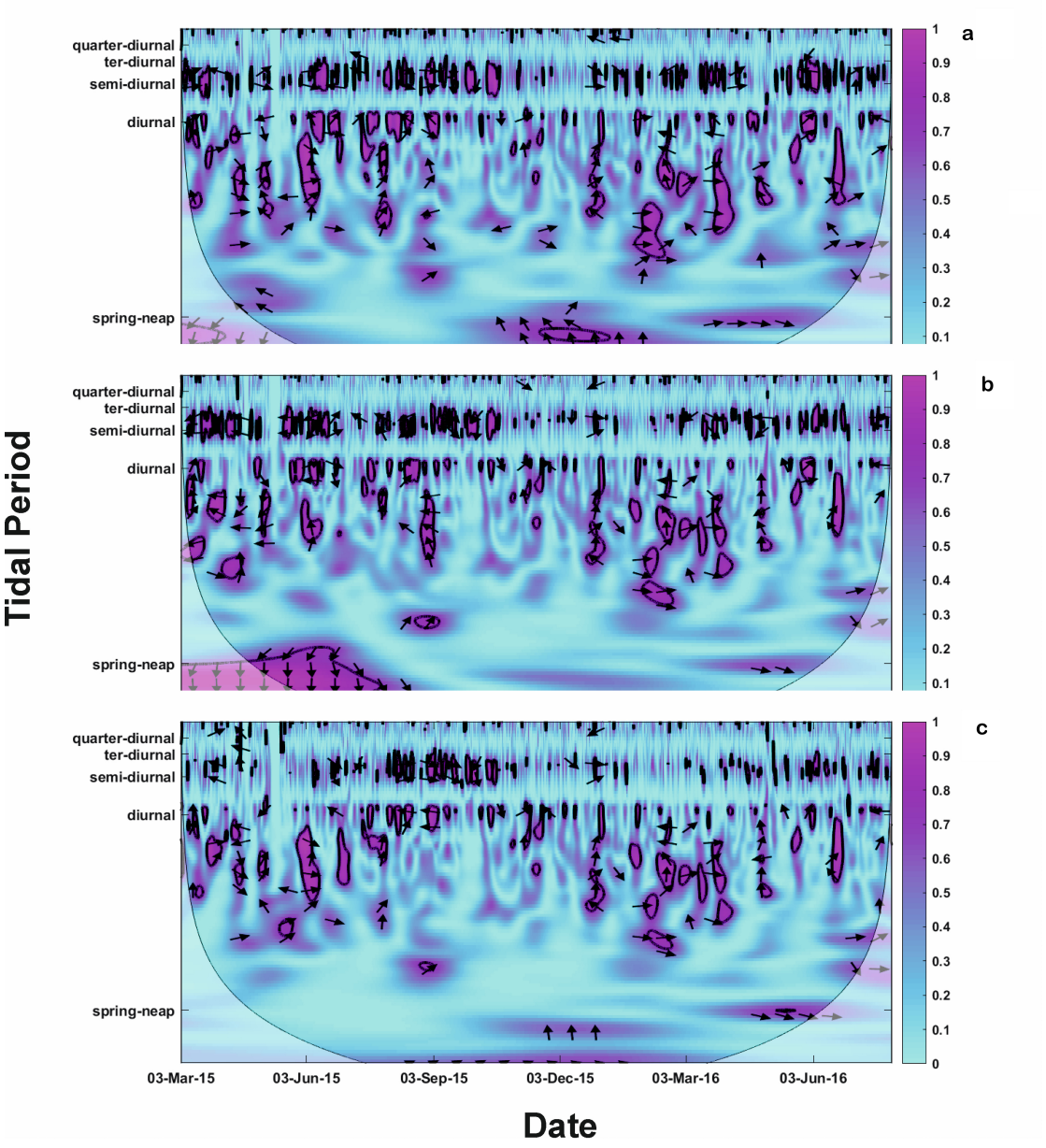

FIGURE 4.8: Squared wavelet coherence between Rhoscolyn tidal and groundwater time series data. Significant areas to the 5% significance level (determined with Monte Carlo methods) are marked purple, with a thick black contour. Semi-diurnal, diurnal and spring neap signals are intermittently significant in well 1 (a), 2 (b) and 3(c).

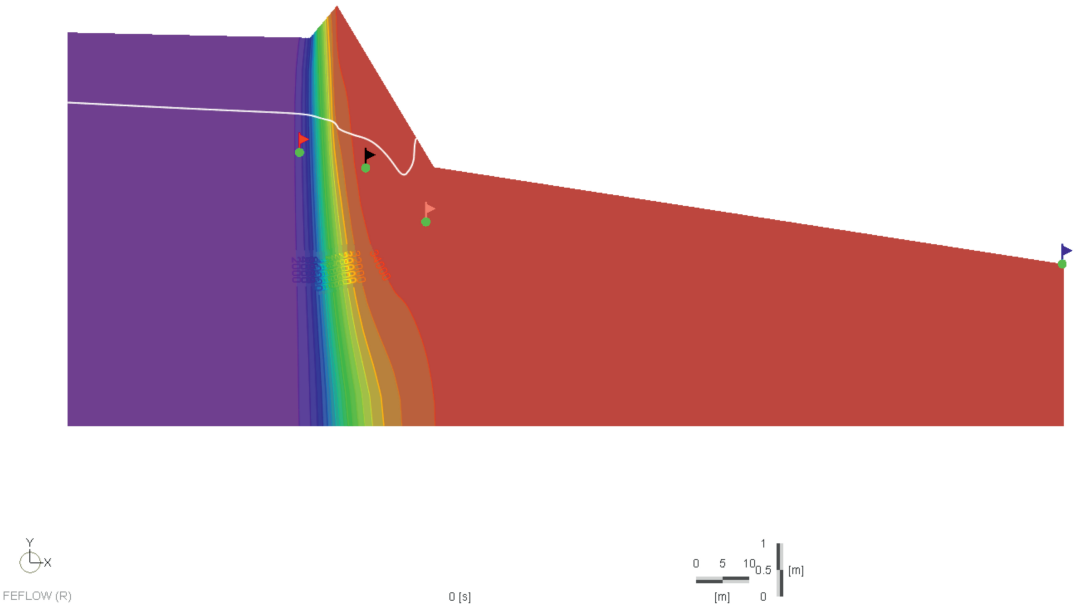

FIGURE 4.9: Cross section of the modelled output for base conditions at Rhoscolyn. Contours show the salinity changes through the groundwater from fully saline (red) to fully fresh (purple). The white line shows groundwater height. Coloured flags represent monitoring wells in the model, displayed in figures 4.12 to 4.15.

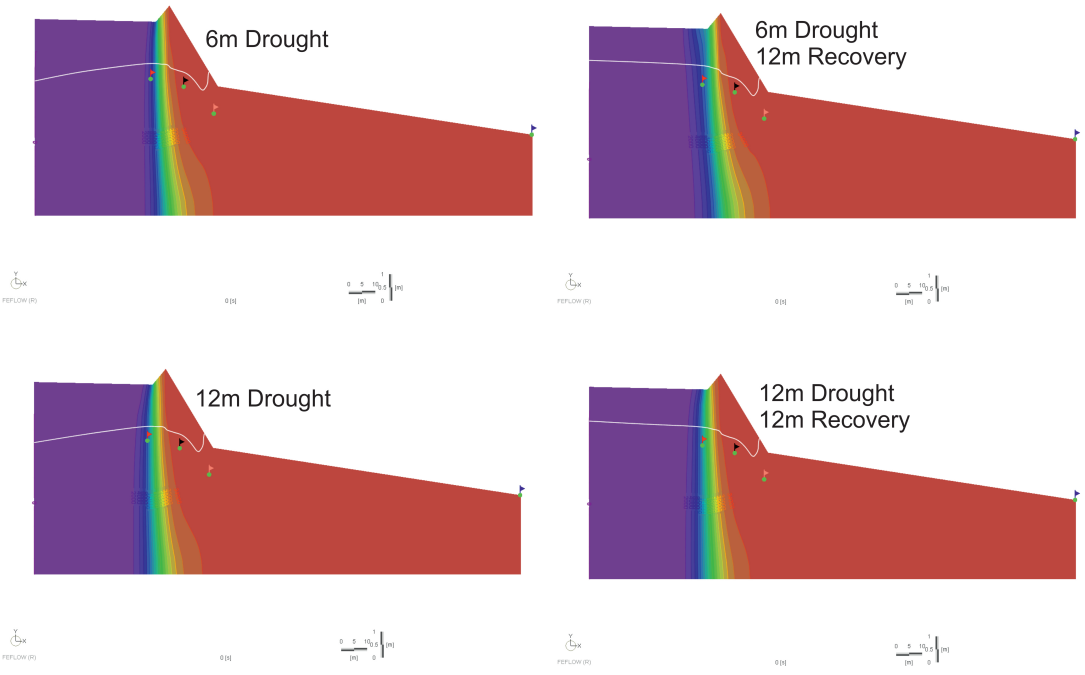

FIGURE 4.10: Cross section of modelled output for drought conditions at Rhoscolyn. Shown are 6 and 12 month drought periods with corresponding 12 month recovery periods. Salinity is represented by contours and groundwater height by the white line. Coloured flags mark the monitoring wells within the model.

the marsh (Figure 4.11). As with the drought model, these were run for six and twelve month periods, followed by a twelve month recovery period. There was no observable difference in recovery between the six and twelve month flooding periods. When flood forcing was removed, the system had returned to base conditions within a twelve month period.

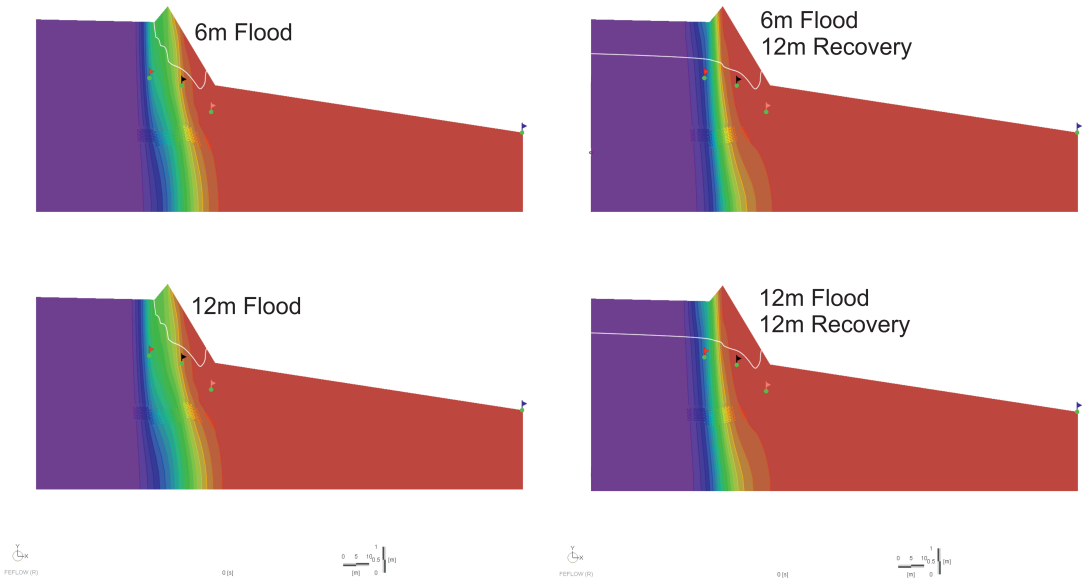

FIGURE 4.11: Cross section of modelled output for flood conditions at Rhoscolyn. Shown are 6 and 12 month flood periods with corresponding 12 month recovery periods. Salinity is represented by contours and groundwater height by the white line. Coloured flags mark the monitoring wells within the model.

Flood conditions didn't fully disconnect groundwater elevation from sea level, although the magnitude of the oscillations dropped by an order of magnitude (Figure 4.12 and Figure 4.13). Once the flood forcing was removed, the base magnitude of tidally induced oscillations was resumed within three spring-neap cycles (c.45 days).

As with flood conditions, drought conditions didn't fully disconnect groundwater elevation from sea level. The reduction in the magnitude of the oscillations is lower than during flood conditions(Figure 4.14 and Figure 4.15). Once the drought forcing was removed, the base magnitude of tidally induced oscillations was resumed within 10 spring neap cycles (150 days).

The well positioned furthest away from the barrier successfully reproduces the spring/neap cycle as identified in the wavelet analysis (Figure 4.8)

These modelling simulations show that should the system be disconnected from the control of sea-level height, during periods of extreme climate, the system very quickly returns to base conditions when the climate returns to normal parameters. This is true for both flooding and dessication events.

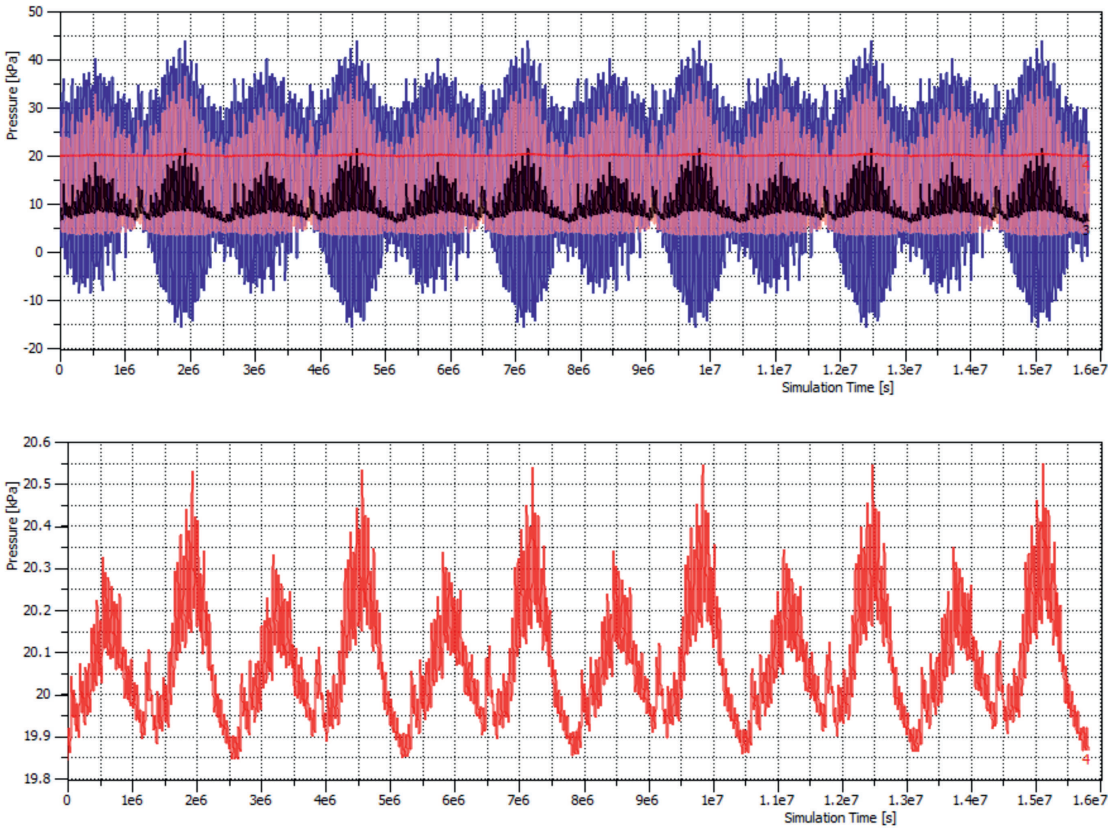

FIGURE 4.12: Modelled tidal oscillations in the groundwater, during flood conditions. Full model (A) colours correspond to wells in Figure 4.9. Marsh groundwater oscillations expanded (B) to show oscillations. All wells show a clear spring-neap cycle of around 1.3e6 seconds.

4.6 Palaeosea-level Determinations

For each SLIP, determinations of palaeosea-level begin with the height of the sample (m OD), the distance behind the barrier from which the sample was collected and an initial indicative meaning, which is taken as the average height of peat formation behind the barrier(Figure 3.8). For Rhoscolyn, the initial indicative meaning is 4.9m OD. The effect of the groundwater gradient is also taken into consideration and a correction is applied. The groundwater gradient for Rhoscolyn is taken as 0.0047, estimated from the topography of the slope (Figure 4.16). The Offshore slope is take as 0.0123, taken from bathymetric maps (Figure 4.17).

This provides the first estimated palaeosea level. However, when the sample was initially formed the barrier would have been further offshore. The palaeo position of the barrier is calculated from Bruun equation (Equation 3.4). This provides a new distance behind the barrier for the sample based on the offshore gradient estimated from bathymetry (Figure 4.17) and as such the correction for the groundwater gradient influence has to be updated. This produces the second estimated palaeosea level. The result of this, is that the position of the palaeobarrier must be

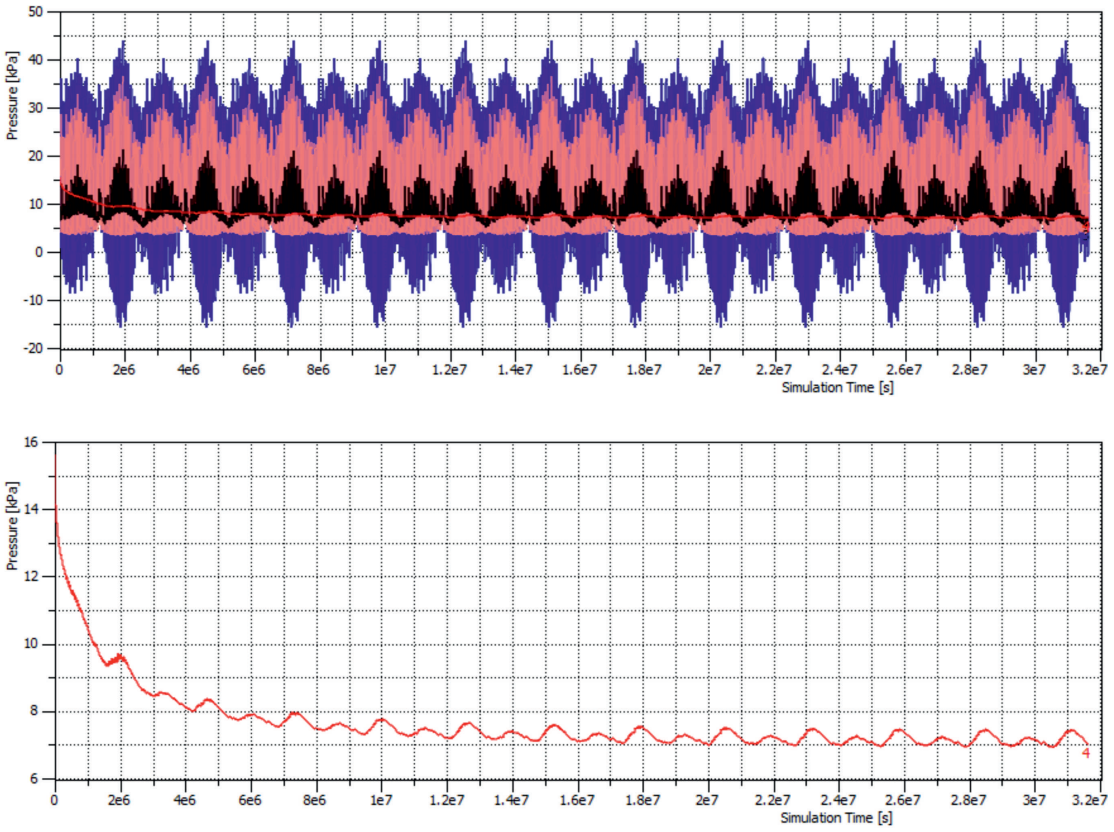

FIGURE 4.13: Modelled tidal oscillations in the groundwater, following the removal of flood conditions. Note the drop in groundwater height in the well situated in the marsh. The spring-neap cycle has increased amplitude compared to those during flood conditions (Figure 4.12).

recalculated. This process is repeated iteratively for each sample (Table A.4), until there is no change in the indicative meaning correction for three iterations.

Two of the dates from this study are accepted as SLIPs for north Wales (Table 6.5) and three are rejected (Figure 4.18). Samples 13 and 14 are in agreement with the existing database, with 14 providing the first SLIP younger than 4000 cal years BP. Samples 9 and 12 are too young, when compared to data from this study and the existing database. As expected, sample 16 was formed in a pre-existing fen or marsh at a time when sea level was not controlling peat formation.

Index Point	Age	Error +	Error -	RSL	RSL +	RSL -
rc13	7381	7447	7303	-5.49	-4.68	-5.97
rc14	1870	2320	1419	-0.33	-0.29	-0.38

TABLE 4.3: New SLIPs established from basal peat at Rhoscolyn and calibrated using CALIB 5.0 ([Stuiver and Reimer, 2018]). Also shown are the associated errors in elevation and age.

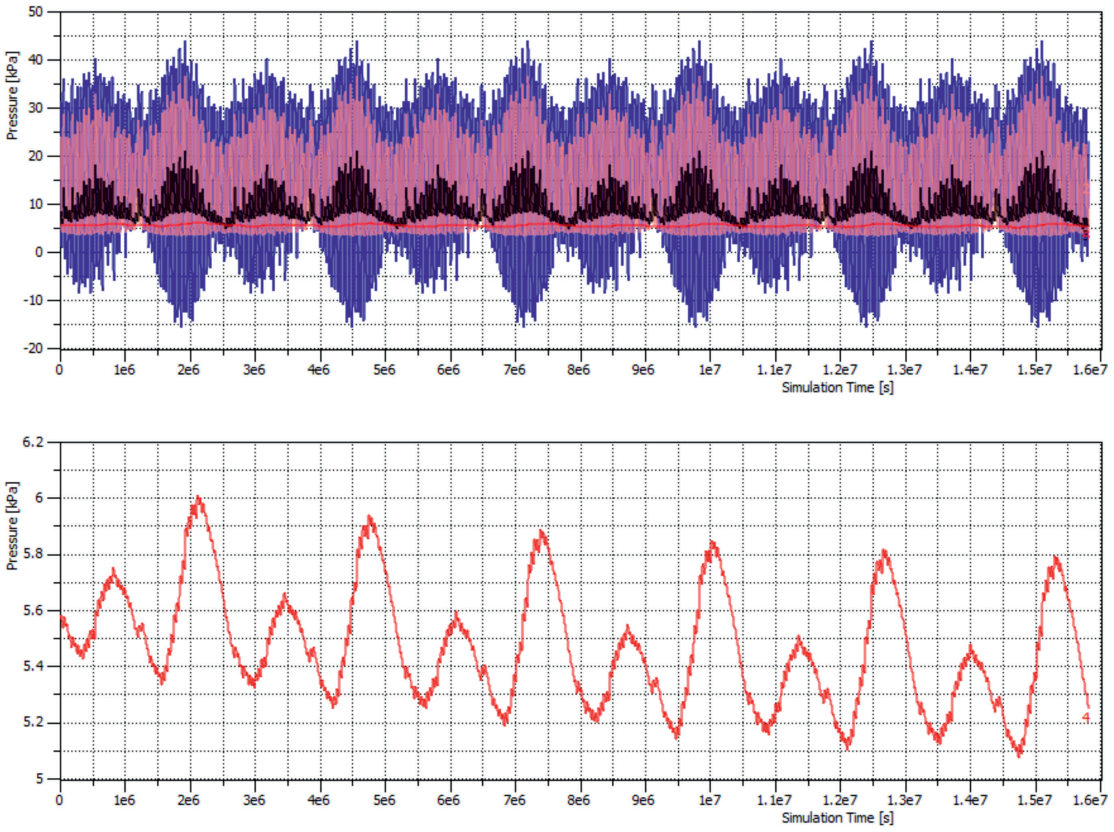

FIGURE 4.14: Modelled tidal oscillations in the groundwater, during drought conditions. Full model (A) colours correspond to wells in figure 4.9. Marsh groundwater oscillations expanded (B) to show oscillations. All wells show a clear spring-neap cycle of around 1.3e6 seconds.

4.7 Synopsis

The groundwater at Rhoscolyn marsh shows a significant connection to ocean oscillations. Wavelet analyses show that correlation between oscillations in the groundwater and the ocean reduce landwards, as a result of tidal efficiency. This demonstrates that the methodology first suggested by Gehrels and Anderson [2014], is suitable for sand/peat barrier systems in addition to gravel/peat systems.

During the course of the Holocene, sea-level rise has resulted in the vertical migration of the marsh. This is captured in the lithostratigraphy, which shows *Phragmites* peat gradually replacing woody peat over time. During this period, the marsh has been subjected overwash and/or slopewash events.

This study provides the first SLIP younger than 4 kyr BP for the north Wales region and add evidence to support the absence of a mid-Holocene highstand. A further SLIP is presented, which is in reasonable agreement to the current data. The lithostratigraphy shows that the fen of Rhoscolyn marsh existed at least c. 14 kyr BP, before sea level was high enough to have an influence on the development of the marsh. This had changed by c. 7300 kyr BP at

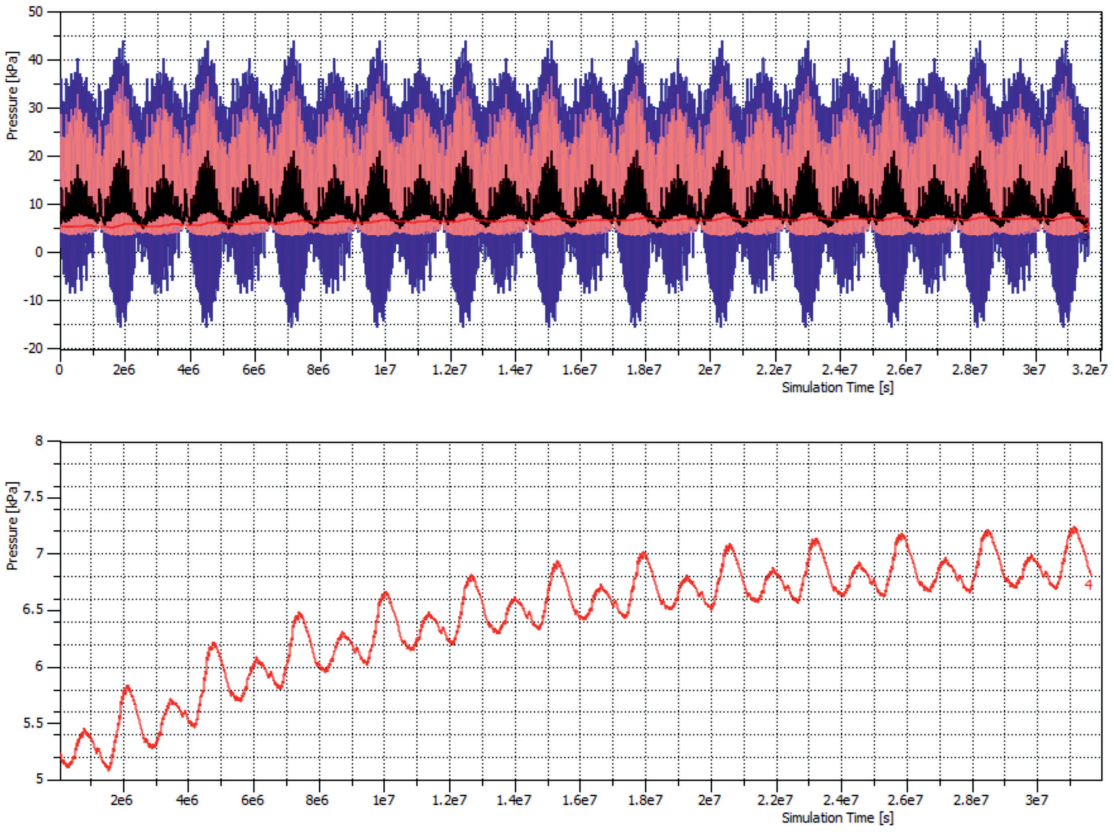

FIGURE 4.15: Modelled tidal oscillations in the groundwater, following the removal of drought conditions. Note the increase in groundwater elevation over time, in the marsh monitoring well.

the latest, towards the end of the period of rapid sea-level rise. The results presented in this chapter demonstrate the suitability of enclosed freshwater peat-sand barrier systems as archives for Holocene sea level.

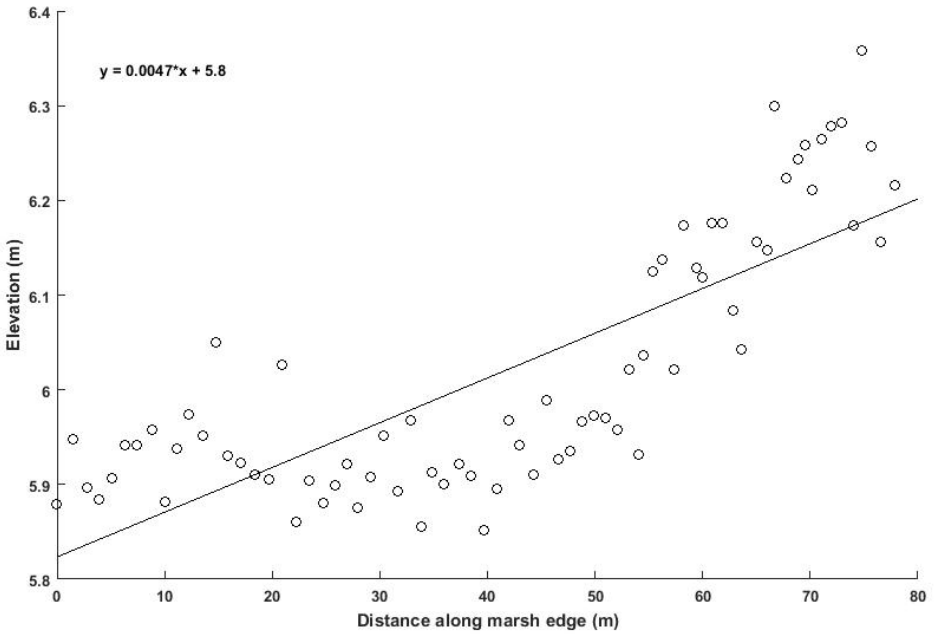

FIGURE 4.16: Measurements of marsh elevation taken along the perimeter of the marsh (Figure 3.1). Groundwater gradient at Rhoscolyn (0.0047m/m) is inferred from topography elevation. SE=0.00043. R^2=0.63. P=0.

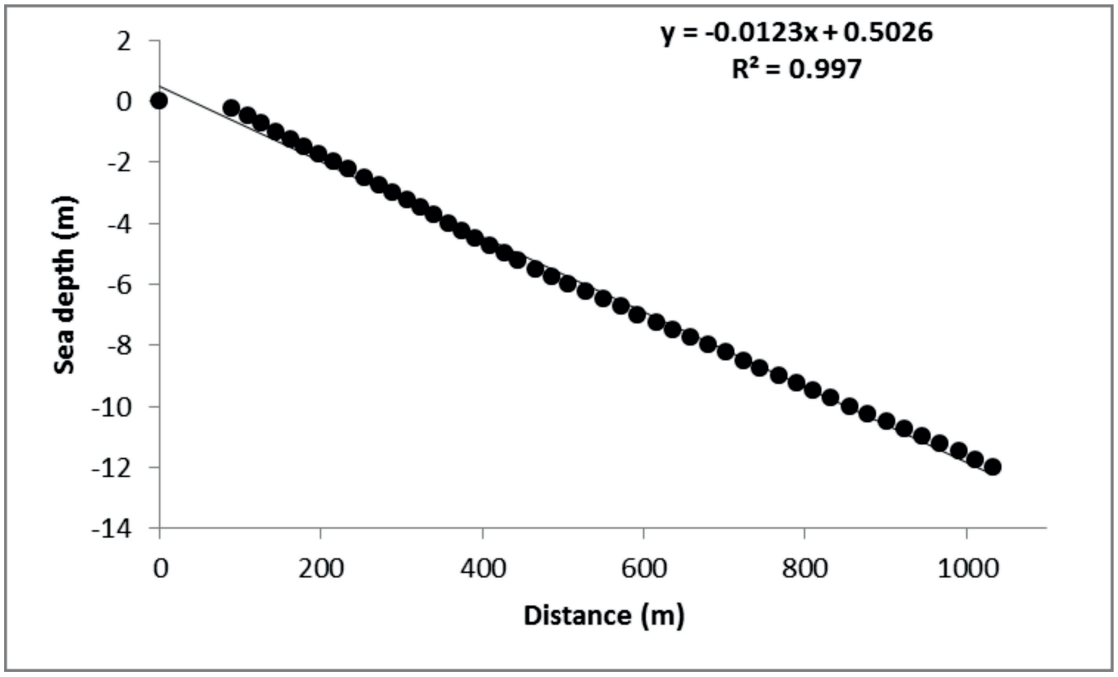

FIGURE 4.17: Offshore gradient at Rhoscolyn (-0.0123m/m), inferred from bathymetry data.

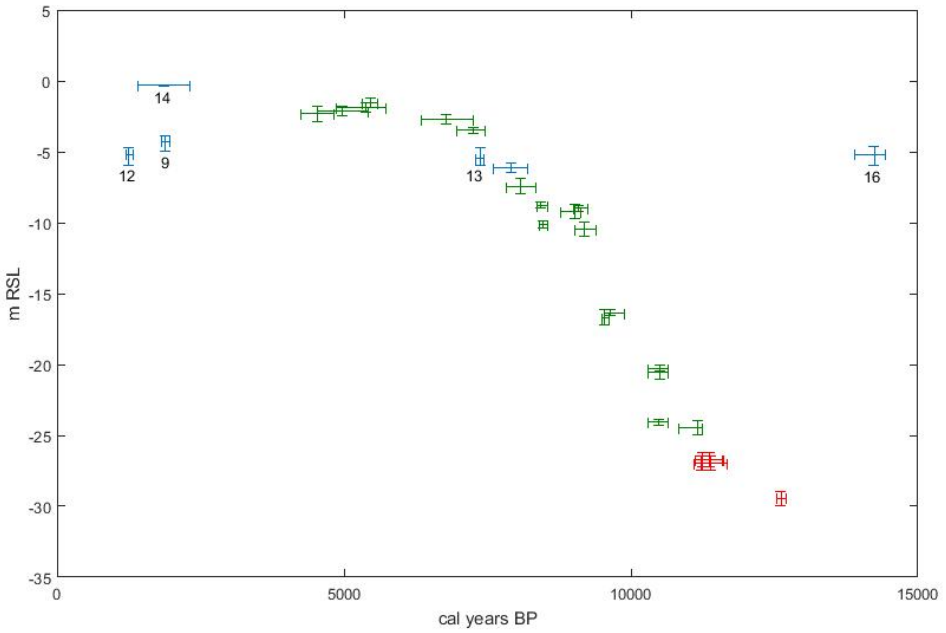

FIGURE 4.18: The basal SLIPs from this study are plotted with the current north Wales database for comparison. SLIPs 13 and 14 are in good agrement with existing data. However, SLIPS 9 and 12 are too young and SLIP 16 is too old.

Chapter 5

Results: Abermawr

5.1 General Introduction

In this chapter six basal SLIPs are presented, collected from a freshwater peat-sandy gravel enclosed back-barrier system at Abermawr in western Pembrokeshire. These SLIPs greatly expand the database, which currently contains only a single index point, and enables more robust testing of modelled Holocene sea-level predictions. In addition to this, the suitability of peat-sandy gravel barrier systems, as archives for Holocene sea level, was assessed.

5.2 Lithostratigraphy

A total of 6 cores were collected for subsampling from two transects, A and B, running parallel to the shoreline (Figure 3.2). A seventh core was obtained from the exposed drowned forest (Figure 3.2). A simplified stratigraphy is shown in Figures 5.1 and 5.2. Both transects are comprised of two distinct stratigraphic units, with *Phragmites* peat overlying woody peat.

A total of 7 cores were taken along transect A (Figure 5.1), which extends 86m, with 4 cores sub-sampled for dating. The underlying pre-Holocene base is a dark grey silty clay, interpreted here as glacial till. The surface of this facies begins at a minimum elevation of -1.87 m OD to a minimum of 1.73 m OD. Overlying the glacial till is a layer of highly humified dark brown peat. The thickest section of this facies is 0.96 cm in the centre of the marsh, tapering towards the edge of the marsh to 0.76 cm. Overlying the humified peat is a thick layer of reddish brown woody peat. Fragments of red wood are present throughout the facies, with the occasional light brown wood fragments at shallow depths in the centre of the marsh. In places, large remains of wood can be found, the size of trunks or large branches. In the centre of the marsh, the woody peat is interrupted by a section of clayey peat, with extends upwards 1.5 m in total. However,

after 0.50 m this is interrupted by a 0.10 m band of clay, before continuing with clayey peat. At the edges of the marsh, this is interrupted by sand, clayey peat and clay to the south-western edge and sand to the north-east. Here, these deposits are interpreted as slope wash. From around 3.5 m OD to the surface is a thick section of *Phragmites* peat, extending the full width of the marsh. Large *Phragmites* remains are preserved in the first meter, which are replaced by smaller *Phragmites* fragments in the deeper section. Potential evidence of standing water is present, with clay deposits to the south-western edge and sand to the north-eastern. There is also a 0.30 m thick deposit of clayey peat, interrupting the *Phragmites* peat in the centre of the marsh. Overall, the general trend is of *Phragmites* peat overlying woody peat, which in turn overlies a pre-Holocene substrate of glacial till.

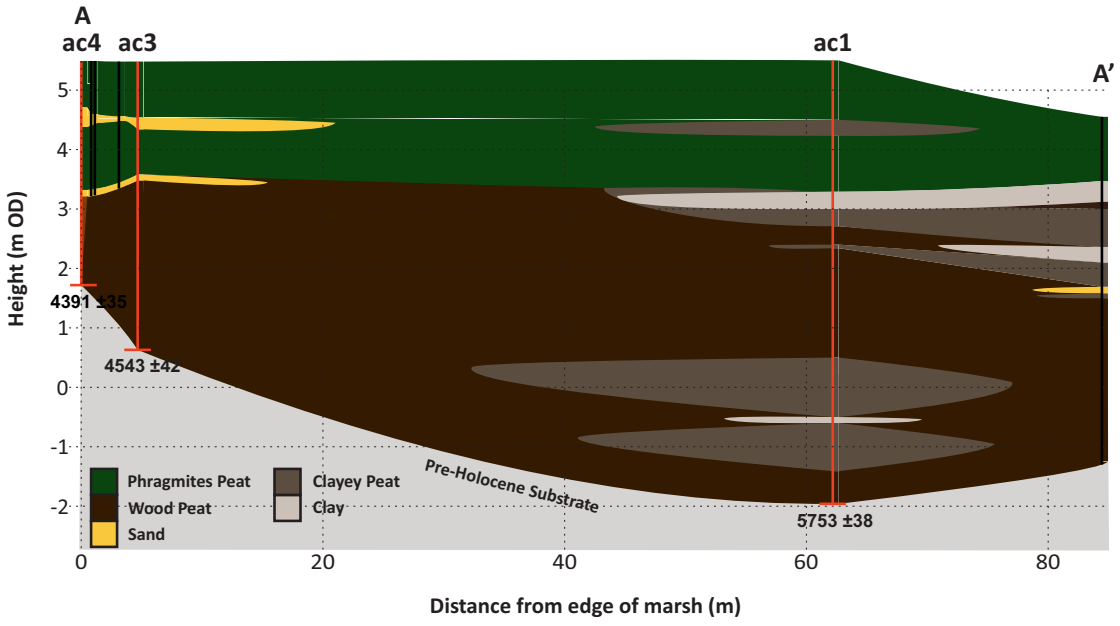

FIGURE 5.1: Shore normal stratigraphy for transect A, running north east (A) to south west (A′), with a simplified stratigraphy from 7 cores. See figure 3.2 for location.

A total of 24 cores were taken from transect B (Figure 5.2), which extends 132m, with 2 cores sub-sampled for dating. Coring the north-eastern edge of transect B was limited to less than 1 m, because of large, flat rocks which extend to just over 25 m into the marsh. The same dark grey glacial till is present as the Holocene base, starting at around 0.5 m OD in the deepest section of the marsh and sharply rising, in two steps, towards the north-eastern edge to a depth of around 5.5 m OD. At the deepest section of the marsh, the base is overlain by a 1.18 m thick layer of dark brown humified peat. This is overlain by woody peat containing large pieces of reddish brown wood. The thickness of the facies varies across the marsh and is thicker towards the north-eastern edge, suggesting that the forest persisted longer at the edges and in keeping with the presence of a modern-day woodland along the current valley slope. The deepest section of the woody peat is interrupted by a thin 0.07 m sand layer, which does not extend to the edges. Overlying the woody peat is a thick layer of *Phragmites* peat, which extends from a maximum

depth of 2.41 m OD to the surface. Apart from the fresh peat at the surface, only small fragments of *Phragmites* are preserved throughout this section. There is no evidence of slope wash to the north-eastern edge but the south-western edge has layers of sandy peat which overlay the rocky area. The general trend is of *Phragmites* peat overlying woody peat, which in turn overlies a pre-Holocene substrate of glacial till.

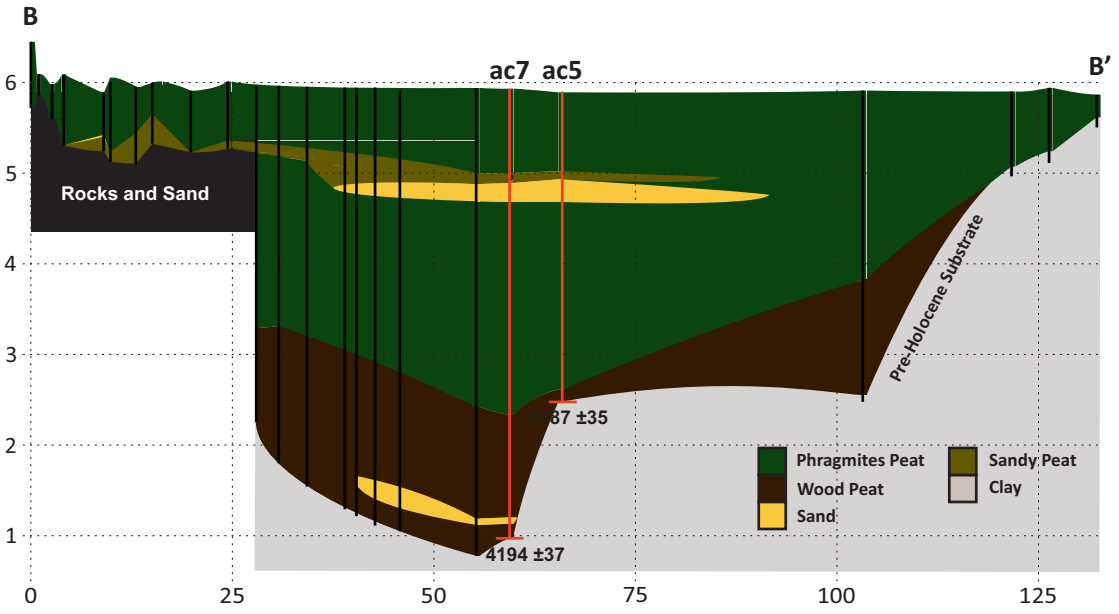

FIGURE 5.2: Shore normal stratigraphy for transect B, running north east (B) to south west (B′), with a simplified stratigraphy from 24 cores. See figure 3.2 for location.

The stratigraphy is indicative of a marine transgressive back barrier system, demonstrating a horizontal shift in the marsh zonation. Older fen/carr deposits, which would have formed during lower sea level, are replaced by *Phragmites* deposits. Neither transects shows evidence of channelisation, supporting the assumption that the barrier has remained closed over time.

5.3 Chronology

The chronology of Abermawr is determined from six AMS ^{14}C dates obtained from plant fragments preserved in basal peat from cores ac1, 3, 4, 5, 6 and 7 (Table 5.1). The dates obtained from cores ac1, 3, 5, 6 and 7 are in good agreement. However, the date obtained from core ac4 suggests a higher than expected sea level (Figure 5.12), in comparison to the other dates obtained. None of the dates collected are inverted when compared to the stratigraphy, and there is nothing to suggest that the samples have been contaminated.

Index number	1	3	4	5	6	7
Radiocarbon lab. number	SUERC-72893	SUERC-72895	SUERC-72901	SUERC-72902	SUERC-72903	SUERC-72904
Core	ac001	ac003	ac004	ac005	ac006	ac007
Material	Plant macrofossil	Plant macrofossil	Plant macrofossil	Plant macrofossil	Plant macrofossil	Plant macrofossil
14C Enrichment (% Modern ± 1σ)	48.86 ± 0.23	56.80 ± 0.30	57.89 ± 0.25	70.69 ± 0.31	46.83 ± 0.21	59.33 ± 0.27
14C age (years BP ± 1σ)	5753 ± 38	4543 ± 42	4391 ± 35	2787 ± 35	6094 ± 35	4194 ± 37
Calibrated BP ± 1σ age ranges	(6496 - 6568)	(5066 - 5111)	(4877 - 4975)	(2850 - 2929)	(6902 - 7001)	(4649 - 4672)
	(6586 - 6626)	(5121 - 5182)	(5017 - 5031)	(2933 - 2943)		(4699 - 4759)
		(5272 - 5312)				(4807 - 4835)
Calibrated BP ± 2σ age ranges	(6453 - 6651)	(5046 - 5205)	(4859 - 5048)	(2789 - 2962)	(6808 - 6811)	(4588 - 4595)
		(5210 - 5319)	(5201 - 5211)		(6856 - 7030)	(4613 - 4766)
		(5428 - 5430)			(7045 - 7049)	(4783 - 4844)
					(7055 - 7069)	
					(7078 - 7085)	
					(7099 - 7156)	
Median calibrated age (cal yrs BP)	6553	5164	4951	2887	6962	4729
Carbon content (% by weight)	61.6	64.3	58.1	54.4	57.3	58.7
$\delta^{13}C_{VPDB}$ ‰(±0.1)	-32	-30.1	-28.9	-28.8	-31.4	-31

TABLE 5.1: Abermawr radiocarbon dates and associated errors. All dates wer obtained from plant microfossils.

5.4 Groundwater Monitoring

5.4.1 Well data

Monitoring wells were positioned 40m (SM 88243 34498), 60m (SM 88253 34483) and 77 m (SM 88265 34471) behind the crest of the barrier. The records cover an uninterrupted period between the start of April 2015, through to the end of July 2017 and monitors changes in groundwater elevation (Figure 5.3) and temperature (Figure 5.4). The long record shows a clear seasonal temperature signal, with temperature peaking around October, before falling to a minimum around May. The long record for elevation is noisy and as such it is not possible to identify any of the tidal constituents in the long record.

5.4.2 Spectral analyses

Spectral analyses of the groundwater data was used to overcome the difficulties of identifying the tidal constituents in the data. The tide gauge data from Fishguard, the nearest available to the site, was also analysed for comparison. To test for significance of the signal, a Fisher G-statistic test was performed. The semidiurnal tide was only identified in well two, with the diurnal tide and spring-neap cycle identified in all the wells (Figure 5.5).

The semidiurnal tide occurs at a frequency of around 20μHz and is significant (p=0) in both the tide gauge and well two data. The diurnal tide occurs at a frequency of around 10μHz and is significant in all three wells and the tide gauge (p=0). Spring neap cycles occur at a frequency of around 0.7μHz and is significant in all three wells (p=0) but not in the tide gauge data. The lack of significance in the tide gauge data is unexpected but could be due to localised effects (Table 5.2).

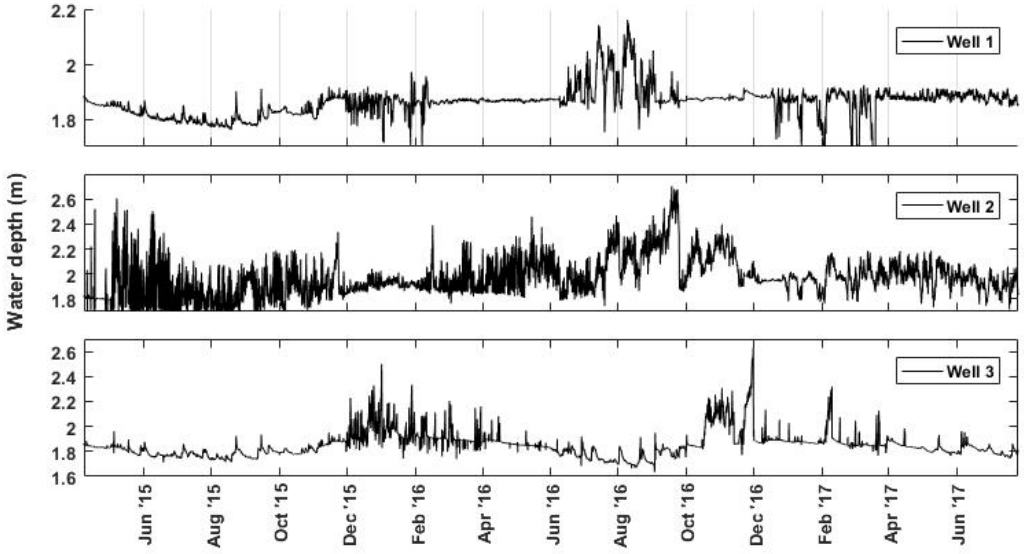

FIGURE 5.3: Monitoring wells 1-3 at Abermawr showing fluctuations in groundwater elevation. Only well 3 shows any seasonality in the elevation.

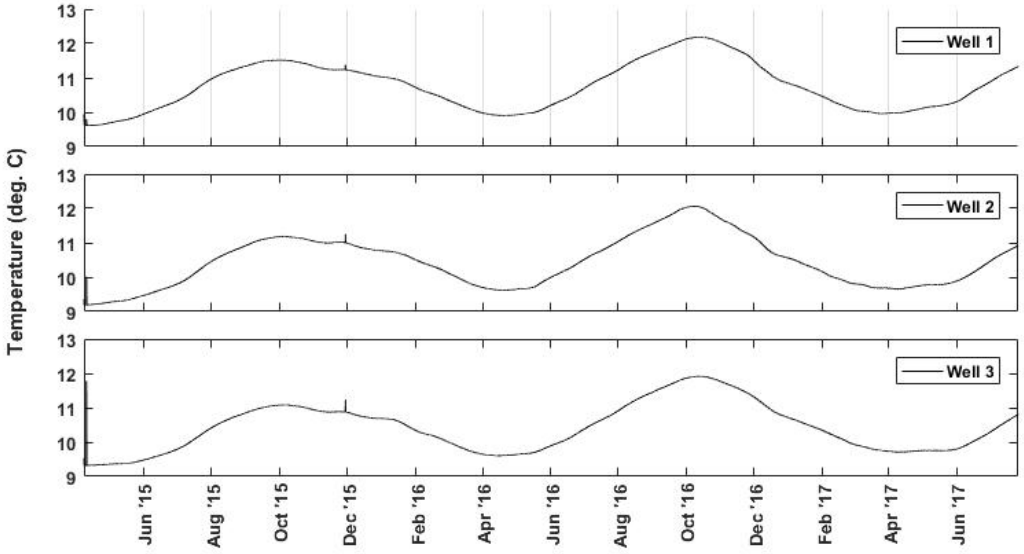

FIGURE 5.4: Monitoring wells 1-3 at Abermawr showing fluctuations in groundwater temperature. All three wells show seasonality in temperature.

5.4.3 Wavelet analyses

Wavelet analysis is used to identify any relationship between the tide gauge record at Fishguard and the groundwater data from the wells at Abermawr. In all three wells, correlation between

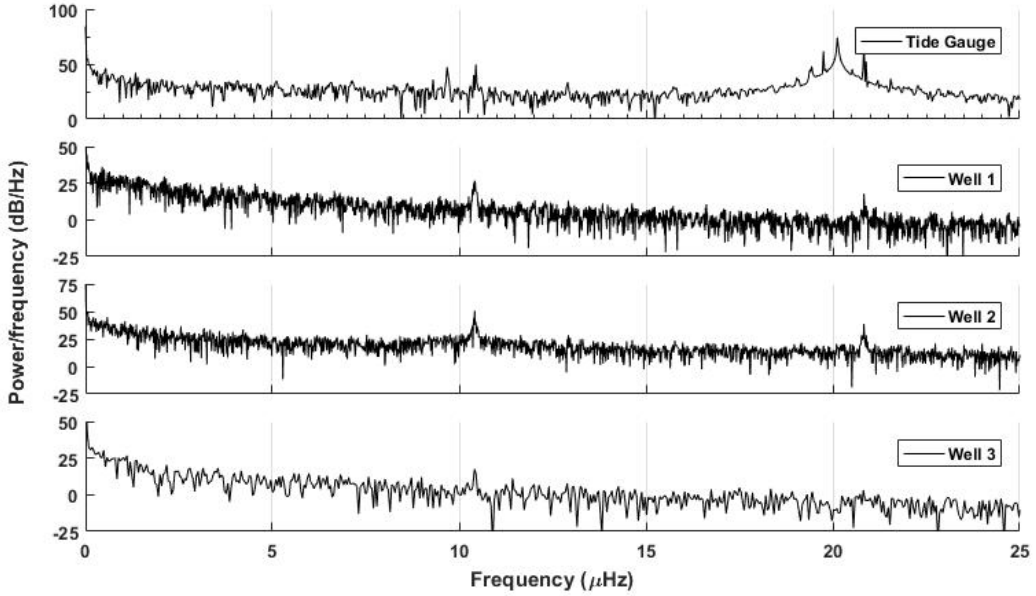

FIGURE 5.5: Spectral Analysis showing the frequency of peaks in water elevation. Groundwater monitoring wells are shown alongside the Fishguard tide guage for comparisson. Semi-diurnal tides occur around 20 μHZ, diurnal tides around 10.4 μHZ and spring-neap tides around 0.75 μHZ.

SITE	SEMI-DIURNAL (μ HZ)	FISHER G	P VALUE	DIURNAL (μ HZ)	FISHER G	P VALUE	SPRING-NEAP (μ HZ)	FISHER G	P VALUE
FISHGUARD	20.1	0.611	0	10.42	0.002	0	0.71	0	2.01×10^{6}
WELL 1	20.82	0	0.645	10.4	0.002	0	0.73	0.005	0
WELL 2	20.82	0.004	0	10.4	0.065	0	0.72	0.004	0
WELL 3	20.77	0	3.66×10^{10}	10.37	0.002	0	0.71	0.008	0

TABLE 5.2: Abermawr peak frequency significance in water elevation, as tested by Fisher G statistic. Reported frequencies represent the highest peak around the expected tidal constituent.

changes in elevation at periods concurrent with semi-diurnal and diurnal tides is significantly correlated to the tide gauge record. This is tested to the 95th significance level against red noise, using Monte Carlo methods (Figure 5.6).

The general pattern of correlation across the three wells shares the same characteristics. The power of the relationship reduces landwards as a result of signal attenuation through the sub-surface, an expected consequence of tidal efficiency. Correlation does not remain significant throughout the year, particularly during the winter of 2015. This is probably a result of increased precipitation masking the tidal signal in the groundwater.

The spring-neap cycle is well recorded in the back-barrier groundwater. All wells show a consistent spring-neap signal throughout the year. This is in contrast to the Rhoscolyn site and is perhaps a result of the barrier material. Although, local tidal effects could also play a part. Taken alongside the spectral analysis, it can be taken with high confidence that the spring-neap cycle is present in the groundwater.

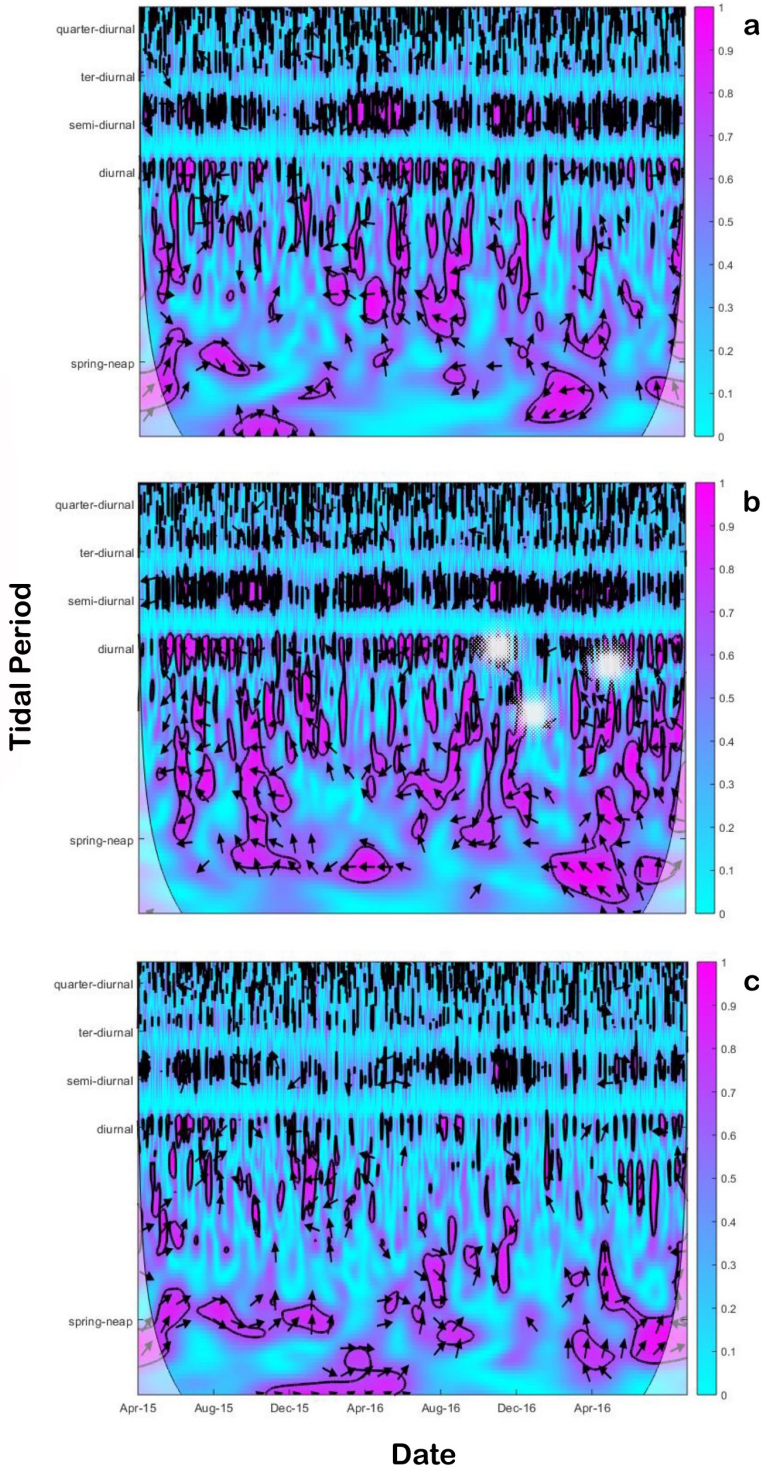

FIGURE 5.6: Squared wavelet coherence between Abermawr tidal and groundwater time series data. Significant areas to the 5 % significance level (determined with Monte Carlo methods) are marked purple, with a thick black contour. Semi-diurnal, diurnal and spring-neap signals are intermittently siginficant in well 1(a), 2(b) and 3(c).

5.5 Groundwater Model

The Abermawr base conditions produced a stable model, which was representative of the field data. The hydraulic conductivity remained the same as the base conditions, with peat set at 0.001 m/d and the barrier 27m/d. Recharge was applied along the top peat boundary, at a rate of 0.00123m/d. The model produced a consistent groundwater height and realistic mixing zone (Figure 5.7), There is a slight gradient in the groundwater table, consistent with the field data.

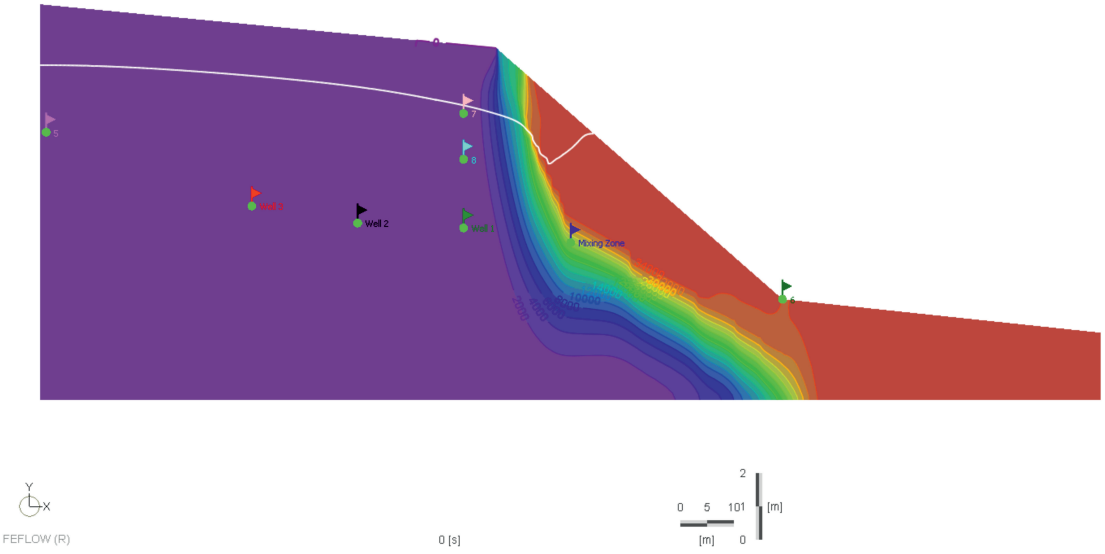

FIGURE 5.7: Cross section of the modelled output for base conditions at Abermawr. Contours show the salinty changes through the groundwater from fully saline (red) to fully fresh (purple). The white line shows groundwater height. Coloured flags represent monitoring wells in the model, displayed in figure 5.9

Drought conditions were simulated by reducing the recharge boundary to 0.00061m/d and the simulation ran for twelve months. The groundwater table remained stable throughout this period (Figure 5.8), showing that the system is resilient to dessication events.

Flood conditions were simulated by increasing the recharge boundary to 0.00246m.d and the simulation ran for six months. As with the drought conditions, the groundwater table remained stable (Figure 5.8). This resilience to climate changes is probably the result of low hydraulic conductivity in the peat, dampening the effects of changing recharge.

Groundwater oscillations were monitored during the drought event, but not during the flood event due to time constraints. They show a clear spring-neap tidal signal in the well closest

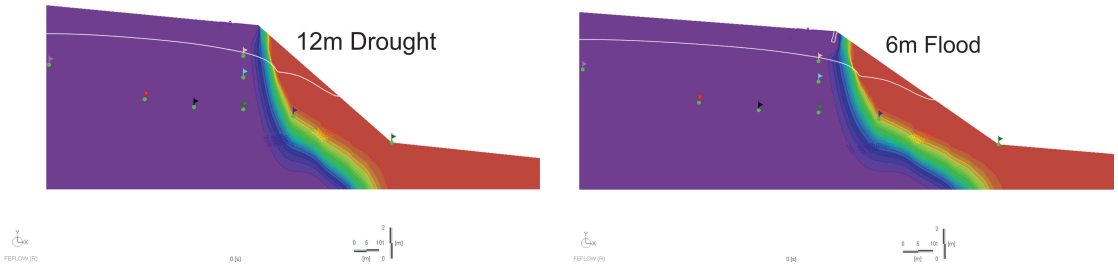

FIGURE 5.8: Cross section of modelled output for flood and drought conditions at Abermawr. Shown are the final conditions for a 12 month drought and 6 month flood event.

the barrier, remaining present during the drought conditions (Figure 5.9). Whilst groundwater height reduces slightly, it is a negligible change.

The model is able to reproduce the spring-neap cycle in the back-barrier marsh. This is inline with the wavelet and spectral analyses performed on the well data. As such, there is some confidence in the models ability to simulate groundwater response to tidal forcing.

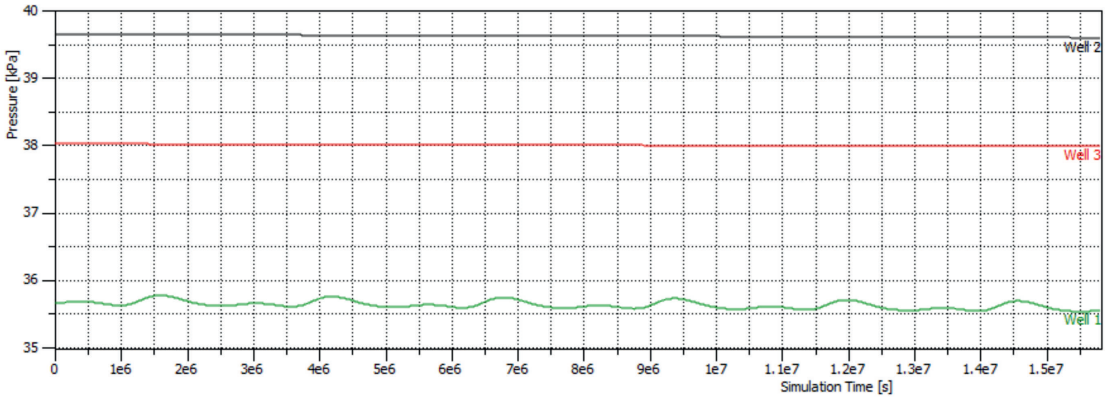

FIGURE 5.9: Modelled tidal oscillations in the groundwater, during drought conditions. Only well 1 maintains a spring-neap tidal signal in the groundwater.

These modelling simulations show that the Abermawr system is resilient to drought and flooding conditions brought about by climate. Tidal oscillations are present in the groundwater and remain so during drought conditions.

5.6 Palaeosea-level Determinations

At Abermawr, the base case indicative meaning is taken as 4.66m OD, the average elevation directly behind the marsh (Figure 3.8). Corrections to the indicative meaning are made, based on the gradient of the groundwater and the offshore slope. The groundwater gradient is inferred

from the topography slope (0.00045) (Figure 5.10) measured along the perimeter of the marsh (Figure 3.8).

Initial calculations for past sea-level are made, allowing for the position of the palaeo-barrier to be established as a function of the offshore slope(0.014), inferred from bathymetry (Figure 5.11). This process is repeated iteratively, until the indicative meaning correction remains unchanged for three iterations.

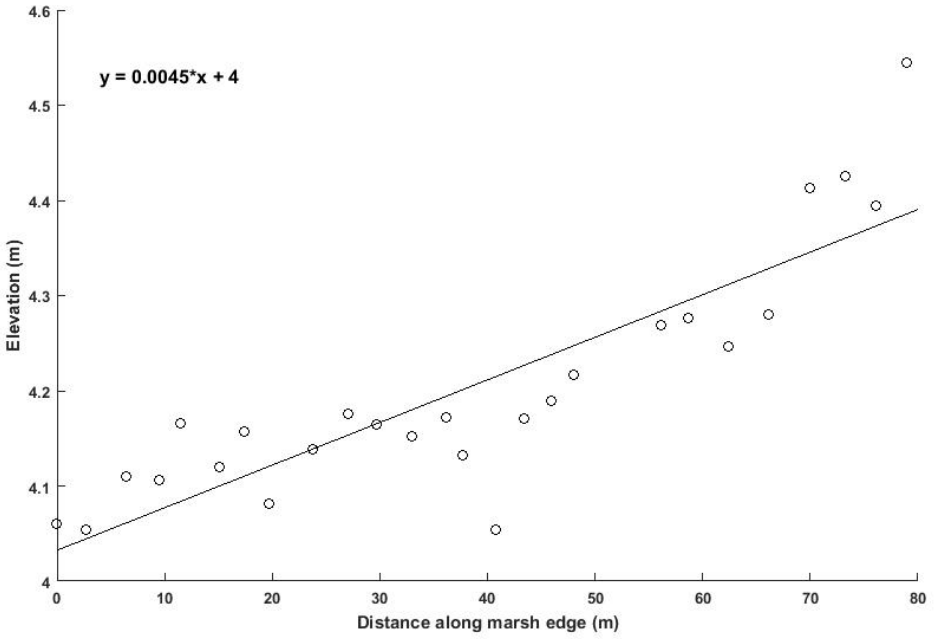

FIGURE 5.10: Measurements of marsh elevation taken along the perimeter of the marsh (Figure3.2). Groundwater gradient (0.0045m/m) inferred from topography elevation. SE=0.00052. P=0. R^2=0.75.

All of the new index points collected (Table 5.3) are accepted into the existing database for Pembrokeshire.These represent a significant increase to the Pembrokeshire sea-level database, which previously consisted of a single SLIP. When compared to the Glamorgan sea-level, they are in good agreement with the existing data (Figure 5.12).

Index Point	Age	Error +	Error -	RSL	RSL +	RSL -
ac1	6553	6651	6453	-9.48	-8.61	-10.54
ac3	5164	5430	5046	-5.86	-5.32	-6.52
ac4	4951	5211	4859	-4.26	-3.87	-4.74
ac5	2887	2962	2789	-3.10	-2.82	-3.45
ac6	6962	7156	6808	-11.25	-10.22	-12.51
ac7	4729	4844	4588	-5.35	-4.86	-5.95

TABLE 5.3: New SLIPs established from basal peat at Abermawr and calibrated using CALIB 5.0 [Stuiver and Reimer, 2018]. Also shown are the associated errors in elevation and age.

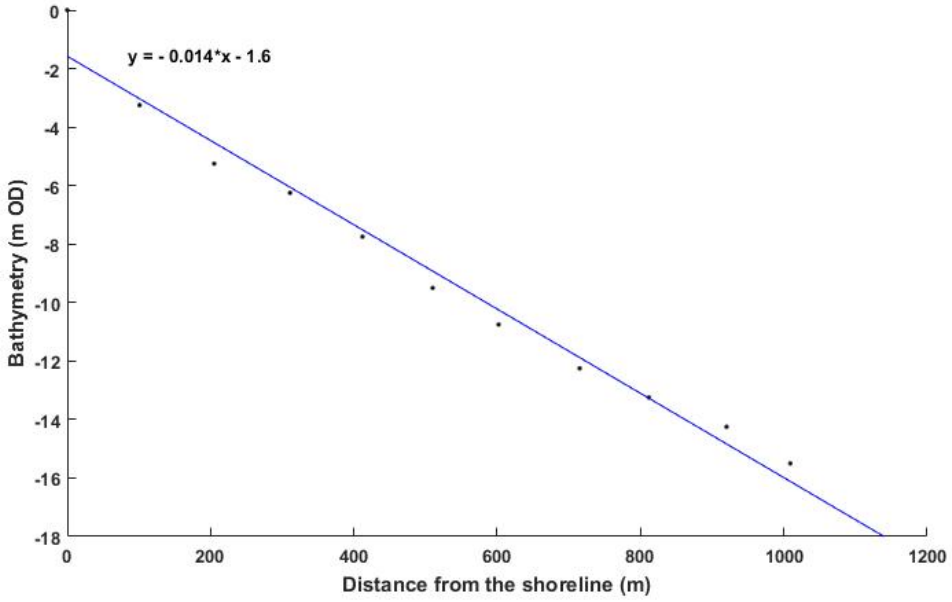

FIGURE 5.11: Offshore gradient at Abermawr inferred from bathymetry data.

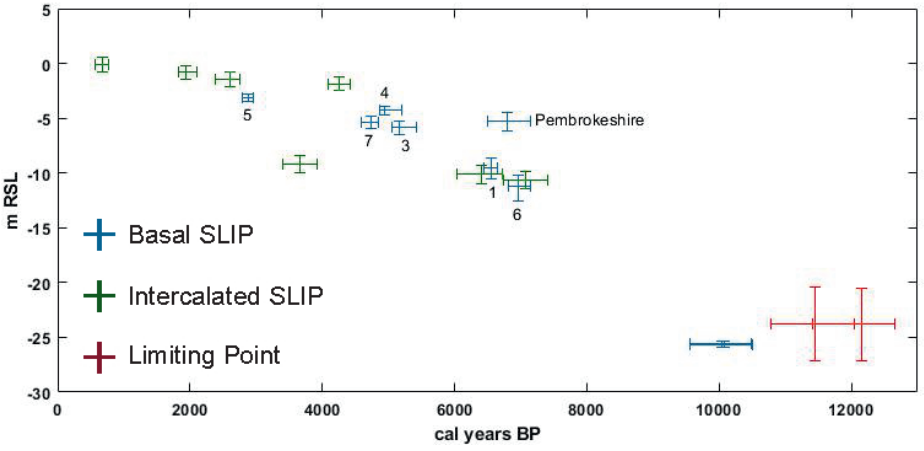

FIGURE 5.12: New basal SLIPs from this study plotted with the current Glamorgan and Pembrokeshire database for comparison. All SLIPs are in good agreement with the existing data.

5.7 Synopsis

Oscillations in the groundwater at Abermawr marsh are significantly correlated with tidal action as recorded by the Fishguard tide gauge. This is supported by both spectral and wavelet analyses. This demonstrates that peat-sandy gravel coastal back-barrier systems are suitable archives of Holocene sea-level data.

There is no evidence of open channels in the marsh stratigraphy, meaning the peat is unlikely to have been reworked. There is evidence of slopewash and/or overwash events in the marsh, with evidence that could suggest standing water at some time. However, this is unlikely to have affected the sampled peat.

Six new basal SLIPs are submitted to the database, expanding the Pembrokeshire database to seven. When compared to the existing Glamorgan data, they are in good agreement. These data fill an important gap during the mod Holocene and allow for more robust testing of RSL changes predicted by GIA models

Chapter 6

Discussion

6.1 Freshwater Barrier Systems as Sea-level Archives

The suitability of freshwater back-barrier systems as sea-level archives, utilising the methodology in this study, was first presented by Gehrels and Anderson [2014]. Four conditions were proposed for a system to be suitable:

1. The back-barrier stratigraphy shows uninterrupted peat sequences that demonstrate that the barrier has remained closed throughout the history of peat accumulation and that processes that instigate reworking of peat (e.g. creek bank erosion) have been insignificant.
2. Field and modelling evidence shows that the influence of sea level on the back-barrier water table is strong and rapid enough to overprint climate-controlled variability.
3. Values of recharge and peat permeability are within the limits that prevent ponding or drying out of the back-barrier marsh and are the primary control on the water table in the back-barrier marsh.
4. The beach is relatively thin and its permeability is not the main control on the elevation of the water table in the back-barrier marsh.

This thesis aims to establish RSL histories for Anglesey and western Pembrokeshire and evaluate the method proposed by Gehrels and Anderson [2014], with regards to sand and sandy gravel barrier systems. As will be demonstrated below, all four conditions are met at both sites and as such the freshwater back-barrier systems are suitable archives of past sea level.

6.1.1 Stratigraphy

At both Abermawr and Rhoscolyn the stratigraphy consists of *Phragmites* peat deposits overlying woody peat deposits and ancient peat crops out on the foreshore at low tide. Both sites are closed

back-barrier freshwater transgressive systems, responding to Holocene RSL rise in the same manner as described by Kraft and Chrzastowski [1985] (Figure 6.1 A). In a closed system, the rollover of the barrier results in onshore migration (Figure 6.1 B); the *Phragmites* swamp replaces the carr as groundwater rises in response to changing hydraulic gradients, driven by RSL rise. As such it is reasonable to expect the carr or fen peat was deposited at the leading edge of the Holocene transgression and can be expected to contain an archive of the history of sea-level rise.

The stratigraphy of the peat sequence in the freshwater back-barrier system at Abermawr is only interrupted by deposits interpreted as over wash and slope wash events. As such, there is no evidence of channelling and so it is concluded that the barrier system has remained closed throughout the time of peat development. The Rhoscolyn stratigraphy has a large sand deposit in transect Y, possibly a storm deposit. The sand does not cut a channel to the base of the peat and it is unlikely to have caused significant reworking and is not of importance to the basal peat deposit. As such, both sites fulfil the first condition of site suitability as proposed by Gehrels and Anderson [2014], that the peat has only been subjected to insignificant processes to cause reworking.

6.1.2 Groundwater Monitoring

Several studies have shown that coastal groundwater is expected to rise in response to rising sea level and that the magnitude of that rise is dependent on both distance from the coast and the hydraulic conductivity of the sediments within an environment [Austin et al., 2013, Gehrels and Anderson, 2014, Geng and Boufadel, 2017, Knott et al., 2018]. Peat contained within freshwater wetlands have low hydraulic conductivities, meaning any rise in groundwater is expected to be dampened. It is possible that overwash deposits could result in a granular sedimentation in the back barrier deposits and increase the hydraulic conductivity of the wetland.

Overwash events could lead to sustained flooding in the back-barrier marsh and decouple the system from sea level. However, there is no evidence of sustained salt-water intrusion at Rhoscolyn, the only site equipped to monitor salinity. There are occasional saline overwash events at the front of the marsh, but salinity levels very quickly return to normal, indicating that recharge and drainage is sufficiently high to prevent ponding of salt water. Although at Abermawr salinity was not recorded, the barrier in that system is gravely sand and has higher hydraulic conductivity than the barrier at Rhoscolyn. As such, it would be expected that any saline overwash would be quickly drained from the site, as demonstrated by Austin et al. [2013], where they show that the height of freshwater lagoons and barrier width prevent saline intrusion.

The dampening of the tidal signal means that the magnitude of the groundwater oscillation is not large enough to observe in the raw data by visual inspection. However, spectral analyses of groundwater fluctuations and tidal movements recorded by the local tide gauge revealed the

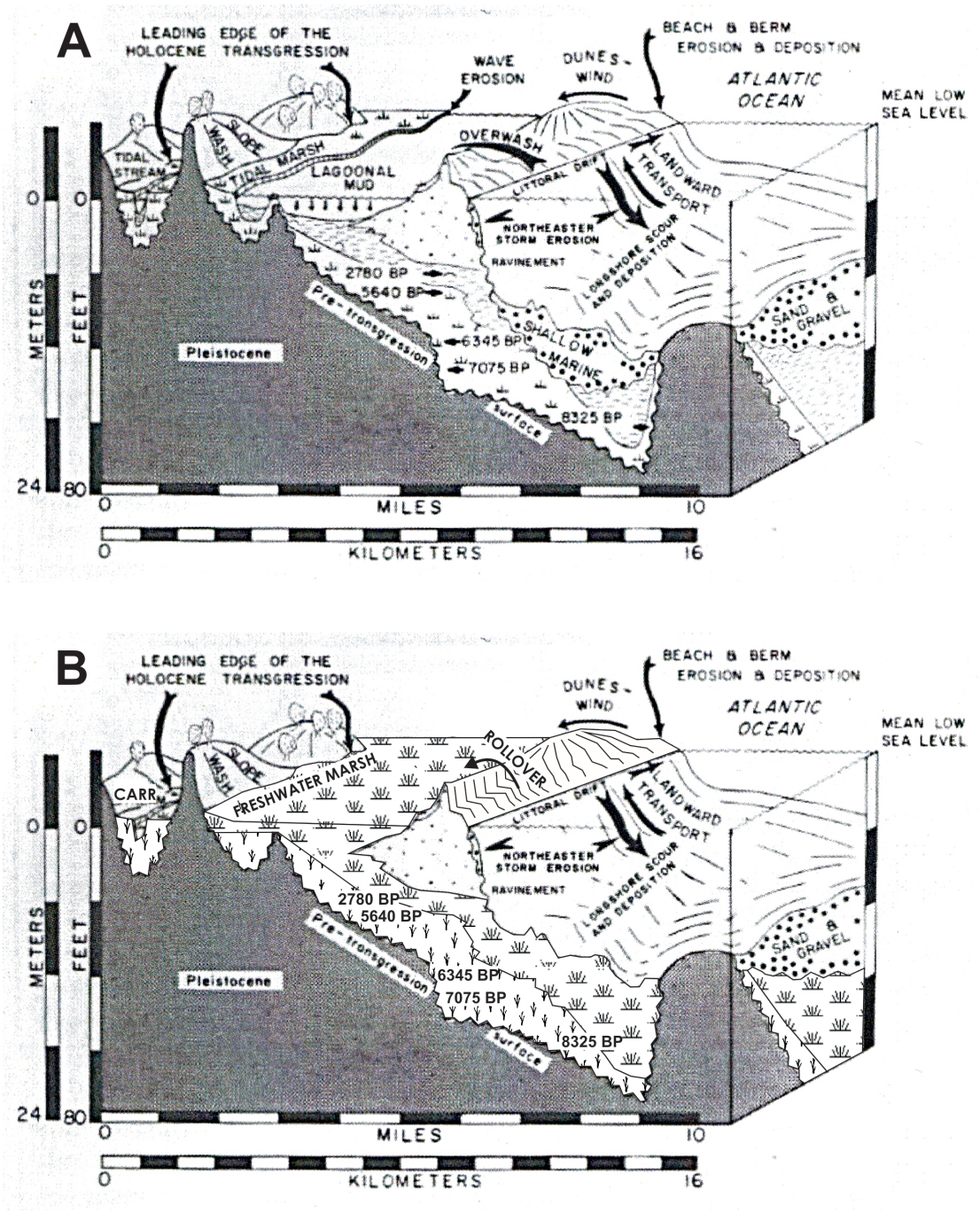

FIGURE 6.1: Schematic showing the response of a back-barrier freshwater marsh to RSL rise (A). Included is the original Kraft and Chrzastowski [1985] schematic for reference (B). Both systems share important features. such as the leading edge of the Holocene transgression.

relationship between the two. As per the study by Gehrels and Anderson [2014], the strongest relationship is with the diurnal tide. This has the potential to be problematic as the same groundwater fluctuation could be the result of evapotranspiration, rather than tidal oscillation. Whilst it would be possible to distinguish between the two in the raw data, as the tidal cycle is not the same length as the night/day cycle, it is not possible to do so with the results from spectral

analyses.

Wavelet analyses, using the technique presented by Grinsted et al. [2004] provide a more robust insight into the tidally induced groundwater oscillations. Cross wavelet power highlights periods that share a high power signal for a particular time period. This is clearly identifiable in the wavelet analyses for the semi-diurnal tide and shows the tidal and groundwater signals are slightly out of phase with each other, which is to be expected as the tidal signal takes time to propagate through the barrier.

The power of wavelet analyses enables a clear identification of a tidal signal in the groundwater, at greater distances than is possible using Fast Fourier Transform based spectral analyses. For both sites, groundwater monitoring shows a significant relationship between groundwater oscillations and the tidal movements of the sea. The groundwater is sensitive enough to oscillate in correlation to the semi-diurnal tide. The signal is consistent through both the sandy barrier at Rhoscolyn (Figure 6.2 A) and the sandy gravel barrier at Abermawr (Figure 6.2 B). However, there is a reduction in power at Rhoscolyn as would be expected as a result of increased dampening caused by the lower hydraulic conductivity of the sand over the sandy gravel.

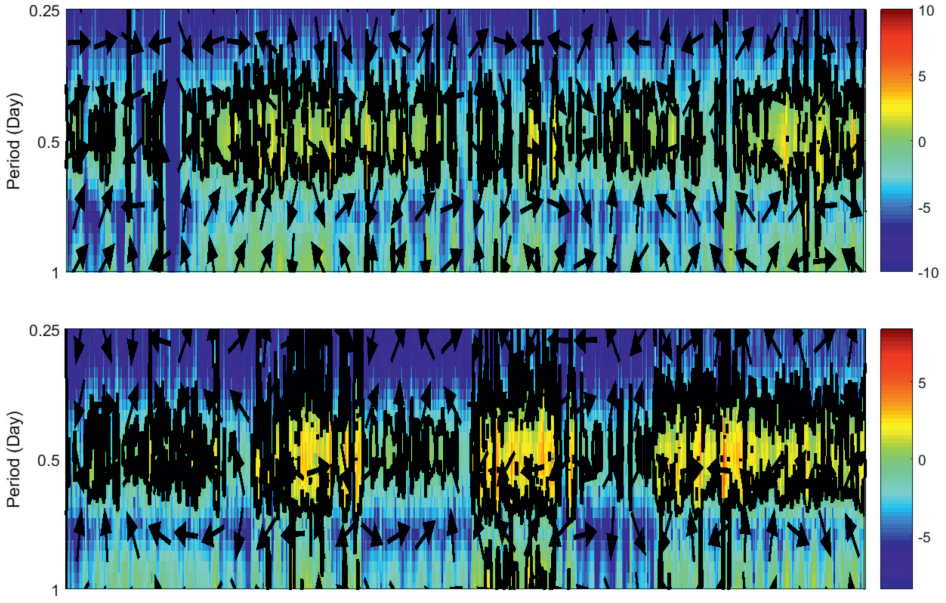

FIGURE 6.2: Comparison between cross wavelet power at Rhoscolyn (A) and Abermawr (B) for the Semi-diurnal tide measured in well one at both sites. Phase offsets are indicated by black arrows. Figure is cropped and focused to provide more detail and as such all results are outside of the cone of influence.

The gravel/sand barrier at Abermawr results in relative dampening of the tidal signal, when compared to the more permeable gravel barrier in the Gehrels and Anderson [2014] study. The impact of a fully sand barrier at Rhoscolyn is negligible when compared to Abermawr, and the

groundwater shows oscillations of similar magnitudes at both sites. The influence of the sea level is shown to be strong and rapid for the majority of the year, only uncoupling during extended wet or dry periods. As such the groundwater monitoring supports the fulfillment of condition two and presents some evidence that condition three is also fulfilled.

6.1.3 Groundwater Modelling

Sensitivity analyses were performed in FEFLOW to examine the impact of climate controlled variability on both sandy-gravel and gravel systems, given a specific peat and barrier permeability. Extreme wet and dry events were simulated for a period of 12 months, apart from a 6 months flood simulation at Abermawr, before returning the model to the base state. For both Abermawr and Rhoscolyn the control on groundwater by sea level is rapidly re-established. As such, the combination of field evidence and modelling supports the fulfilment of the second condition of suitability.

The flooding and dessication sensitivity analyses also support the fulfilment of condition three, that recharge and peat permeability values are at a level to prevent decoupling and are more important than the permeability values of the barrier system. Sensitivity experiments were performed to assess the impact of changes in peat permeability on the level of the groundwater.

Both sites were very sensitive to changes in peat permeability during model calibration, with groundwater dropping to lower levels when permeability was increased and the system flooding when it was decreased. This also supports the idea that the model is a good representation of the real life scenario, as neither site showed these kind of extreme events during a two year monitoring period. This sensitivity analysis shows that condition three is fulfilled for both sites.

The thickness of the beach was estimated from peat outcrops at both sites. Attempts to better quantify this with GPR, ERT and seismics were unsuccessful. The assessed thickness showed the beach to be relatively thin and modelling supported the fulfilment of condition four, that the beach was not the main control of water table height in the marsh.

Despite the modelling generally supporting the conditions required for the sites to be archives of Holocene sea-level histories, it is worth noting several limitations with the modeling carried out as part of this work. Whilst the outputs are probably robust enough for the study sites, the modelling did not present a set of criteria which would enable a judgment on the suitability of these kind of sites in different locations. However, it is worth noting that any previous disconnect between groundwater and sea-level heights would be recorded in the stratigraphic record and could be identified under careful observation.

Deciding on the peat and gravel permeability for the base case model was problematic. None of the wells captured a semi-diurnal tide at any point during the monitoring of groundwater.

Groundwater fluctuations are a composite of several factors, and only during certain periods was a diurnal signal observable. In comparison, the tidal data is dominated by the semi-diurnal fluctuations. As such each second semi-diurnal peak was matched with each diurnal peak, a process which is open to some interpretation. Whilst this is not an ideal approach, it resulted from the nature of the data available and produced base case conditions within the expected range for peat, sand and gravel.

The modelled system for both sites failed to fully reproduce the tidal signals captured in the marsh. Only the spring-neap cycle was reproduced by the model, which matches with observations in the field. This could be the result of using a simple layer model which introduces a degree of heterogeneity which does not represent the field sites. There are several layers of sand and sandy peat within each system, which would result in pockets of higher permeability in the freshwater peat. These possibly improve connectivity to the sea and result in better propagation of the tidal signal than those captured by the model. However, the full range of tidal signals was only observable in the well data via wavelet analysis, which was not carried out on the modelled data. Future work should consider an approach which would allow this type of analysis to be carried out on modelled outputs.

When changing recharge rates to test sensitivity of groundwater elevation to recharge variations, the model became unstable. This could be a further consequence of a simple two layered model. Throughout the simulations it was not possible to reproduce a groundwater elevation consistent with field observations. It is likely that this is a consequence of imprecise knowledge of the barrier stratigraphy at the sites. The thickness of peat under the barrier and the seaward extent of the peat, will play an important role in controlling groundwater elevation and response to variations in recharge. Future work should make further efforts to map out barrier and beach stratigraphy to solve this problem.

6.1.4 Configuration of the back-barrier system

As discussed in chapter 2, the evolution of barrier systems and transgression of barriers under a regime of sea-level rise is a non-trivial matter. Once a barrier is established, there are several drivers of barrier development which can influence the type and orientation of the barrier. Indeed, it is common for barriers to transition between regimes of swash and drift-aligned systems [Forbes et al., 1995].

As sea-level rises and barriers transgress, they go through periods of initiation, establishment, breakup and reinitiation (Figure 6.3. During these transitions it is possible for a barrier to change the angle of orientation to the coastline, dependent upon where the anchor points are located. As such, over the Holocene it is possible that the orientation of the paleo-barrier has not been consistent with the modern day orientation.

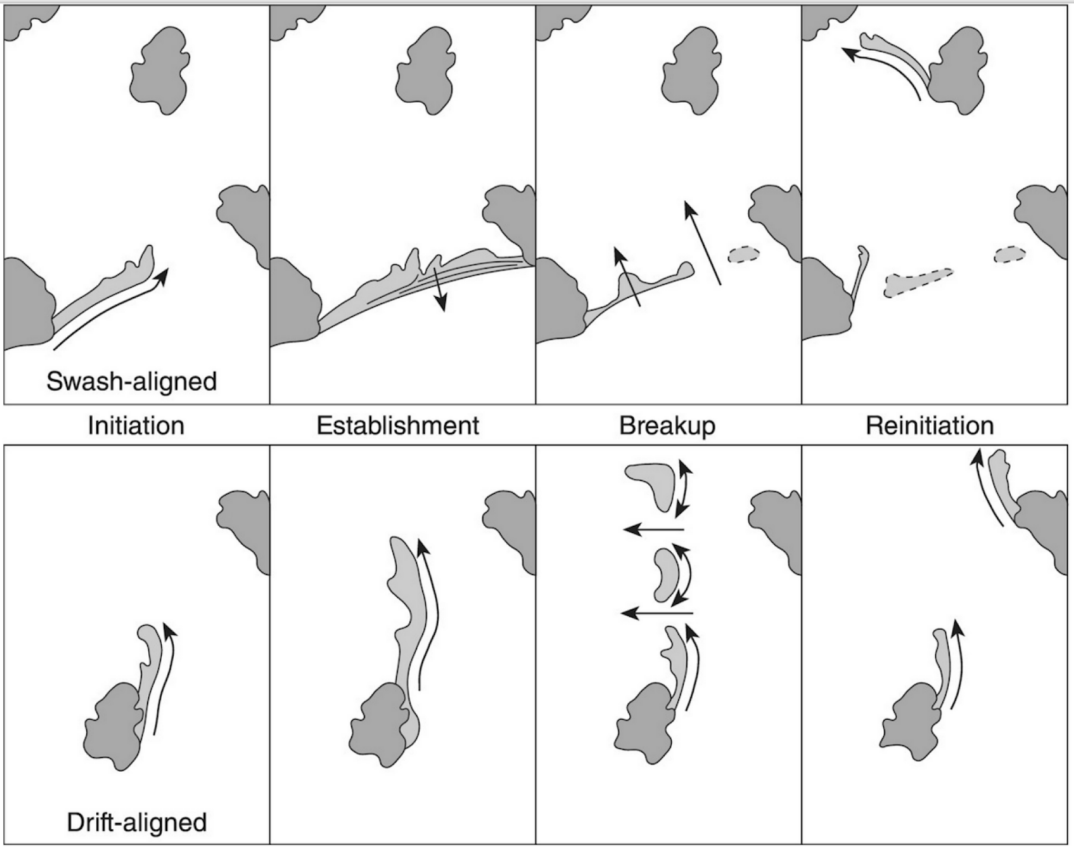

FIGURE 6.3: Phases of development for swash-aligned and drift-aligned barriers during a regime of sea-level rise. Direction of sediment transport is shown by arrows [Forbes et al., 1995]

.

If the palaeo-barrier alignment was different to that of modern day, at the time of basal peat formation, it has implications for the process detailed in section 3.7. Part of the process of determining indicative meaning relies on an estimation of the distance along the groundwater gradient. Variations in barrier orientation could lead to variations in the distance along the gradient (Figure 6.4) and, if this was the case at the time of basal peat formation, variations in the calculated indicative meaning.

Palaeo-ecology would provide a solution to this problem, particularly the use of testate ameobae. Charman [2001] demonstrated how palaeo-groundwater heights could be calculated, using them as a proxy. This could then be compared to a modelled groundwater height, based on the expected distance from the barrier. Whilst this method would require refinement, it provides a potential pathway to the solution of this problem.

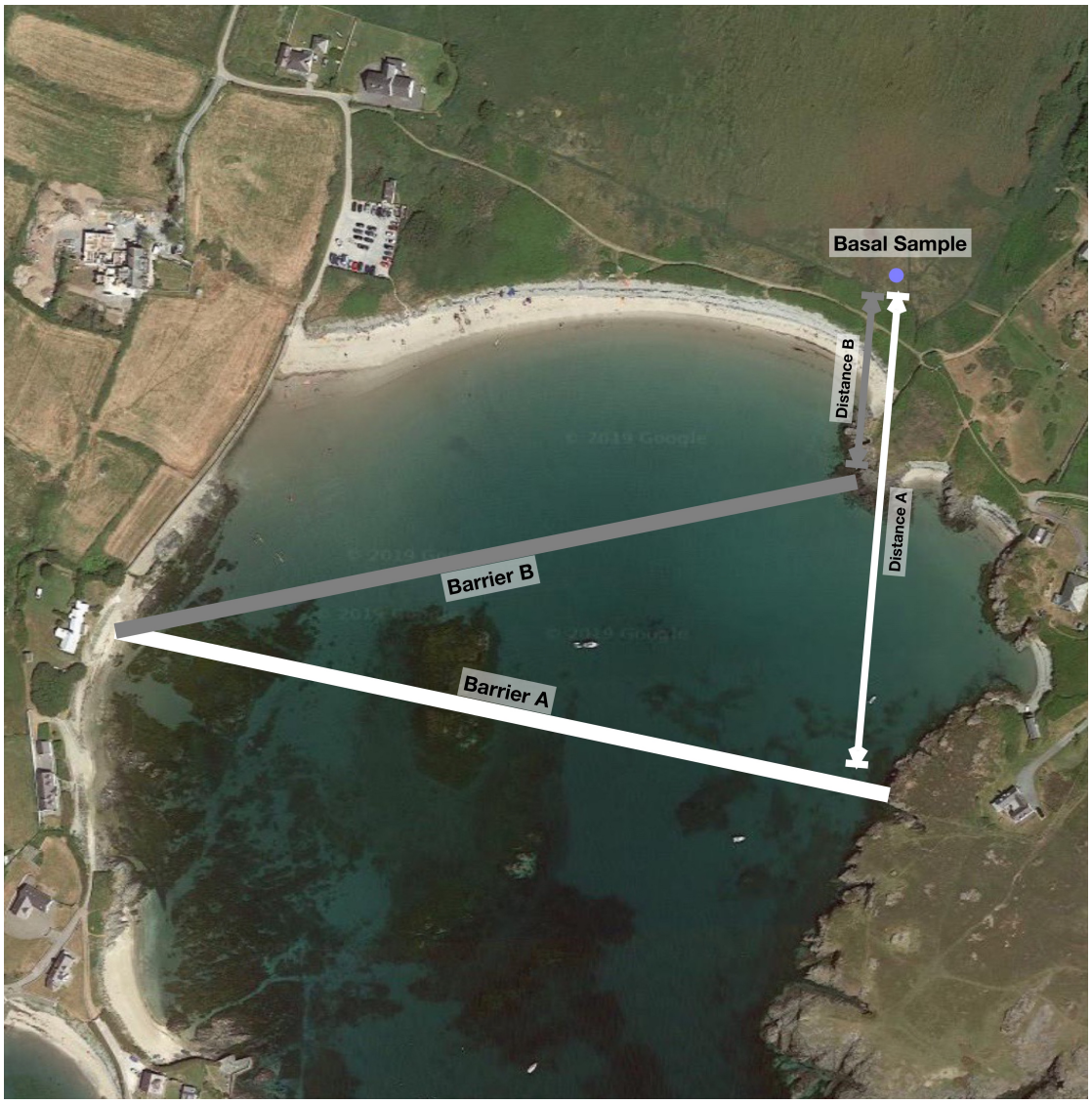

FIGURE 6.4: Caption

6.2 Holocene sea-level Changes in Anglesey

Five Holocene sea-level index points were produced for Anglesey (Figure 4.18), of which two were accepted and three rejected. The new SLIPs for Anglesey are insufficient to address the question of the mid-Holocene highstand. However, they provide a valuable link between any new data from the late Holocene and mid-Holocene. Work by Rushby (PhD in prep.) presents SLIPs from the late Holocene from a c.3000 years old salt marsh. This work presents a SLIP in agreement with Rushby's late Holocene data, as well as being in agreement with the older existing data.

The new data for Anglesey shows a c. 5.2m rise between c. 7400 - 1900 cal years BP. A mid-Holocene basal slip from Rhoscolyn is in good agreement with the existing database, indicating

Period	Cal Years BP	Observations	RSL Rate (m/ka)	SE	r^2	P-Value
Early Holocene	11100-7900	12	6.1	0.0006	0.91	0
Mid Holocene	8400-4500	9	1.7	0.0004	0.73	0.0034
Late Holocene	5300-0	4	0.5	0.0002	0.84	0.0812

TABLE 6.1: Mean RSL rates for the early, mid and late Holocene, calculated from linear regression, using the updated North Wales SLIP database. Correlation and significance values also shown. Lack of data in the late Holocene leads to a lack of significance.

a sea level 5.49 meters lower than present day at c. 7400 cal years BP. A late Holocene basal sample provides the youngest SLIP in the database at c. 1900 cal years BP and indicates a sea level c. 0.3m lower than present day. Whilst it is not possible to conclusively solve the debate surrounding the existence of a mid-Holocene highstand, the new data leave very little room for such a highstand.

Several samples failed to provide accurate SLIPs from Rhoscolyn, either as a result of radiocarbon dating issues or by having dates and indicative meanings that were not compatible with the existing database. Three samples from the shallowest region of the marsh, RC11 (0.8m) RC14 (0.5m) and RC15 (0.9m), were collected to address the aim of filling the gap in the database for the late Holocene, specifically the period younger than c. 4500 cal years BP. Of these samples, RC11 and RC15 returned dates that were modern and as such could not be included in the database. This could be as a result of sampling error or as a result of sea level not providing accommodation space during the late Holocene, with increased potential for deep root penetration by *Phragmites*. Two further samples provided ages younger than the indicative meaning would suggest, when compared to the existing database, RC9 (1890 cal years BP, 2.25m) an RC12 (1251 cal years BP, 1.69m). A further point was too old to be supported by the existing data, RC16 (14258 cal years BP, -5.2m). All of these points were rejected.

The new data from this study were combined with the existing north Wales database to calculate rates of RSL change throughout the Holocene, via linear regression modelling (Figure 6.5). As with the Pembrokeshire calculations, early and mid Holocene predictions are significant but late Holocene predictions are not (Table 6.1).

An early Holocene sea-level rise of c. 19.5m is observed for the period between c.11100 to 7900 cal years BP, at a rate of 6.1 m/ka. The rate of rise slows to 1.7 m/ka in the mid Holocene between c.8400 to 4500 cal years BP, with observed RSL rising 6.63m. The late Holocene has the slowest rate of RSL rise with a rate of 0.5 m/ka and an overall observed increase of 1.75m between c. 5300 cal years BP to present day. There remains a clear gap in the database for the late Holocene, which needs addressing in order to make significant predictions on the rate of RSL rise for that period.

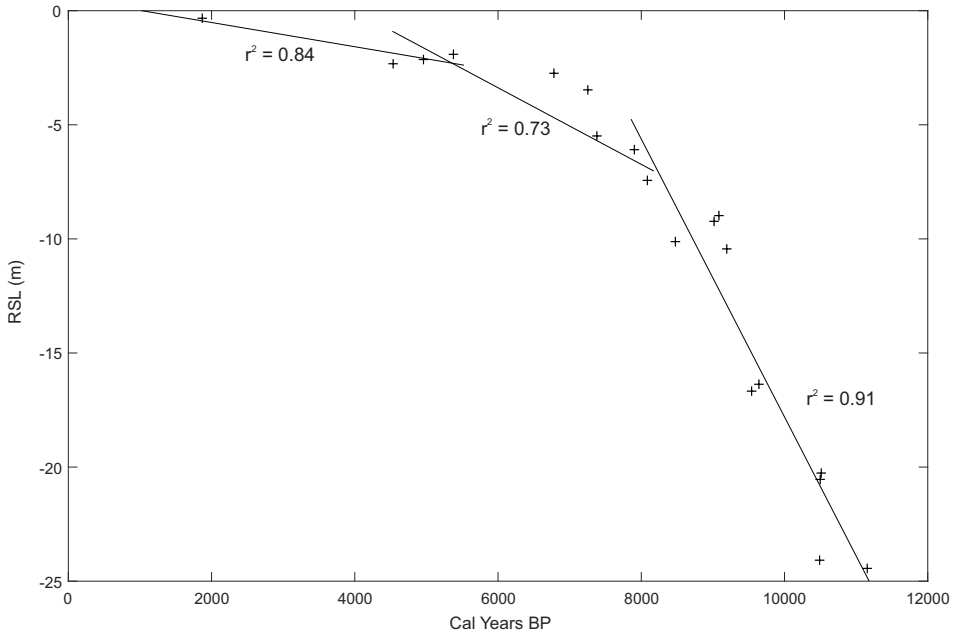

FIGURE 6.5: Linear regression to calculate the rate of RSL change for Early, Mid and Late Holocene periods using the updated north Wales database. Regression line and associated r squared values also shown.

6.3 Holocene Sea-level Changes in Pembrokeshire

Six SLIPs were produced for western Pembrokeshire, all of which were accepted following a quality assessment exercise. These provide greater resolution to the UK postglacial sea-level database, which previously contained only a single SLIP from this region. When compared to SLIPs from Glamorgan, they fill an important temporal gap in the database and span the mid to late-Holocene periods (Figure 5.12).

The new data for Pembrokeshire shows a c. 8.2m rise between c. 7000 and c. 2900 cal years BP. The new SLIPs are in good agreement with the existing Glamorgan database, which is shown to be comparable to Pembrokeshire by Shennan et al. [2018]. SLIPs from Abermawr fill a gap in the data between c. 6500 and c. 4500 cal years BP showing a c. 5.9m rise during this period. It was not possible to collect dates older than c.7000 cal years BP.

Two SLIPs add to the important period c. 7000 ka, when the rate of sea-level change slowed. There is a single SLIP from western Pembrokeshire in the current database, from c. 6800 cal years BP, indicating a sea level c. 5.3m lower than present day. The SLIPs from a similar time period collected during this study are not in agreement with the existing data. Basal SLIPs from Abermawr indicate sea level c. 11.3 and 9.5m lower than present day, at c. 7000 and 6600 cal years BP respectively. However, when compared to SLIPs from a similar period from Glamorgan

Period	Cal Years BP	Observations	RSL Rate (m/ka)	SE	r^2	P-Value
Early Holocene	10000-6400	7	4.9	0.0006	0.93	0.0004
Mid Holocene	8400-4500	9	2.5	0.0006	0.70	0.0046
Late Holocene	5300-0	6	1.5	0.0011	0.32	0.2428

TABLE 6.2: Mean RSL rates for the early, mid and late Holocene, calculated from the updated Pembrokeshire and Glamorgan SLIP databases. Late Holocene correlations lack significance due to scatter in the data.

, the new SLIPs are in good agreement. The Glamorgan database shows sea level at 10.1 meters lower than present day c. 6400 cal years BP and 10.6 meters lower than present day c. 7100 cal years BP.

Three SLIPs fill a gap in the combined database c. 5000 cal years BP. Three basal SLIPs collected from Abermawr cover a period between c.5200 - 4700 cal years BP, showing sea level to rise c. 0.5m from c. -5.9m to -5.4m over this period. The SLIP dated 4950 cal years BP shows sea level to be higher than expected when compared to the other SLIPs in this study. There is no obvious reason why this is the case. A further SLIP is presented for the late Holocene from c. 2900 cal years BP, which fills a gap in the combined database.

All of the SLIPs collected in this study show a lower mean sea level than predicted by GIA models. As all of the SLIPs were collected from freshwater environments, it could be argued that it is more likely that they would show a higher sea level than modelled predictions. Previously, freshwater systems have been considered suitable only for limiting points as they indicate a terrestrial system. As these SLIPs have been corrected for the relationship between groundwater level, mean sea level and groundwater gradient, they are no longer limiting points.

From the data presented in this study and the existing data from the Pembrokeshire and Glamorgan database, linear regression is used to calculate rates of RSL change for periods roughly in line with the Early, Mid and Late Holocene (Figure 6.6). The calculations for the Early and Mid-Holocene period are shown to be significant, whilst the late Holocene fit is not (Table 6.2).

Sea level is observed to have risen c. 17.6m during the early Holocene, between c.10000 to 6400 cal years BP, as a rate of 4.9 m/ka. The rate of change then slows during the mid Holocene to a rate of 2.5 m/ka, with an observed sea-level rise of 7m between c.7000 to 4200 cal years BP. A further reduction in the rate of sea-level change is observed in the late Holocene as RSL rise slows to a rate of 1.5 m/ka, with an observed rise of 6.3m from c.4200 to present day. There is still a visible gap in the database for the early Holocene, which needs addressing. The lack of significance in the late Holocene also needs addressing, by the addition of further data.

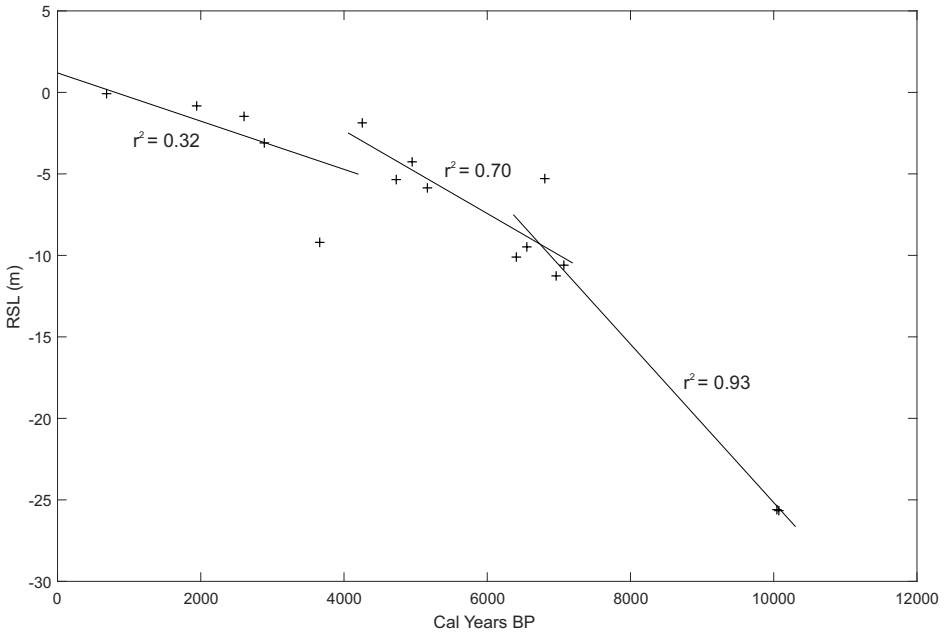

FIGURE 6.6: Linear regression to calculate the rate of RSL change for Early, Mid and Late Holocene periods using the combined updated Pembrokeshire and Glamorgan database. Regression kube and associated r squared values also shown.

6.4 Implications for GIA Models

The model presented by Shennan et al. [2018] presents two versions of the British-Irish Ice Sheet (Figure A.1) and three deglaciation histories for the North Sea. All current SLIPs lack the sensitivity to distinguish between the minor differences in sea level as a result of variations in North Sea deglaciation. However, the SLIPs from this study are precise enough to support the existence of a thicker British-Irish Ice Sheet. This is in agreement to the best fit choice made by Shennan et al. [2018], which utilises the entire SLIP database for the UK. However, these new data are better represented by the ICE5G model presented by Peltier et al. [2002].

The updated British sea-level database for north Wales and Pembrokeshire/Glamorgan is tested against a range of models for north Wales and Pembrokeshire (Table A.6). These models vary the earth model parameters, the global ice model, the regional ice model and North Sea ice coverage. Four of the models combine the regional ice model presented by Shennan et al. [2018] with the global ice model presented by Peltier et al. [2002].

None of the models for north Wales provide a good fit with the data throughout the Holocene (Figure 6.7). During the early to mid Holocene, the collection of models presented by Shennan et al. [2018], with the global ice model from Bradley et al. [2016] provide the best fit for the data. The scatter in the available data means that all of these model fit reasonably well. From the mid

Holocene to the late Holocene, all of the Shennan et al. [2018] models over predict sea level, probably as a result of under predicting rebound [Shennan et al., 2018]. The best fit models for this period are the ICE5G models from Peltier et al. [2002], but with the 71p510 earth model (Table A.6).The lack of data in the late Holocene makes comparison to the models difficult, but the single data point fits the same model as the late-mid Holocene data. The combined Shennan et al. [2018] and Peltier et al. [2002] models are the worst fit and reintroduce the mid Holocene highstand into predictions.

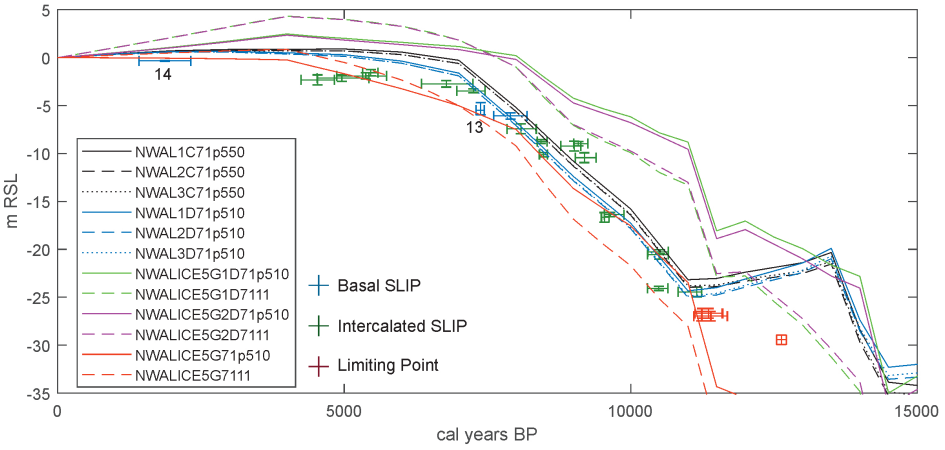

FIGURE 6.7: The updated SLIP database for north Wales, plotted with modelled RSL changes for the region. Variation is ice models are shown as blue and black lines [Bradley et al., 2016] and all other colours [Peltier et al., 2002]. Lithosphere thickness is 71km, with each individual model varying viscosity of the upper and lower mantle (Appendix A.6.

The best fit model (Figure 6.8) for Pembrokeshire, from the mid-late Holocene period, is the ICE5G model from Peltier et al. [2002] with the 71p510 earth model (Table A.6). There is a lack of data in the early Holocene, which makes comparison difficult. However, the limited data supports the use of the scenario C (Table A.6) model presented by Shennan et al. [2018], which also fits some of the data going into the mid-late Holocene. As with the north Wales models, combined Peltier et al. [2002] global ice model and Shennan et al. [2018] regional ice model over predict sea level and introduce a highstand into the predictions.

Whilst the Peltier et al. [2002] ICE5G 71p510 model is a good fit for both regions in this work, they are generally a poor fit for the rest of the UK (S. Bradley, personal communication, August, 2018). This highlights the importance of north and south Wales as an area spanning an isostatic gradient as a result of Holocene subsidence of Pembrokeshire relative to Anglesey. Further data from the late Holocene in north Wales and early Holocene in Pembrokeshire, would allow for more rigorous testing of the model predictions.

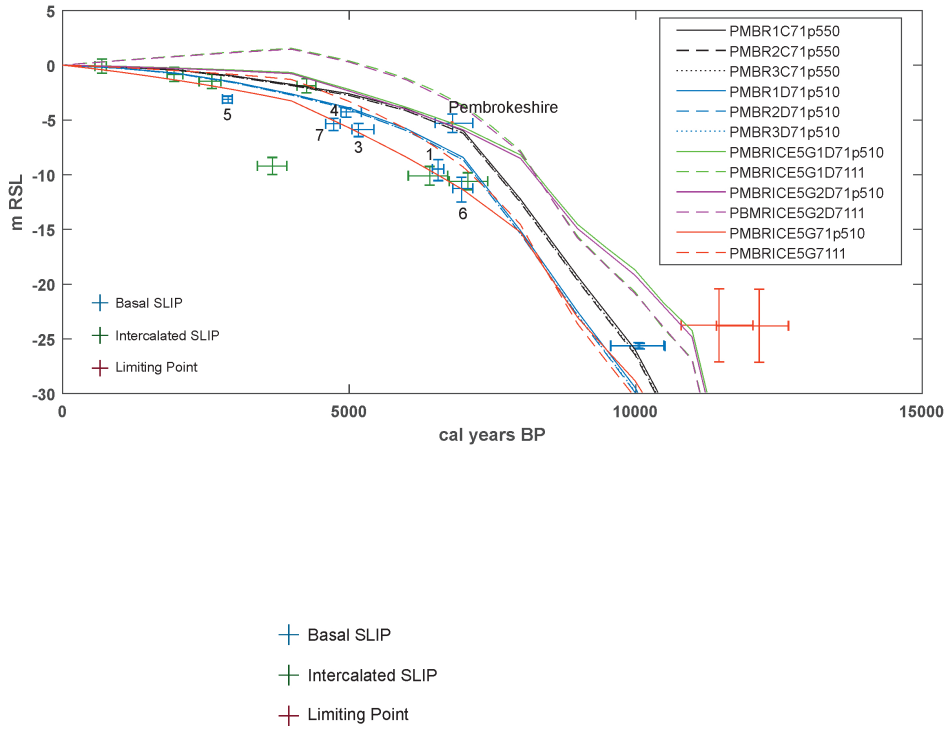

FIGURE 6.8: The updated SLIP database for Pembrokeshire and Glamorgan, plotted with modelled RSL changes for Pembrokeshire. Variations in ice models are shown as blue and black lines [Bradley et al., 2016] and all other colours [Peltier et al., 2002]. Lithosphere thickness is 71km, with each individual model varying viscosity in the upper and lower mantle (Appendix A.6).

Chapter 7

Conclusions

7.1 Original Aims

The aims of this thesis are to:

1. Establish Holocene RSL histories for Anglesey and western Pembrokeshire.
2. Assess current GIA models for Anglesey and western Pembrokeshire.
3. Test the suitability of peat-sandy gravel and peat-sand barrier systems as archives for Holocene sea-level change.

The methodology used to complete these aims was a combination of traditional empirical techniques and a model based approach to generate new SLIPs and to test the suitability of enclosed back-barrier systems more as recorders of sea-level change more generally. Calculating the indicative meaning from these systems is non-trivial and here we adapt the original method presented by Gehrels and Anderson [2014] to include the use of the Bruun equation [Bruun, 1962] for barrier migration calculations.

The barrier systems tested in this work fulfil the four criteria provided by Gehrels and Anderson [2014], as discussed in section 7.3. Modelled sensitivity tests show that whilst dessication and flooding events are capable of decoupling both systems from sea level. However, coupling is re-established within twelve months once the drivers are removed.

7.2 Original Hypothesis

The results of this work are used to test the hypothesis that coastal back-barrier freshwater peat deposits can have a direct relationship to sea level and as such be suitable archives for past sea level.

This work expands the type of systems considered suitable by Gehrels and Anderson [2014], showing that as well as gravel barriers, sea-level index points can also be obtained from sandy gravel and sand enclosed back-barrier systems. The new SLIPs presented here are in good agreement with the existing data and a range of sea-level histories predicted by models. It is concluded that under specified conditions, enclosed freshwater back-barrier marshes are suitable archives of Holocene sea level.

7.3 Freshwater Back-barrier Systems as Holocene Sea-level Archives

Freshwater back-barrier systems are suitable systems as sea-level archives when they fulfil fixed criteria. Firstly, there should be no stratigraphic evidence to suggest that the barrier system has had open channels to the sea. This would result in tidal oscillations been dampened around the channel and the possibility for peat production being controlled by localised groundwater interactions. Stratigraphic surveying at both sites investigated in this study does not show any evidence of channelisation.

Secondly, there has to be a strong tidal control on the level of groundwater, capable of overprinting climate controlled variability. At both sites wavelet analysis showed that groundwater was sensitive to tidal motion and that it oscillated at a diurnal frequency. This demonstrates a response time far more rapid than climate variations are capable of producing. Difficulty in obtaining late Holocene SLIPs from Rhoscolyn means there is some doubt over whether this method is reliable when the rate of sea-level change is slow or stable.

Thirdly, the capability of the system to act as an archive is not liable to periods of dessication or flooding. Groundwater monitoring showed that the system remained stable throughout the study. Sensitivity modelling demonstrated that should the system become decoupled from the sea, as a result of drying out or ponding, coupling was quickly re-established when conditions returned to normal.

Finally, the beach is relativity thin and not the main control on the height of the groundwater. The modelling of different barrier materials shows that the main control on the water table is peat permeability and not the permeability of the barrier.

7.4 Holocene Sea-level Change in Wales

Two SLIPs for north Wales and six SLIPs for western Pembrokeshire were added to the British sea-level database [Shennan et al., 2018]. All SLIPs were basal index points and fill important gaps for both regions. For north Wales the SLIPs provided do not leave any room for the existence

of a mid Holocene highstand. For western Pembrokeshire the SLIPs increase the database from a single point.

Sea level rose 5.16m in north Wales, between c. 7400 and c. 1900 cal years BP. The SLIP from the mid Holocene agrees with the existing data and the late Holocene SLIP provides the first for the region. Early Holocene RSL rates are 6.1 m/ka, mid Holocene rate is 1.7 m/ka and the late Holocene rate is 0.5 m/ka.

In western Pembrokeshire sea level rose 8.16m between c. 7000 and c. 2900 cal years BP. The new SLIPs all agree with the existing data for Pembrokeshire and Glamorgan. Early Holocene RSL rates are 4.9 m/ka, mid Holocene rate is 2.5 m/ka and the late Holocene rate is 1.5 m/ka.

7.5 GIA Models for Wales

The new SLIPs were compared to GIA model predictions by Shennan et al. [2018] and Peltier et al. [2002]. For north Wales, no single model provides the best fit throughout the Holocene. The available sea-level data do not provide sufficient resolution to distinguish between North Sea glaciation histories, but can distinguish between regional ice-sheet thickness. During the early Holocene, the data cannot distinguish between thinner or thicker regional ice sheet as presented by Shennan et al. [2018]. However, the data better fit the thicker ice sheet model predictions by the mid Holocene. The modelled predictions incorporating a regional ice sheet model from Shennan et al. [2018] and ICE-5G from Peltier [2004] over predict the magnitude of sea-level rise. Shennan et al. [2018] point out that the models predict too little rebound, when these parameters are combined. Throughout the Holocene, the 71p510 earth model (with no mid Holocene highstand) provides a better fit than the 71p58 model fromPeltier et al. [2002]. There is little difference between the best fit models during the early Holocene. However, the best fit Peltier et al. [2002] model provides the best prediction for the mid Holocene and the single SLIP in the late Holocene.

No single model provides the best fit throughout the Holocene for western Pembrokeshire. The lack of rebound in the region results in a better fit for the combined ICE-5G and regional ice sheet model presented by Shennan et al. [2018]. However, the model still over predicts the magnitude of sea-level rise. During the early Holocene, there is little available data to compare to the model. The best fit is with the thin regional ice-sheet model presented by Shennan et al. [2018].In the mid Holocene, the data is best fitted to the 71p510 earth model [Peltier et al., 2002]. All the models begin to converge during the late Holocene and the majority of the data support either the thick regional ice-sheet model [Shennan et al., 2018] or the 71p510 earth model [Peltier et al., 2002].

Sea-level predictions from new GIA models presented by Shennan et al. [2018] under predict rebound in north Wales. This results in a misfit between predictions and observations between c. 2000 - 7500 cal years BP. Reliable estimates of relative land change are crucial to future sea-level predictions for north Wales (see section 1.1, Figures 1.1 and 1.2). Once more accurate rebound can be modelled and the misfits closed, then more accurate predictions of future sea-level change for north Wales should be made.

The misfit between the GIA modelled sea level and observations in Pembrokeshire is less, as would be expected due to difference in ice extents between north Wales and Pembrokeshire. Whilst misfits do exist, the scatter in the observed data makes it difficult to quantify. However, the model presented by [Shennan et al., 2018] does have clear misfits in the mid Holocene, which would need to be closed in order to accurately predict future sea-level changes.

7.6 Limitations

It is important to understand the limitations of this work and where improvements can be made for the future. A key consideration is how far behind the palaeobarrier would this method be applicable. This study presents one date from a sample which was formed c. 780m behind the palaeobarrier. Whilst no attempt to quantify the distance are tested during modelling, it is worth noting that Knott et al. [2018] predict SLR induced groundwater rise as much as 4-5km inland. There are four key factors which will influence how far SLR induced groundwater rise will propagate. These are distance, topography, hydraulic conductivity and the presence of streams. As such, each site would need to be individually assessed to determine the maximum propagation distance. A key point is that compaction over time will reduce the hydraulic conductivity of the peat, to values lower than when they originally formed. As such, propagation would have been further than modern day values.

Radiocarbon dating remains an issue during periods of sea-level stability. The lack of accommodation space allows for the extended growth of *Phragmites* roots, which penetrate deep into the peat. It is therefore possible to sample these more modern roots and return younger dates than that of peat formation.

Modelling accuracy would have been improved with better mapping of the subsurface. GPR and seismics would allow for more accurate calculations of barrier thickness and more accurate simulations. However, this study found that it was necessary to reduce model complexity to linear layers in order to keep the model stable. So, whilst these techniques would allow for better mapping of the system, they may be too complex for the model.

The use of testate amoebae would have allowed for a better assessment of groundwater conditions at the time of peat formation. This study uses 2SE to account for groundwater variations. The

use of testate amoebae would have allowed for a more accurate calculation of that error. It is recommended that where preservation of testate amoebae is good, they should be used to investigate the palaeogroundwater height.

7.7 Future Work

This work demonstrates the suitability of a enclosed back-barrier freshwater marshes as archives of Holocene sea-level. Further archives are available throughout Wales, which could be explored to fill important gaps in the British sea-level database. For example, more data from North Wales are needed as there remains a gap. Whilst this work failed to collect more than a single sample suitable as a SLIP, more careful sampling should enable this method to be used to collect the necessary data.

This work demonstrates that SLIPs can successfully be collected from in front of the modern day barrier, as in Abermawr. This allows for the possibility to collect offshore samples to reconstruct early Holocene sea-level. This would be important in regions such as western Pembrokeshire, where such data is scarce. Gehrels and Anderson [2014] identified several similar sites around the world, where this methodology may be suitable. Further to this, there are barrier systems throughout Southeast Asia with organic deposits, such as those described by Murray-Wallace et al. [2002], which may be suitable for this methodology.

GIA modelling needs to resolve the mismatches between observed data and modelled sea-level histories. Whilst advances have been made in the resolution of the models and the representation of the British-Irish Ice Sheet Shennan et al. [2018], the under prediction of rebound needs to be addressed. There is still a need to better resolve the timing and magnitude of melt water pulse 1A, something this methodology may be particularly suited to, due to the possibility in accessing previously untapped archives and the lack of scatter within the SLIPs.

Appendix A

Appendix

ID no.	Site	Laboratory code	Easting	Northing	C14 Age	Error (1 Ss. dev)	Median age (Cal BP)	Cal+	Cal-	RSL (m)	RSL+	RSL-
NW1	Menai Strait	SUERC-2492	258300	373650	9714	49	11155	11238	10825	-24.44	-23.94	-24.94
NW2	Menai Strait	SUERC-2491	258300	373650	9296	53	10490	10652	10291	-24.08	-23.87	-24.29
NW3	Menai Strait	SUERC-2503	259750	374650	9301	54	10498	10654	10294	-20.54	-20.04	-21.04
NW4	Menai Strait	SUERC-2502	259750	374650	9308	45	10513	10655	10300	-20.26	-20.05	-20.47
NW5	Menai Strait	SUERC-2498	259750	374650	8581	40	9541	9622	9489	-16.67	-16.17	-17.17
NW6	Menai Strait	SUERC-2497	259750	374650	8698	43	9643	9883	9543	-16.37	-16.16	-16.58
NW7	Menai Strait	SUERC-2512	258450	373350	8227	40	9194	9394	9031	-10.44	-9.93	-10.95
NW8	Menai Strait	SUERC-2511	258450	373350	7689	38	8476	8548	8407	-10.12	-9.89	-10.35
NW9	Menai Strait	SUERC-2510	258450	373350	8084	41	9016	9129	8780	-9.23	-8.72	-9.74
NW10	Menai Strait	SUERC-2509	258450	373350	8152	38	9085	9250	9008	-8.98	-8.75	-9.21
NW11	Rhyl	HV 4348	303100	382610	4725	65	5463	5587	5320	-1.58	-1.25	-1.91
NW12	Clwyd Plain	HV 17810	296370	377510	4345	145	4959	5432	4527	-2.14	-1.8	-2.48
NW13	Clwyd Plain	HV 17811	296370	377510	4685	175	5377	5739	4872	-1.91	-1.57	-2.25
NW14	Clwyd Plain	HV 17812	296370	377510	5935	190	6781	7248	6350	-2.74	-2.4	-3.08
NW15	Clwyd Plain	HV 17814	296600	377120	7080	155	7903	8192	7609	-6.09	-5.75	-6.43
NW16	Malltraeth	HV 17820	247350	374450	4035	100	4535	4827	4249	-2.33	-1.81	-2.85
NW17	Malltraeth	HV 17819	247350	374450	7225	130	8085	8352	7839	-7.44	-6.92	-7.96
NW18	Morfa	HV 17815	282180	380790	6335	115	7254	7460	6965	-3.47	-3.26	-3.68
NW19	Llandudno	SRR 61	277540	381910	7635	52	8433	8542	8369	-8.76	-8.54	-8.98
NL1	Menai Strait	SUERC-2493	258300	373650	9945	48	11360	11607	11241	-26.68	-26.18	-27.18
NL2	Menai Strait	SUERC-2578	258300	373650	9834	67	11248	11595	11123	-26.68	-26.18	-27.18
NL3	Menai Strait	SUERC-2496	258300	373650	9965	49	11397	11687	11246	-26.97	-26.47	-27.47
NL4	Menai Strait	SUERC-2579	258300	373650	9817	67	11233	11399	11099	-26.97	-26.47	-27.47
NL5	Menai Strait	SUERC-2506	257950	374650	10654	53	12630	12715	12544	-29.43	-28.93	-29.93

TABLE A.1: The Holocene sea-level data for north Wales.

ID no.	Site	Laboratory code	National grid reference	C14 Age	Error (1 Ss. dev)	Median age (Cal BP)	Cal+	Cal-	RSL (m)	RSL+	RSL-
MD1	Clarach	HAR1575	SN 5880 8380	2560	70	2620	2782	2379	-1.16	-0.36	-1.96
MD2	Clarach	HAR1576	SN 5880 8381	4410	80	5028	5288	4851	-2.89	-2.09	-3.69
MD3	Clarach	HAR301	SN 5875 8395	5740	80	6540	6731	6324	-4.09	-3.27	-4.91
MD4	Clarach	HAR300	SN 5880 8380	5170	90	5930	6185	5717	-3.78	-2.97	-4.59
MD5	Clarach	HAR299	SN 5875 8395	5130	100	5873	6178	5653	-3.56	-2.74	-4.38
MD6	Clarach	HAR1572	SN 5880 8380	1140	80	1066	1261	927	-0.41	-0.19	-0.63
MD7	Clarach	HAR1579	SN 5880 8380	3800	80	4195	4418	3976	-1.96	-1.16	-2.76
MD8	Ynyslas	HAR1016	SN 6200 9250	1510	70	1410	1538	1299	-0.83	-0.61	-1.05
MD9	Ynyslas	HAR1019	SN 6200 9340	4700	70	5435	5585	5312	-2.36	-1.95	-2.77
MD10	Borth Bog	Q712	SN 6100 8900	2900	110	3049	3339	2787	-0.86	-0.56	-1.16
MD11	Ynyslas	HAR1017	SN 6200 9250	3050	70	3248	3441	3037	-1.53	-1.31	-1.75
MD12	Ynyslas	HAR1018	SN 6200 9340	3740	70	4136.5	4381	3892	-1.21	-0.99	-1.43
MD13	Ynyslas	Q382	SN 6100 9300	5898	135	6727	7155	6405	-3.36	-3.15	-3.57
MD14	Ynyslas	HAR1020	SN 6200 9340	5150	90	5902	6178	5663	-2.89	-2.67	-3.11

TABLE A.2: The Holocene sea-level data for mid Wales.

ID no.	Site	Laboratory code	National grid reference	C14 Age	Error (1 Ss. dev)	Median age (Cal BP)	Cal+	Cal-	RSL (m)	RSL+	RSL-
PM1	West Pembrokeshire	Q530	SM 8800 0000	5960	120	6804	7156	6501	-5.29	-4.45	-6.13
GM1	Margam	Q265	SS 7811 8714	3402	108	3661	3913	3397	-9.20	-8.42	-9.98
GM2	Margam	Q274	SS 7811 8714	5605	126	6406	6717	6051	-10.10	-9.25	-10.95
GM3	Margan	Q275	SS 7811 8714	6184	143	7070	7416	6714	-10.60	-9.84	-11.38
GM4	Stavel Hagar	CAMS41310	SS 4983 9236	1990	50	1943	2099	1824	-0.83	-0.19	-1.47
GM5	Stavel Hagar	CAMS41309	SS 4983 9236	2540	60	2604	2760	2381	-1.47	-0.83	-2.11
GM6	Port Talbot	Q663	SS 7609 8942	8970	160	10045	10489	9564	-26.60	-25.34	-26.86
GM7	Port Talbot	Q662	SS 7609 8942	8990	170	10072	100511	9564	-25.66	-25.40	-25.92
GM8	Stavel Hagar	CAMS41308	SS 4983 9236	3840	60	4255	4418	4088	-1.87	-1.23	-2.51
GM9	Stavel Hagar	CAMS41307	SS 4983 9236	740	50	685	762	563	-0.08	0.56	-0.56
LG1	Port Talbot	Q661	SS 7609 8942	9920	170	11454	12046	10792	-23.76	-20.43	-27.09
LG2	Port Talbot	Q664	SS 7609 8942	11980	180	13849	14404	13419	-34.86	-31.53	-38.19
LG3	Port Talbot	Q660	SS 7609 8942	10350	170	12156	12666	11411	-23.81	-20.48	-27.14

TABLE A.3: The Holocene sea-level data for Pembrokeshire and Glamorgan.

Iteration	Core	rc9	rc12	rc13	rc14	rc16
	Height (m OD)	5.16	4.26	4.19	5.19	5.77
	Depth (m)	2.91	2.57	2.65	0.49	4.05
	Sample Height (m OD)	2.25	1.69	1.54	4.7	1.72
	Initial Indicative Meaning (m OD)	4.90	4.90	4.90	4.90	4.9
1	Shore Distance (m)	53	30	23	67	20
	IM Correction	0.25	0.14	0.11	0.31	0.09
	Sea-level	-2.90	-3.35	-3.47	-0.51	-3.27
2	Shore Distance (m)	239.58	276.93	286.61	42.55	270.57
	IM Correction	1.13	1.30	1.35	0.20	1.27
	Sea-Level	-3.78	-4.51	-4.71	-0.40	-4.45
3	Shore Distance (m)	312.05	372.84	388.99	33.06	367.89
	IM Correction	1.47	1.75	1.83	0.16	1.73
	Sea-Level	-4.12	-4.96	-5.19	-0.36	-4.91
4	Shore Distance (m)	340.20	410.09	428.76	29.37	405.69
	IM Correction	1.60	1.93	2.02	0.14	1.91
	Sea-Level	-4.25	-5.14	-5.38	-0.34	-5.09
5	Shore Distance (m)	351.14	424.56	444.21	27.93	420.37
	IM Correction	1.65	2.00	2.09	0.13	1.98
	Sea-Level	-4.30	-5.21	-5.45	-0.33	-5.16
6	Shore Distance (m)	355.38	430.18	450.21	27.38	426.07
	IM Correction	1.67	2.02	2.12	0.13	2.00
	Sea-Level	-4.32	-5.23	-5.48	-0.33	-5.18
7	Shore Distance (m)	357.03	432.36	452.54	27.16	428.29
	IM Correction	1.68	2.03	2.13	0.13	2.01
	Sea-Level	-4.33	-5.24	-5.49	-0.33	-5.19
8	Shore Distance (m)	357.67	433.21	453.44	27.08	429.15
	IM Correction	1.68	2.04	2.13	0.13	2.02
	Sea-Level	-4.33	-5.25	-5.49	-0.33	-5.20
9	Shore Distance (m)	357.92	433.54	453.79		429.48
	IM Correction	1.68	2.04	2.13		2.02
	Sea-Level	-4.33	-5.25	-5.49		-5.20
10	Shore Distance (m)		433.67			429.61
	IM Correction		2.04			2.02
	Sea-Level		-5.25			-5.20

TABLE A.4: Rhoscolyn base case conditions for sea-level calculations, along with the iterations for each index point.

Iteration		ac1	ac3	ac4	ac5	ac6	ac7
	Height (m OD)	5.59	5.48	5.49	5.89	-1.08	5.93
	Depth (m)	7.45	4.85	3.76	3.36	2.00	4.95
	Sample Height (m OD)	-1.86	0.63	1.73	2.53	-3.08	0.98
	Initial Indicative Meaning (m OD)	4.66	4.66	4.66	4.66	4.66	4.66
1	Shore Distance (m)	90	61	96	59	0	59
	IM Correction	0.41	0.27	0.43	0.27	0.00	0.27
	Sea-level	-6.93	-4.30	-3.36	-2.40	-7.74	-8.01
2	Shore Distance (m)	481	299	233	166	537	556
	IM Correction	2.16	1.35	1.05	0.75	2.42	2.50
	Sea-Level	-8.68	-5.38	-3.98	-2.88	-10.16	-6.18
3	Shore Distance (m)	603	373	276	200	705	429
	IM Correction	2.71	1.68	1.24	0.90	3.17	1.93
	Sea-Level	-9.23	-5.71	-4.17	-3.03	-10.91	-5.61
4	Shore Distance (m)	641	396	290	210	758	390
	IM Correction	2.89	1.78	1.30	0.95	3.41	1.75
	Sea-Level	-9.41	-5.81	-4.23	-3.08	-11.15	-5.43
5	Shore Distance (m)	653	404	294	214	774	377
	IM Correction	2.94	1.82	1.32	0.96	3.48	1.70
	Sea-Level	-9.46	-5.85	-4.25	-3.09	-11.22	-5.38
6	Shore Distance (m)	657	406	295	215	779	373
	IM Correction	2.96	1.83	1.33	0.97	3.51	1.68
	Sea-Level	-9.48	-5.86	-4.26	-3.10	-11.25	-5.36
7	Shore Distance (m)	658	407	296	215	781	372
	IM Correction	2.96	1.83	1.33	0.97	3.51	1.68
	Sea-Level	-9.48	-5.86	-4.26	-3.10	-11.25	-5.36
8	Shore Distance (m)	658	407	296	215	782	372
	IM Correction	2.96	1.83	1.33	0.97	3.52	1.67
	Sea-Level	-9.48	-5.86	-4.26	-3.10	-11.25	-5.35
9	Shore Distance (m)					782	372
	IM Correction					3.52	1.67
	Sea-Level					-11.26	-5.35
10	Shore Distance (m)					782	372
	IM Correction					3.52	1.67
	Sea-Level					-11.26	-5.35

TABLE A.5: Abermawr base case conditions for sea-level calculations, along with the iterations for each index point.

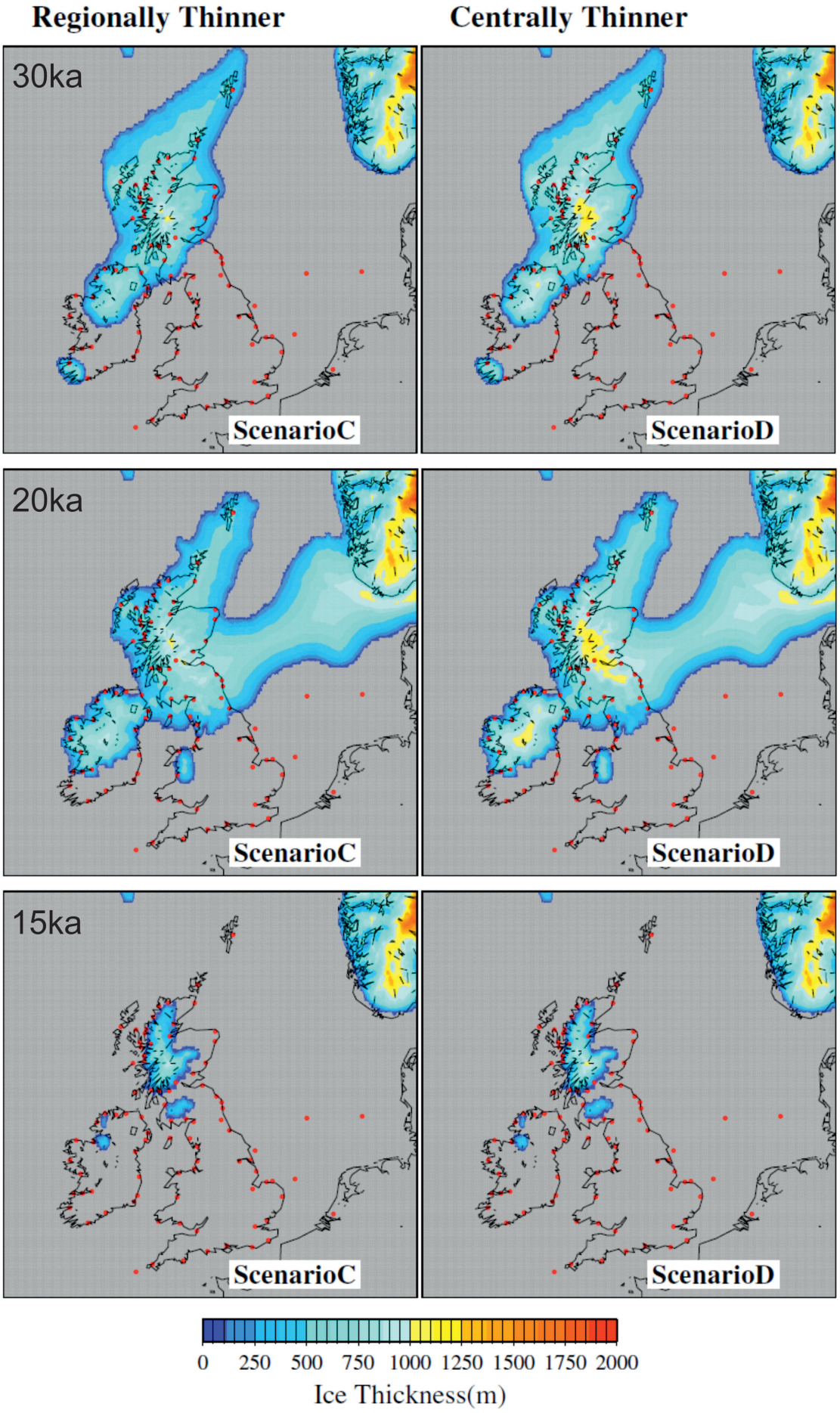

FIGURE A.1: Thickness of the British-Irish Ice sheet for scenarios C and D. Scenario D uses a thicker ice sheet over the UK.

Scenario	Global Ice	Reg. Ice	Lith. (km)	U.Mantle (Pa.s)	L.Mantle (Pa.s)
PmBR1C71p550	Bradley et al. [2016]	Shennan et al. [2018]	71	$5x10^{20}$	$5x10^{22}$
PmBR2C71p550	Bradley et al. [2016]	Shennan et al. [2018]	71	$5x10^{20}$	$5x10^{22}$
PmBR3C71p550	Bradley et al. [2016]	Shennan et al. [2018]	71	$5x10^{20}$	$5x10^{22}$
PmBR1D71p510	Bradley et al. [2016]	Shennan et al. [2018]	71	$5x10^{20}$	$1x10^{22}$
PmBR2D71p510	Bradley et al. [2016]	Shennan et al. [2018]	71	$5x10^{20}$	$1x10^{22}$
PmBR3D71p510	Bradley et al. [2016]	Shennan et al. [2018]	71	$5x10^{20}$	$1x10^{22}$
PmBRICE5G1D71p510	Peltier et al. [2002]	Shennan et al. [2018]	71	$5x10^{20}$	$1x10^{22}$
PmBRICE5G1D7111	Peltier et al. [2002]	Shennan et al. [2018]	71	$1x10^{21}$	$1x10^{21}$
PmBRICE5G2D71p510	Peltier et al. [2002]	Shennan et al. [2018]	71	$5x10^{20}$	$1x10^{22}$
PmBRICE5G2D7111	Peltier et al. [2002]	Shennan et al. [2018]	71	$1x10^{21}$	$1x10^{21}$
PmBRICE5G71p510	Peltier et al. [2002]	Peltier et al. [2002]	71	$5x10^{20}$	$1x10^{22}$
PmBRICE5G7111	Peltier et al. [2002]	Peltier et al. [2002]	71	$1x10^{21}$	$1x10^{21}$

TABLE A.6: GIA model parameters used for Holocene sea-level reconstructions.

Bibliography

Anderson Jr., W. P. [2015]. *Coastal Groundwater*, John Wiley and Sons, Ltd.
URL: *https://onlinelibrary.wiley.com/doi/abs/10.1002/9781119117261.ch6*

Austin, M. J., Masselink, G., McCall, R. T. and Poate, T. G. [2013]. Groundwater dynamics in coastal gravel barriers backed by freshwater lagoons and the potential for saline intrusion: Two cases from the uk, *Journal of Marine Systems* **123-124**: 19 – 32.
URL: *http://www.sciencedirect.com/science/article/pii/S0924796313000870*

Bassett, S. E., Milne, G. A., Mitrovica, J. X. and Clark, P. U. [2005]. Ice sheet and solid earth influences on far-field sea-level histories, *Science* **309**(5736): 925–928.

Bedlington, D. [1994]. *Holocene sea-level changes and crustal movements in North Wales and Wirral*, PhD thesis, PhD thesis, University of Durham, Durham.

BGS [2016a]. Digmapgb-50 [esri shapefile geospatial data], scale 1:50,000, tile(s): ew192 209 stdavids bedrock,, *EDINA Geology Digimap Service* **8.24**.

BGS [2016b]. Digmapgb-50 [esri shapefile geospatial data], scale 1:50,000, tile(s): ew192 209 stdavids superficial, *EDINA Geology Digimap Service* **8.24**.

Bibby, H. C. [1940]. The submerged forests at rhyl and abergele, north wales, *New Phytologist* **39**(2): 220–225.
URL: *http://dx.doi.org/10.1111/j.1469-8137.1940.tb07133.x*

Boorman, L. [2003]. Saltmarsh review:an overview of coastal saltmarshes, their dynamic and sensitivity characteristics for conservation and management, *JNCC Report 334* .

Bradley, S. L., Milne, G. A., Shennan, I. and Edwards, R. [2011]. An improved glacial isostatic adjustment model for the british isles, *Journal of Quaternary Science* **26**(5): 541–552.

Bradley, S., Milne, G., Horton, B. and Zong, Y. [2016]. Modelling sea level data from china and malay-thailand to estimate holocene ice-volume equivalent sea level change, *Quaternary Science Reviews* **137**: 54–68.

Bruun, P. [1962]. Sea-level rise as a cause of shore erosion, *Journal of the Waterways and Harbors Division* **88**: 117–132.

Bruun, P. [1988]. The bruun rule of erosion by sea-level rise: A discussion on large-scale two- and three-dimensional usages, *Journal of Coastal Research* **4**(4): pp. 627–648.
URL: *http://www.jstor.org/stable/4297466*

Canjander, A. [1913]. Studies of Finnish Mires, *Finnish Mires Acta Forestalia* **2**(3): 1–208.

Charman, D. J. [2001]. Biostratigraphic and palaeoenvironmental applications of testate amoebae, *Quaternary Science Reviews* **20**(16âĂŞ17): 1753 – 1764. European Quaternary Biostratigraphy.
URL: *http://www.sciencedirect.com/science/article/pii/S0277379101000361*

Collins, A. and Buchan, C. [2004]. Provenance and age constraints of the south stack group, anglesey, uk: UâĂŞpb sims detrital zircon data., *Journal of the Geological Society* **161**(5): 743–746.
URL: *http://jgs.lyellcollection.org/content/161/5/743.abstract*

Crane, P. [2004]. Archaeological monitoring of the intertidal and coastal zone pembrokeshire.

CRAWFORD, R. M. M., JEFFREE, C. E. and REES, W. G. [2003]. Paludification and Forest Retreat in Northern Oceanic Environments, *Annals of Botany* **91**(2): 213–226.
URL: *https://dx.doi.org/10.1093/aob/mcf185*

Davidson-Arnott, R. G. D. [2005]. Conceptual model of the effects of sea level rise on sandy coasts, *Journal of Coastal Research* pp. 1166–1172.
URL: *http://dx.doi.org/10.2112/03-0051.1*

Duigan, C., Rimington, N. and Howe, M. [2014]. Welsh coastal storms, december 2013 and january 2014 an assessment of environmental change.

Edwards, R. J. [2006]. Mid-to late-holocene relative sea-level change in southwest britain and the influence of sediment compaction, *The Holocene* **16**(4): 575–587.
URL: *https://doi.org/10.1191/0959683606hl941rp*

Erskine, A. D. [1991]. The effect of tidal fluctuation on a coastal aquifer in the uk, *Groundwater* **29**(4): 556–562.

FitzGerald, D. M., Fenster, M. S., Argow, B. A. and Buynevich, I. V. [2008]. Coastal impacts due to sea-level rise, *Annual Review of Earth and Planetary Sciences* **36**(1): 601–647.
URL: *http://dx.doi.org/10.1146/annurev.earth.35.031306.140139*

Forbes, D., Orford, J., Carter, R., Shaw, J. and Jennings, S. [1995]. Morphodynamic evolution, self-organisation, and instability of coarse-clastic barriers on paraglacial coasts, *Marine Geology* **126**(1âĂŞ4): 63 – 85. Large-Scale Coastal Behavior.
URL: *http://www.sciencedirect.com/science/article/pii/0025322795000668*

Gehrels, W. R. [1999]. Middle and late holocene sea-level changes in eastern maine reconstructed from foraminiferal saltmarsh stratigraphy and ams ^{14}c dates on basal peat, *Quarternary Research* **52**: 350–359.

Gehrels, W. R. [2010]. Late holocene land-and sea-level changes in the british isles: implications for future sea-level predictions, *Quaternary Science Reviews* **29**(13): 1648–1660.

Gehrels, W. R. and Anderson, W. P. [2014]. Reconstructing holocene sea-level change from coastal freshwater peat: A combined empirical and model-based approach, *Marine Geology* **353**: 140–152.

Gehrels, W. R., Belknap, D. F. and Kelley, J. T. [1996]. Integrated high-precision analyses of holocene relative sea-level changes: Lessons from the coast of maine, *Geological Society of America Bulletin* **108**(9): 1073–1088.
URL: *http://gsabulletin.gsapubs.org/content/108/9/1073.abstract*

Geng, X. and Boufadel, M. C. [2017]. Spectral responses of gravel beaches to tidal signals, *Scientific Reports* .
URL: *http://www.nature.com/articles/srep40770*

Grinsted, A., Moore, J. and Jevrejeva, S. [2004]. Application of the cross wavelet transform and wavelet coherence to geophysical time series, *Nonlinear Processes in Geophysics* **11**: 561–566.

Gu, C., Anderson Jr, William, P., Colby, Jeffrey, D. and Coffey, Christopher, L. [2014]. Air-stream temperature correlation in forested and urban headwater streams in the southern appalachians, *Hydrological Processes* .

Harkness, D. and Wilson, H. [1974]. Scottish universities research and reactor centre radiocarbon measurements ii., *Radiocarbon* **16**(2).
URL: *https://journals.uair.arizona.edu/index.php/radiocarbon/article/view/394*

Hassani, H., Covey-Crump, S. J. and Rutter, E. H. [2004]. On the structural age of the rhoscolyn antiform, anglesey, north wales, *Geological Journal* **39**(2): 141–156.
URL: *http://dx.doi.org/10.1002/gj.949*

Heyworth, A. and Kidson, C. [1982]. Sea-level changes in southwest england and wales, *Proceedings of the Geologists' Association* **93**(1): 91 – 111.
URL: *http://www.sciencedirect.com/science/article/pii/S0016787882800345*

Holgate, S. J., Matthews, A., Woodworth, P. L., Rickards, L. J., Tamisiea, M. E., Bradshaw, E., Foden, P. R., Gordon, K. M., Jevrejeva, S. and Pugh, J. [2013]. New data systems and products at the permanent service for mean sea level, *Journal of Coastal Research* **29**: 493–504.

Jennings, S., Orford, J. D., Canti, M., Devoy, R. J. N. and Straker, V. [1998]. The role of relative sea-level rise and changing sediment supply on holocene gravel barrier development: the example of porlock, somerset, uk, *The Holocene* **8**(2): 165–181.
URL: *http://hol.sagepub.com/content/8/2/165.abstract*

Knott, J. F., Jacobs, J. M., Daniel, J. S. and Kirshen, P. [2018]. Modeling groundwater rise caused by sea-level rise in coastal new hampshire, *Journal of Coastal Research* **0**(0): null.
URL: *https://doi.org/10.2112/JCOASTRES-D-17-00153.1*

Kraft, J. C. and Chrzastowski, M. [1985]. Coastal stratigraphic sequences, *in* J. Davis, RichardA. (ed.), *Coastal Sedimentary Environments*, Springer New York, pp. 625–663.

Lambeck, K. [1993a]. Glacial rebound of the british islesâĂŤi. preliminary model results, *Geophysical Journal International* **115**(3): 941–959.
URL: *http://dx.doi.org/10.1111/j.1365-246X.1993.tb01503.x*

Lambeck, K. [1993b]. Glacial rebound of the british islesâĂŤii. a high-resolution, high-precision model, *Geophysical Journal International* **115**(3): 960–990.
URL: *http://dx.doi.org/10.1111/j.1365-246X.1993.tb01504.x*

Lambeck, K., Johnston, P., Smither, C. and Nakada, M. [1996]. Glacial rebound of the british islesâĂŤiii. constraints on mantle viscosity, *Geophysical Journal International* **125**(2): 340–354.
URL: *http://dx.doi.org/10.1111/j.1365-246X.1996.tb00003.x*

Lisle, R. J. [1988]. Anomalous vergence patterns on the rhoscolyn anticline, anglesey: Implications for structural analysis of refolded regions, *Geological Journal* **23**(3): 211–220.
URL: *http://dx.doi.org/10.1002/gj.3350230303*

Loáiciga, Hugo, A., Pingel, Thomas, J. and Garcia, Elizabeth, S. [2011]. Sea water intrusion by sea-level rise: Scenarios for the 21st century, *Groundwater* **50**: 27–47.

Lowe, J., Howard, T., Pardaens, A., Tinker, J., Holt, J., Wakelin, S., Milne, G., Leake, J., Wolf, J., Horsburgh, K. et al. [2009]. Uk climate projections science report: Marine and coastal projections.

Lowe, J., W. M. J. [2015]. *Reconstructing Quaternary Environments*, London: Routledge.

Michael, H. A., Mulligan, A. E. and Harvey, C. F. [2005]. Seasonal oscillations in water exchange between aquifers and the coastal ocean, *Nature* **436**: 1145–1148.

Milne, G. A. [2015]. *Sea Level*, John Wiley and Sons Ltd, pp. 28–51.
URL: *http://dx.doi.org/10.1002/9781119117261.ch2*

Milne, G., Shennan, I., Youngs, B., Waugh, A., Teferle, F., Bingley, R., Bassett, S., Cuthbert-Brown, C. and Bradley, S. [2006]. Modelling the glacial isostatic adjustment of the uk region, *Philosophical Transactions of the Royal Society of London A: Mathematical, Physical and Engineering Sciences* **364**(1841): 931–948.

Moore, W. S. [1999]. The subterranean estuary: a reaction zone of ground water and sea water, *Marine Chemistry* **65**(1âĂŞ2): 111 – 125.
URL: *http://www.sciencedirect.com/science/article/pii/S0304420399000146*

Murray-Wallace, C. V., Jones, B. G., Nghi, T., Price, D. M., Vinh, V. V., Tinh, T. N. and Nanson, G. C. [2002]. Thermoluminescence ages for a reworked coastal barrier, southeastern vietnam: a preliminary report, *Journal of Asian Earth Sciences* **20**(5): 535 – 548.
URL: *http://www.sciencedirect.com/science/article/pii/S1367912001000402*

Orford, J. D., Carter, R. W. and Jennings, S. C. [1991]. Coarse clastic barrier environments: evolution and implications for quaternary sea level interpretation, *Quaternary International* **9**: 87–104.

Orford, J. D., Forbes, D. L. and Jennings, S. C. [2002]. Organisational controls, typologies and time scales of paraglacial gravel-dominated coastal systems, *Geomorphology* **48**(1âĂŞ3): 51 – 85. 29th Binghamton Geomorphology Symposium: Coastal Geomorphology.
URL: *http://www.sciencedirect.com/science/article/pii/S0169555X02001757*

Otvos, E. [2012]. Coastal barriers - nomenclature, processes and classification issues, *Geomorphology* **139–140**: 39–52.

Peltier, W. [2004]. Global glacial isostasy and the surface of the ice-age earth: the ice-5g (vm2) model and grace, *Annu. Rev. Earth Planet. Sci.* **32**: 111–149.

Peltier, W., Shennan, I., Drummond, R. and Horton, B. [2002]. On the postglacial isostatic adjustment of the british isles and the shallow viscoelastic structure of the earth, *Geophysical Journal International* **148**(3): 443–475.

PSMSL [2017].
URL: *http://www.psmsl.org/data/obtaining/*

Roberts, M. J. [2006]. *Holocene sea-level change in North Wales: the evolution of the Menai Strait.*, PhD thesis, University of Wales, Bangor,.

Roberts, M., Scourse, J., Bennell, J., Huws, D., Jago, C. and Long, B. [2011]. Late devensian and holocene relative sea-level change in north wales, uk, *Journal of Quaternary Science* **26**(2): 141–155.

Robinson, C., Li, L. and Barry, D. [2007]. Effect of tidal forcing on a subterranean estuary, *Advances in Water Resources* **30**(4): 851 – 865.
URL: *http://www.sciencedirect.com/science/article/pii/S0309170806001217*

Roper, H. [1992]. Superposed structures in the mona complex at rhoscolyi ynys gybi, north wales, *Geological Magazine* **129**: 475–490.

Schwartz, M. L. [1967]. The bruun theory of sea-level rise as a cause of shore erosion, *The Journal of Geology* **75**(1): pp. 76–92.
URL: *http://www.jstor.org/stable/30084988*

Shennan, I., Bradley, S. L. and Edwards, R. [2018]. Relative sea-level changes and crustal movements in britain and ireland since the last glacial maximum, *Quaternary Science Reviews* **188**: 143 – 159.
URL: *http://www.sciencedirect.com/science/article/pii/S0277379118300040*

Shennan, I., Bradley, S., Milne, G., Brooks, A., Bassett, S. and Hamilton, S. [2006]. Relative sea-level changes, glacial isostatic modelling and ice-sheet reconstructions from the british isles since the last glacial maximum, *Journal of Quaternary Science* **21**(6): 585–599.

Shennan, I. and Horton, B. [2002]. Holocene land- and sea-level changes in great britain, *Journal of Quaternary Science* **17**(5-6): 511–526.
URL: *http://dx.doi.org/10.1002/jqs.710*

Shennan, I., Lambeck, K., Horton, B., Innes, J., Lloyd, J., McArthur, J., Purcell, T. and Rutherford, M. [2000]. Late devensian and holocene records of relative sea-level changes in northwest scotland and their implications for glacio-hydro-isostatic modelling, *Quaternary Science Reviews* **19**(11): 1103–1135.

Shennan, I., Milne, G. and Bradley, S. [2012]. Late holocene vertical land motion and relative sea-level changes: lessons from the british isles, *Journal of Quaternary Science* **27**(1): 64–70.

Shennan, P. I., Long, P. A. J. and Horton, D. B. P. [2015]. *Handbook of Sea-Level Research*, Chichester, West Sussex, UK ; Hoboken, NJ, USA : Wiley.

Smith, Anthony, J. [2004]. Mixed convection and density-dependent seawater circulation in coastal aquifers, *Water Resources Research* **40**.

Stuiver, M., R. P. and Reimer, R. [2018]. Calib 7.1 [www program] at http://calib.org.
URL: *http://calib.org/calib/*

Treagus, S., Treagus, J. and Droop, G. [2003]. Superposed deformations and their hybrid effects: The rhoscolyn anticline unravelled, *Journal of the Geological Society* **160**(1): 117–136.

Troels-Smith, J. [1955]. *Characterization of Unconsolidated Sediments*, Danmarks Geologiske Undersøgelse, Reitzels Forlag.
URL: *https://books.google.co.uk/books?id=DZHEtgAACAAJ*

Vallejos, A., Sola, F. and Pulido-Bosch, A. [2015]. Processes influencing groundwater level and the freshwater-saltwater interface in a coastal aquifer, *Water Resources Management* **29**: 679–697.

Vleeschouwer, F. D., Chambers, F. and Swindles, G. [2010]. Coring and sub-sampling of peatlands for palaeoenvironmental research, *Mires and Peat* **7**(1).

Wheeler, B. and Shaw, S. [1995]. *Coastal Groundwater*, London : HMSO.

Wilks, P. J. [1977]. *FLANDRIAN SEA-LEVEL CHANGE IN THE CARDIGAN BAY AREA*, PhD thesis.

Xun, z., Chai, S., Ting and Ruige, G. [2015]. Estimation of aquifer parameters using tide-induced groundwater level measurements in a coastal confined aquifer, *Environmental Earth Sciences* **73**: 2197–2204.